Piezoelectric composites : design, fabrication and performance analysis

DOI:
[10.6100/IR760468](https://doi.org/10.6100/IR760468)

Document status and date:
Published: 01/01/2013

Document Version:
Publisher's PDF, also known as Version of Record (includes final page, issue and volume numbers)

Please check the document version of this publication:

• A submitted manuscript is the version of the article upon submission and before peer-review. There can be important differences between the submitted version and the official published version of record. People interested in the research are advised to contact the author for the final version of the publication, or visit the DOI to the publisher's website.
• The final author version and the galley proof are versions of the publication after peer review.
• The final published version features the final layout of the paper including the volume, issue and page numbers.

[Link to publication](#)

PIEZOELECTRIC COMPOSITES

Design, fabrication and performance analysis

PROEFSCHRIFT

ter verkrijging van de graad van doctor aan de Technische Universiteit Eindhoven, op gezag van de rector magnificus prof.dr.ir. C.J. van Duijn, voor een commissie aangewezen door het College voor Promoties, in het openbaar te verdedigen op maandag 11 november 2013 om 16:00 uur

door

Indu Babu

geboren te Trichur, India

Dit proefschrift is goedgekeurd door de promotoren en de samenstelling van de promotiecommissie is als volgt:

voorzitter: prof.dr.ir. J.C. Schouten
1^e promotor: prof.dr. G. de With
2^e promotor: prof.dr. R.A.T.M. van Benthem
leden: prof.dr. J.Th.M. de Hosson
                         (University of Groningen)
                     prof.dr. S.J. Picken
                         (Delft University of Technology)
                     dr.ing. C.W.M. Bastiaansen

To Babu, Iva Maria (Ponnu) and parents

Table of contents

Chapter 1

Introduction

In this chapter a concise introduction and an overview to piezoelectricity and piezoelectric materials are given. Important piezoelectric materials, properties and piezo composites are briefly reviewed, while pointing to aspects relevant to current and emerging applications. Furthermore the purpose of the research and an outline of the structure of the thesis are described.

---

*Part of this chapter has been submitted for publication as: I. Babu, N. Meis and G. de With, "Review of piezoelectric composites," Journal of Materials Chemistry (2013).

1. 1. Introduction

Piezoelectricity is the property of certain crystalline materials to develop electric charge in response to applied mechanical stress. The word piezoelectricity means electricity resulting from pressure [1]. The German physicist Wilhelm G. Hankel gave this phenomenon the name piezoelectricity, derived from the Greek 'piezo' or 'piezein' which means to squeeze or press, and electric or electron, which stands for amber, an ancient source of electric charge [2, 3]. The direct piezoelectric effect refers to the generation of electric polarization by mechanical stimulation and conversely, the indirect effect refers to the generation of a strain in a material due to the electric stimulation (Figure 1). Although piezoelectricity has been discovered by the French physicists Jacques and Pierre Curie already in 1880, the effect was not technically useful until the first quartz crystal oscillator was developed by Walter Cady in 1921 and until the need for good frequency stability for radio systems was recognized. The development of the modern piezo technology was not possible until barium titanate ($BaTiO_3$) was discovered to be ferroelectric by von Hippel and co-workers and until R.B. Gray of the Erie Resistor Company recognized that a poling process is necessary to make $BaTiO_3$ ceramics piezoelectric. Discovery of PZT (($PbZr_xTi_{1-x})O_3$) gave an important improvement on piezo technology, as compared to barium titanate, because of higher and lower Curie temperatures. The nature of the piezoelectric effect is closely related to the occurrence of electric dipole moments on crystal lattice sites with asymmetric charge surroundings as in $BaTiO_3$ and PZT [4].

Piezoelectricity had been first observed in 1880 in Quartz and Rochelle salt which occur naturally [1]. From the application point of view it has been realized that the piezoelectric properties are very stable in natural crystals as compared to synthetic ones. Since then, piezoelectricity has introduced a wide range of applications and most of them can be broadly classified into sensor (direct effect, e.g. pressure sensor), actuator (converse effect, e.g. ultrasonic motor), resonance (both direct and converse effect, e.g. hydrophone) and energy conversion (direct effect, e.g. high voltage generator) applications. This has initiated exciting developments and led to an enormous wide field of applications based on piezoelectric materials [5-10].

Piezoelectric materials have yielded several interesting properties which are used for a large number of sensor and transducer applications that are important in a variety of fields such as medical instrumentation, naval sonar devices, industrial process control, environmental monitoring, communications, information systems and tactile sensors. In parallel, the need for functioning under varied conditions, in wider operation ranges, in extreme environment such as high temperatures, high electric

fields or pressures, high frequencies continues to grow and this lead to the development of new piezoelectric materials and processing technologies. A wide variety of materials are piezoelectric which include crystals (natural and synthetic), ceramics and polymers [11].
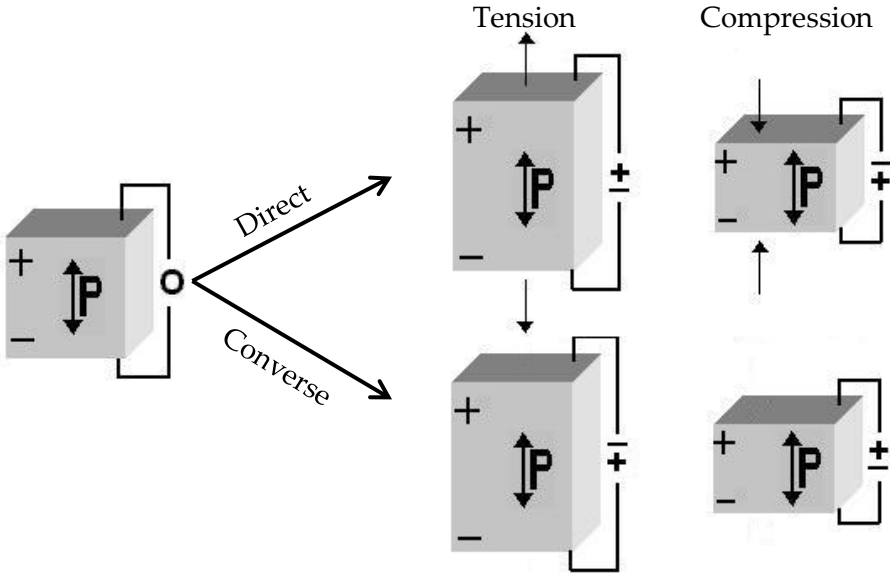
Figure 1. *Direct and converse piezoelectric effect.*
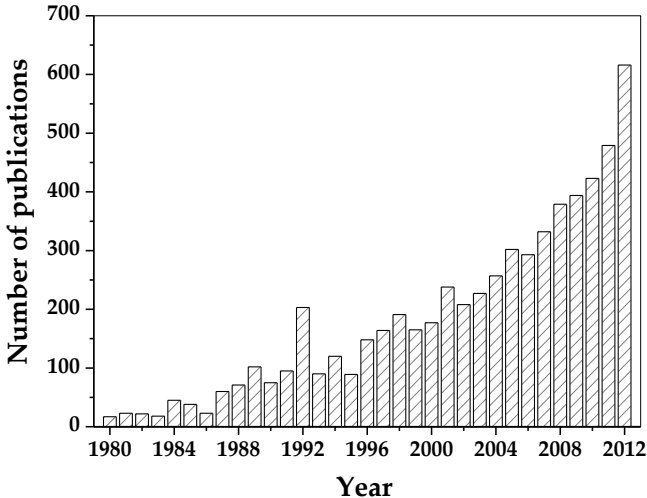
Figure 2. *Number of publications on piezoelectric composites from 1980 till 2013.*

Applied piezoelectric materials include bulk ceramics, ceramic thin films, multi-layer ceramics, single crystals, polymers and ceramic-polymer composites. Figure 2 shows the growth of the use of composite piezoelectrics in research by the number of peer reviewed articles published each year (based on Web of Science (ISI Web of Knowledge), search terms ((Polymer AND Ceramic composite) AND (Piezoelectric OR Piezoelectric composite).

1.2. Piezoelectric materials

Piezoelectric materials exhibit intrinsic polarization and the characteristic of this state is the thermodynamically stable and reversibility of the axis of polarization under the influence of an electric field. The reversibility of the polarization, and the coupling between mechanical and electrical effects are of crucial significance for the wide technological utilization of piezoelectric materials. Piezoelectric materials can be classified in to crystals, ceramics and polymers. The most well-known piezoelectric crystal is quartz SiO_2. Most of the piezoelectric materials are ceramic in nature though these ceramics are not actually piezoelectric but rather exhibit a polarized electrostrictive effect. These include lead zirconate titanate PZT $(PbZr_xTi_{1-x})O_3$, lead titanate $(PbTiO_2)$, lead zirconate $(PbZrO_3)$, and barium titanate $(BaTiO_3)$. There are some polymeric materials which are piezoelectric and polyvinylidene fluoride is one of them [12-13].

The perovskite $Pb(Zr_xTi_{1-x})O_3$ piezoelectric ceramic is playing a dominant role in piezoelectric materials. PZT and its related materials have been extensively investigated because of its high dielectric constant and excellent piezoelectric properties. Above a temperature known as the Curie point T_c, these crystallites exhibit simple cubic symmetry, the elementary cell of which is shown in figure 3. This perovskite structure of PZT consisting of a cubic structure ABO_3 with the A-cation in the middle of the cube, the B-cation in the corner and the anion in the faces. The A and B represents the large cation, such as Ba^{2+} or Pb^{2+} and medium size cation such as Ti^{4+} or Zr^{4+}. In cubic lattice structure, the cations are located at the centers of the oxygen cages with the positive and negative charge sites coincides with no dipoles. This structure is termed as centrosymmetric with zero polarization. Below the Curie point these crystallites take on tetragonal symmetry in which the cations are shifted off the center. This creates the positive and negative charge sites with buit-in electric dipoles that can be switched to certain allowed directions by the application of an electric field. The structure is non-centro symmetric with net polarization as shown in figure 4.

In order to make these materials piezoelectrically active a process called poling is required. Poling switch the polarization vector of each domain to the crystallographic direction which is the nearest to the direction of the applied field. Once aligned, these dipoles form regions of local alignment known as Weiss domains. Application of stress (tensile or compression) to such a material will result in the separation of charges leading to a net polarization. Polarization varies directly with the applied stress and is linearly dependent. The effect is also direction dependent, the compressive and tensile stresses will generate electric fields and hence voltages of opposite polarity. If an electric field is applied, the dipoles within the domains either contract or expand

(resulting in a change in the volume). Doping with conductive fillers (CB, CNTs and metals) will enhance the electrical conductivity which leads to improved poling efficiency.
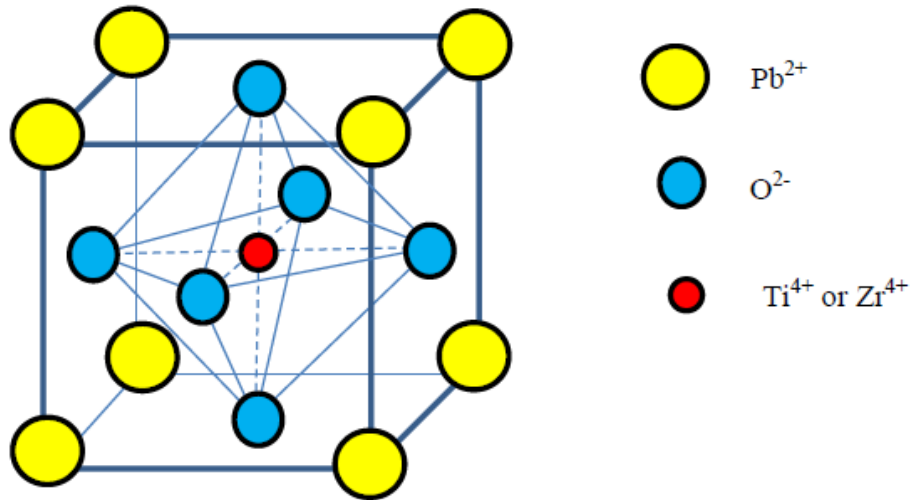
Figure 3. *The perovskite structure of PZT with a cubic lattice (Centrosymmetric with zero polarization).*
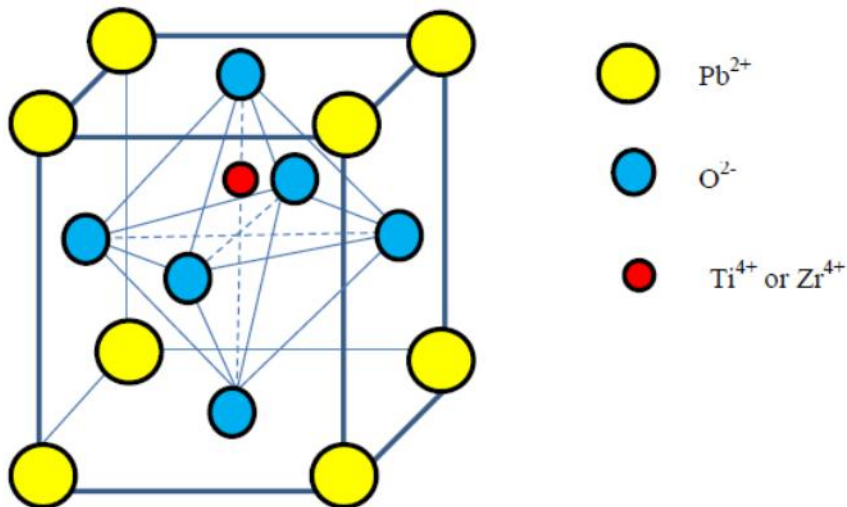
Figure 4. *The perovskite structure of PZT with a tetragonal lattice (Non-centrosymmetric with a net polarization).*

1.3. Piezoelectric properties

The piezoelectric effect is anisotropic and strongly depends on polarization direction. Piezoelectric materials can be polarized with an electric field and also by application of a mechanical stress. Application of stress to a piezoelectric material in a particular

direction, will strain the material in not only the direction of the applied stress but also in directions perpendicular to the stress as well. The linear relationship between the stress applied on a piezoelectric material and the resulting polarization generated is known as the direct piezoelectric effect. Conversely strain generated (contract or expand) in a piezoelectric material when an electric field is applied is called converse piezoelectric effect. Since the piezoelectric coupling is described by a linear relationship between the first-rank tensor (D or E) and the second-rank tensor (σ or ε), the corresponding coupling coefficients form a third-rank tensor. Both the direct and converse piezoelectric effects can be described mathematically through the tensor notation in the following form (i, j, k = 1, 2, 3), [14].

$$D_i = d_{ijk}\, \sigma_{jk} \qquad\qquad \text{Direct effect} \qquad (1)$$
$$\varepsilon_{jk} = d_{ijk}\, E_i \qquad\qquad \text{Converse effect} \qquad (2)$$

where D_i is the dielectric displacement, σ_{jk} is the applied stress, ε_{jk} is the strain generated, E_i is the applied field and d_{ijk} is the piezolectric coeiffficient. The units of direct piezoelectric effect are C/N (Coulomb/Newton) and for the converse piezoelectric effect are m/V (meter/Volt).
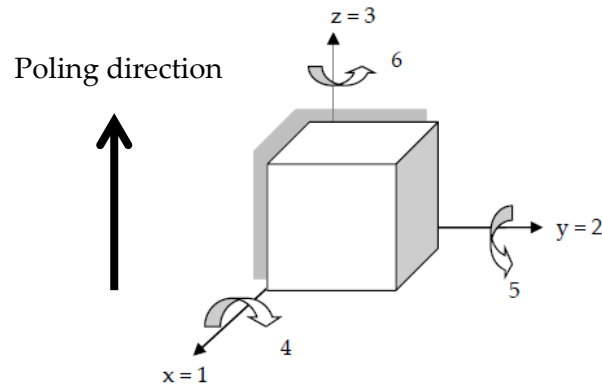
Figure 5. *Conventional notation of the axes and directions.*

In accordance with the IEEE standard on piezoelectricity [15], the three-dimensional behavior of the piezoelectric material (electric, elastic and piezoelectric) are based on an orthogonal coordinate system as shown in Figure 5. In this Figure, the z or 3 direction is determined as the poling direction, and all the directions perpendicular to the poling direction are considered as direction 1. The piezoelectric coefficients of poled ceramics are d_{33} (longitudinal piezoelectric coefficient), $d_{31} = d_{32}$ (transverse piezoelectric coefficient) and $d_{15} = d_{24}$ (shear piezoelectric coefficient). The d_{33} represents the induced polarization in direction 3 (parallel to direction in which ceramic element is polarized)

13

per unit stress applied in direction 3. Conversely it is the strain generated in the direction 3 due to an electric field applied in the direction 3. While the d_{31} stands for (induced polarization in direction 3 (parallel to direction in which ceramic element is polarized) per unit stress applied in direction 1 (perpendicular to direction in which ceramic element is polarized). The three principal axes are assigned as x, y and z (1, 2 and 3) while 4, 5, and 6 describe mechanical shear stress which acts tangentially to the areas defining the coordinate system.

1.4. Piezoelectric composites

Realization of excellent properties is acquired in piezoelectric composites by the combination of its constituent phases. As a result the demand for piezoelectric composites is growing and developing such materials is a common way to tailor the material properties for particular applications. The arrangement of the constituent phases in a composite is critical for the electromechanical coupling of the composites. The research on composite piezoelectrics has been stimulated by the introduction of the concept of connectivity developed by Newnham et al. in the late 1970s [16]. Out of 10 connectivity patterns as shown in Figure 6 [16] (0-0, 0-1, 0-2, 0-3, 1-1, 1-2, 2-2, 1-3, 2-3 and 3-3), 0-3 and 1-3 have received the most attention and is briefly described in the following sections.
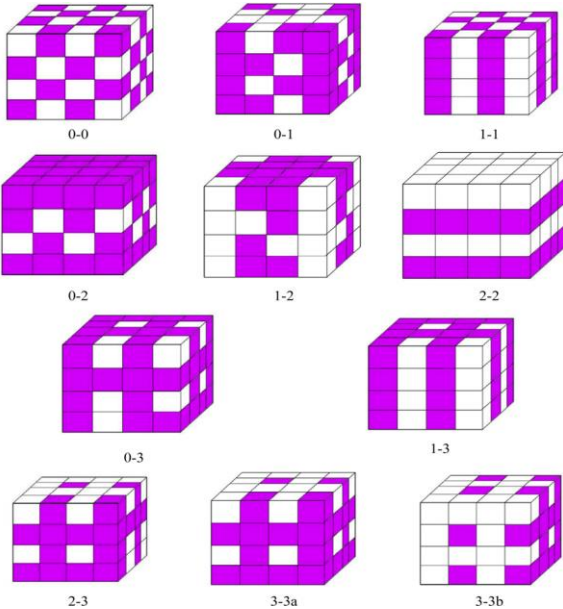
Figure 6. *Connectivity patterns for two-phase piezocomposites.*

In this connectivity pattern, the first number denotes the physical connectivity of the active phase (ceramic) and the second number refers to the passive phase (polymer).

The simplest type is the 0-3 connectivity, in which the polymer matrix is incorporated with ceramic inclusions and 0-3 stands for the three dimensionally-connected polymer matrix filled with ceramic inclusions. Based on the connectivity patterns, various piezoelectric ceramic-polymer composites were designed and a few of them is shown in Figure 7 [18]. A useful figure of merit of these types of composites is the improved performance compared to single phase piezoceramics.
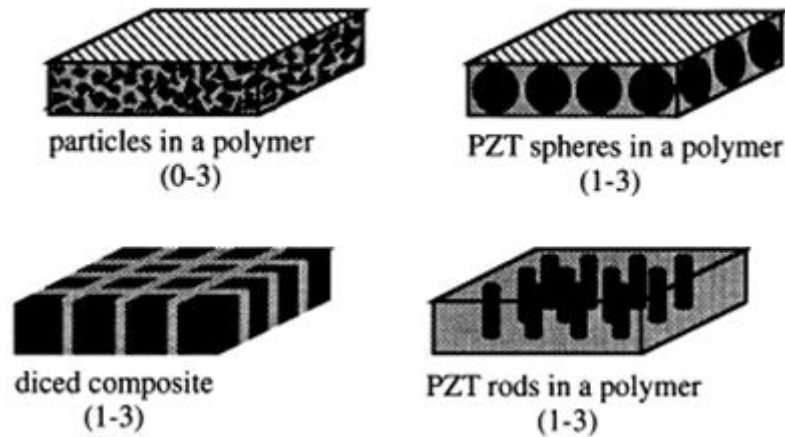
Figure 7. *Schematic diagram of piezocomposites with 0-3 and 1-3 connectivity.*

1.4.1. Piezocomposites with 0-3 connectivity

The simplest type of piezocomposites is with the 0-3 connectivity, which consists of a polymer matrix incorporated with ceramic inclusions. In many ways, these types of composites is similar to polyvinylidene fluoride (PVDF). Both consists of a crystalline phase embedded in an amorphous matrix which are reasonably flexible. Polymer composites with 0-3 connectivity have several advantages over other types of composites: their ease of production, their ability for the properties to be tailored by varying the volume fraction of the ceramic inclusions and the ease of obtaining different sizes and shapes. First attempts to fabricate composites with 0-3 connectivity were made by Kitayama et al., Pauer et al. and Harrison et al. [19] with a comparable d_{33} to PVF$_2$ and lower d_h value to that of PZT and PVF$_2$. An improved version of these types of composite was fabricated by Banno et al. [20] using modified lead titanate incorporated in chloroprene rubber. These composites provides better piezo properties than the previous ones. Safari et al. [21] fabricated flexible composites with $PbTiO_3$-$BiFeO_3$ as fillers in eccogel polymer. The as-developed composites exhibit outstanding hydrostatic sensitivity. Later several researchers developed composites with 0-3 connectivity with different inclusions and these include PZT $(PbZr_xTi_{1-x})O_3$, $(PbTiO_2)$, $(PbZrO_3)$, and $BaTiO_3$ [22-32].

1.4.2. Piezocomposites with 1-3 connectivity

In composites with 1-3 connectivity, the ceramic rods or fibers are self-connected one dimensionally in a three dimensionally connected polymer matrix. In this type of composites, the PZT rods or fibers are aligned in a direction parallel to the poling direction. These types of composites have relatively good hydrostatic piezoelectric constants. First attempts to fabricate composites with 1-3 connectivity were developed by Klicker et al. [33] by incorporating PZT rods in porous polyurethane matrix. Lynn et al. [34] also developed these types of composites by incorporating PZT rods in different types of polymer matrices. Since the high Poisson ratio of the polymer plays a negative role in the piezo properties of the composites, porous polymer matrices are used for the fabrication of 1-3 types composites. Fabrication of these types of composites is not easy and a recent study shows that the PZT particles can align in one dimension by dielectrophoresis (DEP) by applying an electric field to a composite incorporated with PZT particle [35].

1.5. Fabrication process

Piezoceramic materials are available in a large variety of shapes and forms. Consequently, these materials are manufactured in many different ways: sputtering, metal organic chemical vapor deposition (MOCVD), chemical solution deposition (CSD), the sol gel method and pulsed laser deposition (PLD) which is a physical method by thermal evaporation. These new technologies all techniques have (large) drawbacks. The MOCVD process has a fundamental drawback, in that the stable delivery of metal-organic precursors is difficult to achieve with conventional bubbler technology, because of the lack of suitable precursors. Moreover, precursors tent to degrade at elevated temperatures and vapor pressure in the bubbler varies with time, and therefore constant delivery is hard to achieve. The CSD method has the disadvantage that it can not be utilized for high density memory devices because the substrate must undergo the planarization process in order to spin-coat ferroelectric films. In sol-gel methods cracks are liable to occur in the post-annealing process when the thickness of the PZT film is larger than several hundred of angstroms. Therefore, forming many thin layers of film is usually done in order to prevent cracks. However, many time repetition of spin coating, pre-baking and post-annealing is time consuming and also increases the probability of contamination [36-40].

PLD technique is the most popular and powerful one in terms of stoichiometric transfer from the multi component oxide target to the growing film and its easy applications of PZT material. However, PLD has shortcomings too, in particular the

oxygen content in the deposited layer may differ from that of the target and sometimes large entities are deposited, leading to a particulate nature of the films realized. The size of these particulates may be as large as few micrometers. Such particulates will greatly affect the growth of the subsequent layers as well as the electrical properties of the films, which can be detrimental for PZT material [41, 42].

The traditional PZT production process consists of several steps (see Figure 8). The first step is where the lead, zirconium and titanium oxides powders are weight in their appropriate amounts and mechanically mixed. Usually, a few modifying or stabilizing agents are added, *e.g.* manganese, calcium, antimony and niobium oxides. The mixture is mechanically activated by dry or wet milling in a planetary ball mill. Under high shear rotation with several balls a certain homogeneous mixture and particle size is obtained and also aggregations are eliminated. Often a liquid or dispersing agent (wet milling) is added to obtain a slurry. When a slurry is added, the mixture is dried and fragmented into small pieces.

In the next step, the mixture is reacted in a calcining step at elevated temperatures (*T* varies from 800-1000 °C), where the oxides react to form the perovskite. The activated material is then pressed into pellets or remains as powder form and is sintered at temperatures exhibiting the perovskite structure, usually for 1-4 hours at approximately 1100-1300 °C in air. This step is to densificate the mixture. Hereafter a poling step is performed or can be postponed when making a composite.

| Ball-mixed raw material with solvent | Drying | Calcination and sintering | Electroding and poling |

Figure 8*. Manufacturing process of PZT.*

A piezoelectric composite, incorporation of a piezoelectric-ceramic in a polymer, takes the advantage of the flexibility of a polymer and the piezoelectric effect and rigidity of the piezoelectric-ceramics. Main advantage on these materials is the ease of formability / flexibility into any shape. Moreover, this can also reduce the cost of the material. Conventionally, piezocomposites are fabricated by two ways; solid- and liquid- phase processes. Solid-phase processes usually involve mechanical approaches

like direct compounding and melt compounding. Liquid-phase processes involve solvent assisted dispersion of the piezo-material in the polymer monomer followed by in-situ polymerization processes [17].

The major ingredient in PZT is lead oxide, which is a hazardous material with a relatively high vapor pressure at calcining temperatures. Consequently, last decades PZT also attracted attention from an environmental perspective. Concerns about the lead compound in PZT, which can during calcination and sintering release volatiles causing pollution. More concern is about the recycling and disposal of devices containing PZT, especially those used in consumers products. Extensive effort in research has been made to arrive with alternatives for PZT, which do not contain lead such as $BaTiO_3$, $Na_{0.5}Bi0.5TiO_3$, $K_{0.5}Bi_{0.5}TiO_3$, $Na_{0.5}K_{0.5}NbO_3$ and many more [43-48]. However, till today, none of the alternatives encounters better performance as compared to PZT for ferroelectric and piezoelectric properties (converting very efficient electrical energy into mechanical energy or vice versa).

1.6. Theory

Various theoretical models have been proposed for the permittivity and piezoelectric properties of the 0-3 composites. Some of the mostly used analytic expressions are briefly discussed here. For a brief review we refer to [49] while [50] provides an extensive discussion. One of the first, if not the first, model for understanding the dielectric behavior of composites, still widely used, was given in 1904 by Maxwell Garnett [50]. In this model spherical inclusions are embedded in a polymer matrix without any kind of interaction resulting in:

$$\varepsilon = \varepsilon_P \{1 + [3\phi_c (\varepsilon_c - \varepsilon_P/\varepsilon_c + 2\varepsilon_c)] / [1 - \phi_c (\varepsilon_c - \varepsilon_P/\varepsilon_c + 2\varepsilon_c)]\} \qquad (2)$$

where ϕ_c is the volume fraction of the inclusions and ε, ε_c and ε_P are the relative permittivity of the composite, ceramic particles and matrix, respectively. Lichtenecker [51] provided in 1923 a rule of mixtures, also still widely used, that reads:

$$\varepsilon = \varepsilon_c^{\varphi_c} \varepsilon_p^{1-\varphi_c} \qquad (3)$$

Although initially largely empirical, in 1998 Zakri et al. [52] provided a theoretical underpinning of this rule.

In 1982 Yamada et al. [22] proposed a model to explain the behavior of the permittivity, piezoelectric constant and elastic constant of a composite in which ellipsoidal particles are dispersed in a continuous medium aligned along the electric

field. Their model shows excellent agreement with experimental data of PVDF-PZT composites. Their final equations read:

$$\varepsilon = \varepsilon_p \left[1 + \frac{n\varphi_c(\varepsilon_c - \varepsilon_p)}{n\varepsilon_p + (\varepsilon_c - \varepsilon_p)(1 - \varphi_c)} \right] \qquad (4)$$

$$d = \alpha_p \varphi_c G d_c \qquad (5)$$

$$E = E_p \left[1 + \frac{\varphi_c(E_c - E_p)}{E_p + n'(E_c - E_p)(1 - \varphi_c)} \right] \quad \text{with} \quad n' = \frac{1 + \nu_p}{3(1 - \nu_p)} \qquad (6)$$

where $n = 4\pi/m$ is the parameter attributed to the shape of the ellipsoidal particles. Further, α is the poling ratio, $G = n\varepsilon / [n\varepsilon + (\varepsilon - \varepsilon)]$ is the local field coefficient and d_c is the piezoelectric constant of the piezoceramic while d is the piezoelectric constant of the composite. Finally the elastic modulus E contains, apart from the above mentioned quantities, a factor n' directly calculated from Poisson's ratio ν_p of the matrix. The condition that the particles are considered to be oriented ellipsoids might seem to be a significant restriction but it has been shown [52] that composites with an arbitrary distribution of ellipsoids with respect to the electric field direction can be transformed in to an equivalent composite with ellipsoids aligned along the electric field direction but with different aspect ratio's for the ellipsoids. This largely removes the restriction mentioned, although the interpretation in micro structural terms becomes more complex.

Another model relatively simple model for the permittivity was provided by Jayasundere et al. [53]. The final expression reading:

$$\varepsilon = \frac{\varepsilon_p \varphi_p + \varepsilon_c \varphi_c [3\varepsilon_p/(\varepsilon_c + 2\varepsilon_p)][1 + 3\varphi_c(\varepsilon_c - \varepsilon_p)/(\varepsilon_c + 2\varepsilon_p)]}{\varphi_p + 3\varphi_c \varepsilon_p /(\varepsilon_c + 2\varepsilon_p)[1 + 3\varphi_p(\varepsilon_c - \varepsilon_p)/(\varepsilon_c + 2\varepsilon_p)]} \qquad (7)$$

is a modification of the expression for a composite dielectric sphere by including interactions between neighboring spheres.

Many other models resulting in analytical expressions have been proposed. We mention here only the models by Furukawa et al. [23], Bruggeman et al. [54], Maxwell-Wagner [49], Bhimasankaram et al. [49] and Wong et al. [55]. Most models deal only with part of the full piezoelectric problem and only partially combined solutions were given. e.g. based on the Bruggeman method [54, 56], taking permittivity and conductivity into account, or based on the Marutake method [57], taking permittivity piezoelectric coefficients and elastic compliance into account. The

latter already requires numerical solution. Recently complete numerical solutions to the fully coupled piezoelectric equations for ellipsoidal inclusions of the same orientation have been provided [58] predicting giant piezoelectric and dielectric enhancement. No experimental evidence for this effect was presented though while a significant conductivity is required rendering the options for practical applications probably less useful.

1.7. Purpose of the research

Piezoelectric composites with 0-3 connectivity have several unique properties and have been widely utilized in a large number of sensor and transducer applications. Due to the continued and increased demands for an enormous wide field of applications, extensive research has been carried out in recent years. This leads to the development of new piezoelectric materials and processing technologies. In general, the performance of these composite materials is optimized depending on specific applications. These composite systems have several advantages: their ease of production, their ability for the properties to be tailored by varying the volume fraction of the ceramic inclusions and the ease of obtaining different sizes and shapes and excellent high temperature stability. However, in spite of the developments throughout the years, the need for highly flexible, soft and thin composites having excellent piezoelectric properties have not been fulfilled yet and this limit the usefulness of the composite materials for potential soft-touch applications. The development and characterization of novel piezoelectric composites may overcome this limitation and has potential applications in the fields of fundamental as well as applied research and opens new ways to 'soft touch' applications in a variety of transducer and sensor applications.

The general aim of this research is to design and fabricate fairly flexible composites with high permittivity and piezoelectric charge constant for transducer and sensors applications. In this research, we have developed novel single-piezo layer (unimorph) and double-piezo layer (bimorph) 0-3 piezoelectric composites. The functional and mechanical properties of these composites were quantified using experimental and theoretical methods. We also investigated the feasibility of fabricating these novel composites in the form of films and the reliability of laminated films. The correlation of the chemistry of matrix material to the adhesion of the PZT particles in the matrix and the resulting properties were also studied.

The novel composites developed in this study possess the ability to attain various sizes and shapes, each with high flexibility and combined with good functional properties. Furthermore, we report for the first time on the enhancement of electromechanical properties by incorporating nano-size conductive fillers like carbon

nano tubes and carbon black into composite matrix. The newly developed bimorphs have several advantages in terms of ease of fabrication, tailoring the properties and low price and renders as a useful alternative for high temperature applications. The excellent properties and the relatively simple fabrication procedure of different unimorph and bimorph composites developed in this research make them promising candidates in piezoelectric sensors, actuators and high efficiency capacitors.

1.8. Outline of the thesis

Chapter 2 describes the processing and characterization of new series of fairly flexible 0-3 PZT/LCT/PA (Lead Zirconate Titanate $Pb(Zr_{1-x}Ti_x)O_3$/Liquid crystalline thermotropic/Polyamide) piezoelectric composites with high permittivity and piezoelectric charge constant by incorporating PZT5A4 into a matrix of LCT and polyamide (PA11). For comparison PZT/PA composites were studied. Commercially available PZT powder was calcined at different temperatures for the optimization of the composite properties. The phase transition during calcination of the powder was studied by X-ray diffraction and the particle size by light scattering and scanning electron microscopy. The experimental results for relative permittivity ε_r, piezoelectric charge constant d_{33}, piezoelectric voltage coefficient g_{33} obtained for these composites were compared with several theoretical models (Jayasundere, Yamada and Lichtenecker).

   Chapter 3 describes realization of highly flexible piezoelectric composites with 0-3 connectivity, with filler volume fractions up to 50 vol. % and having no pores. Composites were fabricated by solution casting of dispersions of $(Pb(Zr_xTi_{1-x})O_3$ (PZT) in poly-(dimethylsiloxane) (PDMS). The electrical, dielectrical and mechanical properties were investigated as a function of ceramic volume fraction and frequency. The experimental results were compared with theoretical models (Yamada and Jayasundere). These PZT/PDMS composites offer the advantage of high flexibility in comparison with other 0-3 composites, even with 50 vol. % PZT. These composites possess the ability to attain various sizes and shapes, each with high flexibility due to the exceptional elastic behavior of PDMS, combined with good functional properties. The high flexibility combined with excellent properties of these composites opens new ways to 'soft touch' applications in a variety of transducer and sensor applications.

   Chapter 4 reports on the enhancement of electromechanical properties of 0-3 PZT/PDMS composites incorporated with nano-size conductive fillers like carbon nano tubes (CNT) and carbon black (CB). Highly flexible piezoelectric 0-3 PZT/PDMS (lead zirconate titanate - poly dimethyl siloxane) composites incorporated with carbon

nanotubes (CNT) and carbon black (CB) were fabricated by solution casting technique using a constant PZT/PDMS ratio of 40/60 and conductive fillers ranging from 0 to 0.5 vol.%. The electromechanical properties and the characterization of the composites were studied as a function of the volume fraction and frequency. In this study we realized a simple fabrication procedure for highly dense piezoelectric composites containing CNTs and CB with a combination of high dielectric constant and low dielectric loss. The excellent (di-)electrical properties and the relatively simple fabrication procedure of these composites make them promising candidates in piezoelectric sensors, actuators and high efficiency capacitors.

Chapter 5 describes design, fabrication and performance analysis of two new disc-type composite bimorphs with series connection by compression molding (PZT/PA-rigid) and solution casting (PZT/PDMS-flexible) technique. The bimorph consists of two circular piezoelectric disks, which are separated by a metal plate aluminium, which act as central electrode and also as reinforcement. We have used two types of composites, PZT/PA and PZT/PDMS, both using lead zirconate titanate (PZT) as piezoelectric filler and the matrix consisted of polyamide (PA) and poly dimethyl siloxane (PDMS). Electric force microscopy (EFM) is used to study the structural characterization and the piezoelectric properties of the materials realized. The newly developed bimorphs have several advantages in terms of ease of fabrication, tailoring the properties and low price. The absence of any bonding agent in the fabrication process renders these bimorphs a useful alternative for high temperature applications.

Chapter 6 describes the contribution of the electric field dependence of the strain, i.e. dx/dE, to the experimentally determined d_{33} due to the mechanical load is applied to realize proper measurements of the piezoelectric charge constant d_{33} of materials. The samples were characterized with respect to their piezoelectric properties in terms of a static preload, imposing a varying load and constant frequency of 110 Hz using a d_{33} meter. We used 0-3 composites (PZT/LCT/PA, PZT/PA and PZT/PDMS) and compared measurements as a function of load for these materials with ceramic reference samples (PZT disks). While for stiff reference materials this contribution is small, ~ 1.5%, for the compliant composite materials it is about 15%. Hence for an accurate determination of the *d*-value the experimental data extrapolated to load zero. Since equipment to measure the d_{33} is conventionally used for stiff, ceramic-like materials and the expected load dependence for polymer matrix piezo-composites is expected to larger than for ceramics, a study on the load dependence of d_{33} for polymer matrix composites was done.

Finally, *chapter 7* describes a summary of the results of this research project and discusses the future applications and potentials of the results described in this thesis.

References

[1]   B. Jaffe, W.R. Cook and H. Jaffe, Piezoelectric ceramics, New York, 1971, p. 49-50.

[2]   G.W. Taylor, Piezoelectricity, New York, 1985, p. 3-5.

[3]   G. Gautschi, Piezoelectric Sensorics, Germany, 2002, p. 5-7.

[4]   N. Setter, Piezoelectric materials in devices, Switzerland, 2002, p. 29-30.

[5]   M.S. Vijaya, Piezoelectric materials and devices, New York, 2013, p. 39-40.

[6]   W. Wersing, M. Schnoller and H. Wahl, Ferroelectrics, 68, 1986, p. 145-156.

[7]   Z.M. Dang, Y.H. Lin, C.W. Nan, Adv Mater, 2003, 15, 1525-9.

[8]   R. Newnham, L.J. Bowen, K. Klicker and L.E. Cross, Material Engineering, 1980, 2, 93-9.

[9]   K. Uchino, Piezoelectric actuators and ultrasonic motors, USA, 1997, p. 2-20.

[10]   J. Lu, K.S. Moon, J. Xu, C.P. Wong, J. Mater Chem, 2006, 16, 1543-8.

[11]   P. Muralt, J. Micromech. microeng., 2000, p. 136-146.

[12]   C.Z. Rosen, B.V. Hiremath and R.E. Newnham, Piezoelectricity, New York, 1992, p. 10-15.

[13]   H. Nalwa, Ferroelectric polymers, New York, 1995, p. 13-15

[14]   M.R. Kermani, Applied vibration suppression using piezoelectric materials, USA, 2008, p. 5-7.

[15]   IEEE standard on piezoelectricity, IEEE Ultrasonics, Ferroelectrics, and Frequency Control Society, USA, 1987, p. 21-22.

[16]   R.E. Newnham, D.P. Skinner and L.E. Cross, Mat. Res. Bull. 1978, 13, p. 525-536.

[17]   Z.M. Dang, J.K. Yuan, J.W. Zha, T. Zhou, S.T. Li and G.H. Hu, Progress in materials Science, 2012, 57, 660-723.

[18]   J.F. Tressler, S. Alkoy, A. Dogan, R.E. Newnham, Composites Part A: Applied Science and Manufacturing, 1999, 30, p. 477-482.

[19]   C.Z. Rosen, B.V. Hiremath and R.E. Newnham, Piezoelectricity, New York, 1992, p. 195-204.

[20]   H. Banno, Ferroelectrics, 1983, 50, p. 3-12.

[21]   A. Safari, G. Sa-gong, J. Giniewicz and R.E. Newnham, Proceedings of the 21st university conference on ceramic sciences, 1986, 20, 445-454.

[22]   T. Yamada, T. Udea and T. Kitayama, J. Appl. Phys., 1982, 53, p. 4328-4332.

[23]   T. Furukawa, K. Ishida and E. Fukada, J. Appl. Phys., 1979, 50, p. 4904-4912.

[24]   T. Bhimasankaran, S.V. Suryanarayana and G. Prasad, Cur. Sci. 74, 1998, 11, p. 967-976.

[25]   E. Venkatragavaraj, B. Satish, P.R. Vinod, M.S. Vijaya, J. Phys. D: Appl. Phys. 2001, 34, p. 487.

[26]   D. Khastgir, K. Adachi, J. Polym. Sci., Part B: Polym. Phys. 1999, 37, p. 3065.

[27]   W.K. Sakamoto, E.d. Souza and D.K. Das-Gupta, Materials Research 2001, 4, p. 201-204

[28]   G. Rujijanagul, S. Boonyakul and T. Tunkasiri, J. mater. Sci. Ltrs, 2001, 20, p. 1943-1945.

[29]   B. Satish, K. Sridevi and M.S. Vijaya, J. Phys. D: Appl. Phys., 2002, 35, p. 2048–2050.

[30]   D.A. van den Ende, P de Almeida and S. van der Zwaag, J. Mater. Sci., 2007, 42, p. 6417-6425.

[31]   I. Babu, D. A. v. d. Ende, G. de. With, J. Phys. D: Appl. Phys. 2010, 43, 425402.

[32]   I. Babu and G. de. With, Composites Science and Technology. 2013; Submitted.

[33]   K.A. Klicker, J.V. Biggers and R.E. Newnham, J. Am. Ceram. Soc., 1982, 64:5.

[34]   S.Y. Lynn, R. E. Newnham, K. A. Klicker, K. Rittenmyer, A. Safari and W. A. Schulze, 1983, Ferroelectrics, 1981, 38, p. 955-958.

[35]   D. A. van den Ende, S. E. van Kempen, X. Wu, W. A. Groen, C. A. Randall, and S. van der Zwaag, J. Appl. Phys. 2012, 111, 124107.

[36]   S. B. Krupanidhi, N. Maffei, M. Sayer, and K. El-Assal, J. Appl. Phys. 1983, 54, 6601-09.

[37]   M. Toyama, R. Kubo, E. Takata, K. Tanaka, K. Ohwada, Sensors and Actuators A: Physical, 1994, 45, 2, 125–129.

[38]   S. Jeong, J. Shi-Zhao, H.R. Kim, D.Y. Park, C. S. Hwang, Y. K. Han, C. H. Yang, K. Y. Oh, S. H. Kim, D.S. Lee and J. Ha, J. Electrochem. Soc. 2003, 150, 10, C678-C687.

[39]   J.S. Zhao, D.Y. Park, M. J. Seo, C. S. Hwang, Y. K. Han, C. H. Yang and K. Y. Oh J. Electrochem. Soc. 2004 151(5): C283-C291.

[40]   Y. Sakashita, T. Ono, H. Segawa, K. Tominaga, and M. Okada, J. Appl. Phys. 1991, **69**, 8352.

[41]   G. Yi, Z. Wu, and M. Sayer, J. Appl. Phys. 1988, **64**, 2717.

[42]   K. W. Seo, S. H. Cho, S.H. Lee, Korean Journal of Chemical Engineering, 2001, 18, Issue 1, pp 75-80.

[43]   D. Damjancovic, N. Klein, J. Li, V. Porokhonskyy, 2010, Functional Materials Letters, 3, 5-13.

[44]   M. Demartin Maeder, D. Damjanovic, N. Setter, 2004, Journal of Electroceramics, 13, 385-392.

[45]   D. Xiao, D. Lin, J. Zhu, P. Yu, 2008, Journal of Electroceramics, 21, 34-38.

[46]   E.A. Gurdal, S.O. Ural, H.-Y. Park, S. Nahm, K. Uchino, 2011, The Japan Society of Applied Physics, 50, 027101.

[47]   E. Aksel, J.L. Jones, 2010, Sensors, 10, 1935-1954.

[48]   H. Li, W.-H. Shih, W.Y. Shih, 1993, Journal of the American Ceramic Society, 1852-1855.

[49]   S. Firmino Mendes, C.M. Costa, V. Sencadas, J. Serrado Nunes, P. Costa, R. Gregorio jr., S. Lanceros-Méndez, *J. Appl. Phys. A*, 2009, 96, p. 899-908.

[50]   A. Sihvola, *Electromagnetic mixing formulas and applications*, 1999, London, p. 166-167.

[51]   K. Lichtenecker, *Physikalische Zeitschrift*, 1926, 27, p. 115-158.

[52]   T. Zakri, J.P. Laurent and M.J. Vauclin, *j. Phys. D: Appl. Phys., 1998,* 31, p. 1589-1594.

[53]   N. Jayasundere and B.V. Smith, *J. Appl. Phys.*, 1993, 5, p. 2462-2466

[54]   D.A.G. Bruggeman, *Ann. Physik*, 1935, 24, p. 636-664.

[55]   C.K. Wong, Y. M. Poon, F.G. Shin, *J. Appl. Phys.*, 2001, 90, p. 4690-4700.

[56]   J.A. Reynolds and J.M. Hough, *Proc. Phys Soc.*, 1957, London, B70, p. 769-774.

[57]   M. Marutake, *J. Phys Soc. Japan*, 1956, 11, p. 807-814.

[58]   A.V. Turik, A.I. Chernobabov, G.S. Radchenko and S.A. Turik, *Physics of the Solid State*, 2004, 46, p. 2213-2216.

Chapter 2

Processing and characterization of piezoelectric 0-3 PZT/LCT/PA composites*

PZT/LCT/PA (Lead Zirconate Titanate $Pb(Zr_{1-x}Ti_x)O_3$/Liquid crystalline thermotropic/Polyamide) composites of 0-3 connectivity were fabricated by hot-pressing. Commercially available PZT powder was calcined at different temperatures for the optimization of the composite properties. The phase transition during calcination of the powder was studied by X-ray diffraction and the particle size by light scattering and scanning electron microscopy. The relative permittivity ε_r, piezoelectric charge constant d_{33}, conductivity σ and elastic modulus E of the composites were found to increase with increasing ceramic volume fraction ϕ. The obtained d_{33} and g_{33} values of this newly developed PZT/LCT/PA composite with 50 volume percent PZT using a low poling voltage of 60 kV/cm and poling time of 30 minutes are 42 pC/N and 65 mVm/N, respectively, which are high values for this volume fraction in comparison with the other 0-3 composites reported. Good agreement was found between the experimental data of relative permittivity and piezoelectric constants with several theoretical models (Jayasundere, Yamada and Lichtenecker) of 0-3 composites. In order to assess the correlation of the experimental data with the theoretical models, the experimental data obtained from PZT/PA composites were also included.

2.1. Introduction

Sensors and actuators based on piezoelectric ceramic-polymer composites, so-called smart materials, offer a high potential for high tech systems. These composite materials provide superior overall performance over conventional pure ceramics in having good elastic compliance while maintaining good durability. Usually they are optimized for special applications and the demand for these materials has led to extensive research during the past three decades [1-4]. One of the most used piezoceramics in these types of composites is lead zirconate titanate $Pb(Zr_{1-x}Ti_x)O_3$ (PZT) which is a typical piezoelectric material having the perovskite crystal structure. PZT shows excellent electromechanical piezoelectric properties at the morphotropic phase boundary due to the coexistence of the tetragonal and rhombohedral phases and its properties are influenced by the variation in composition [5].

The types and number of phases, composition, and connectivity of the individual phases determine the properties of the composites. Newnham et al. [6] introduced the concept of 0-3 connectivity (a three dimensionally-connected polymer matrix filled with ceramic particles) for the classification of composites. Polymer composites with 0-3 connectivity have several advantages over other types of composites: their ease of production, their ability for the properties to be tailored by varying the volume fraction of the ceramic inclusions and the ease of obtaining different sizes and shapes.

Recently, a number of articles were published on 0-3 composites showing an increased demand on this type of composites [7-10]. The recently developed PZT/ liquid crystalline thermotropic (LCT) [11] composites by van den Ende et al. [12] showed excellent high temperature stability. However, although these composites are more flexible than PZT ceramics, they are rather brittle, limiting their potential applications. To overcome this limitation and be able to realize fairly flexible composites with high permittivity and piezoelectric charge constant, we developed a new series of 0-3 piezoelectric composites (PZT/LCT/PA) by incorporating PZT5A4 into a matrix of LCT and polyamide (PA11).

In this chapter we report on the processing and characterization of these new 0-3 piezoelectric composites. Hot-pressing was utilized for the fabrication and the effect of the volume fraction of PZT on the composite properties was studied. For comparison also PZT/PA composites were studied. A comparison of the experimental results for relative permittivity ε_r, piezoelectric charge constant d_{33}, piezoelectric voltage coefficient g_{33} obtained for these composites with several theoretical models were made.

2.2. Experimental

2.2.1. Materials

The PZT powder used in this research is a half-product of the commercial PZT ceramic PZT5A4 (Morgan Electro Ceramics, Ruabon UK), a soft PZT with 1 mol% Nb added as dopant. The LCT polymer used are phenylethynyl end-capped oligomers based on 6-hydroxy-2-naphthoic acid (HNA) and 4-hydroxybenzoic acid (HBA) (M_n = 9000 g mol^{-1}, HBA/HNA ratio of 73/27), obtained from TU Delft. The amide was PA11, obtained from Aldrich Chemical Company (T_g = 46 °C, T_m = 198 °C). The PZT powder was calcined at different temperatures (Table 1) with a heating rate of 3 °C/min and a 60 minute hold at the required temperature and cooling to room temperature with a temperature ramp of 3 °C/min. Per calcination temperature 20 gram PZT powder was used in an alumina crucible covered with an alumina lid.

2.2.2. Fabrication of composites

Two types of composites were fabricated. PZT/PA composites were made in order to optimize the calcination temperature and to correlate the theoretical results with PZT/LCT/PA composites. PZT/LCT/PA composites were made with the optimized PZT. Temperatures in the range of 800 to 1300 °C were utilized for optimization.

In order to optimize the calcination temperature, PZT/PA composites were fabricated with 40 volume percent calcined PZT at different temperatures and 60 volume percent PA11. For the correlation of the results with PZT/LCT/PA composites, PZT/PA composites were fabricated with five different volume percent of PZT. The raw materials were initially mixed by hand with a spatula at room temperature and further ball milled for 60 minutes at 800 rpm. Composites with specific dimensions of 14 mm in diameter and 280-300 μm thickness were fabricated by hot-pressing with an applied force of 90 kN.

Figure 1 shows the various PZT/LCT/PA composites fabricated. The corresponding volume percent of PZT and LCT were premixed in an aluminum boat by hand with spatula. This aluminum boat was placed on a hot plate at 285 °C and thoroughly mixed with a glass rod until all the LCT was molten. After reaching room temperature, the PA powder was added and mixed well. The above mixture was powdered with a pestle and mortar and thereafter subjected to ball-milling for 60 minutes at 800 rpm. Composites with specific dimensions of 14 mm in diameter and 300-375 μm thickness were fabricated by hot-pressing with an applied force of 90 kN.

The LCT was allowed to melt at 280 °C for 30 min and after that the temperature was increased to 320 °C and kept at that temperature for 30 min for curing the LCT. Circular gold electrodes of thickness 300 nm and an area of $7.85 \times 10^{-5} \, m^2$ are sputtered on both sides of the composites using an Edwards sputter coater (model S150B). The poling of the electroded sample is performed by applying an electric field of 60 kV/cm with a Heinziger 10 kV high voltage generator for 30 min at 100 °C (PZT/PA) and 120 °C (PZT/LCT/PA) in a silicone oil bath to ensure uniform heating. The electric field was kept on while cooling to room temperature.
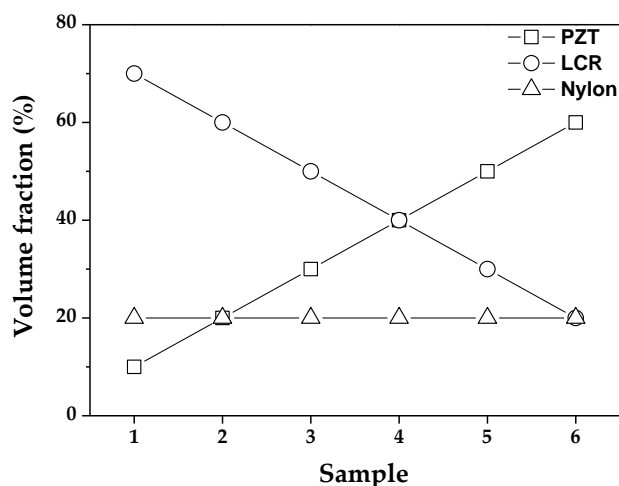

Figure 1. *Volume fraction of PZT/LCT/PA composites fabricated with PZT calcined at 1100 °C.*

2.2.3. Measurements

The phase identification was done at room temperature with an X-ray diffractometer (Rigaku) with CuKα radiation of wavelength 0.15418 nm. The diffraction spectra were recorded in the 2θ range of 10-80° with a step size of 0.01° and a scanning speed of 0.4°/minute. The microstructure of the calcined PZT powder and the composites were examined by SEM (FEI, Quanta 3D FEG). The particle size of the calcined powders was determined by light scattering (Beckman Coulter LS230) and also by SEM. The aspect ratio of the particles was estimated by Image J software [15] on the SEM pictures of the calcined and milled powder.

In order to calculate the ac conductivity σ, relative permittivity ε_r and the loss tangent $\tan \delta$ of the composites, impedance data were collected by an impedance analyzer (EG&G Princeton Applied Research, Model 1025) coupled with a potentiostat (Potentiostat/Galvanostat, Model 283) at room temperature in a frequency range of 50 Hz – 5 MHz. The dc conductivity (Table 2) is measured as follows. The electrical current was provided by a source measure unit Keithley 237 while the voltage was measured

by an electrometer Keithley 6517A. The piezoelectric charge constant d_{33} was measured with a d_{33} meter (Piezotest, PM300) at a fixed frequency of 110 Hz. The d_{33} and ε_r obtained at 110 Hz is used to calculate piezoelectric voltage coefficient g_{33} according to

$$g_{33} = d_{33} / \varepsilon_o \, \varepsilon_r \qquad (1)$$

where d_{33} is the piezoelectric charge constant in pC/N, ε_o is the permittivity of free space (8.85×10^{-12} F/m) and ε_r is the relative permittivity of the composite. The elastic moduli of the composites were tested in three-point bending in static mode on a TA Instruments Q800 series DMA at room temperature. The dimensions of the specimens tested were 20 mm x 10 mm x 2 mm and for each composition two specimens were measured.

2.3. Theory

Various theoretical models have been proposed for the permittivity and piezoelectric properties of the 0-3 composites. Some of the mostly used analytic expressions are briefly discussed here. For a brief review we refer to [20] while [24] provides an extensive discussion.

One of the first, if not the first, model for understanding the dielectric behavior of composites, still widely used, was given in 1904 by Maxwell Garnett [24]. In his model spherical inclusions are embedded in a polymer matrix without any kind of interaction resulting in

$$\varepsilon = \varepsilon_p \{1 + [\, 3\phi_c \, (\varepsilon_c - \varepsilon_p / \varepsilon_c + 2\varepsilon_c)] \, / \, [1 - \phi_c \, (\varepsilon_c - \varepsilon_p / \varepsilon_c + 2\varepsilon_c)]\} \quad (2)$$

where ϕ_c is the volume fraction of the inclusions and $\varepsilon, \varepsilon_c$ and ε_p are the relative permittivity of the composite, ceramic particles and matrix, respectively. Lichtenecker provided in 1923 a rule of mixtures, also still widely used, that reads

$$\varepsilon = \varepsilon_c^{\varphi_c} \varepsilon_p^{1-\varphi_c} \qquad (3)$$

Although initially largely empirical, in 1998 Zakri et al. [26] provided a theoretical underpinning of this rule.

In 1982 Yamada et al. [18] proposed a model to explain the behavior of the permittivity, piezoelectric constant and elastic constant of a composite in which ellipsoidal particles are dispersed in a continuous medium aligned along the electric field. Their model shows excellent agreement with experimental data of PVDF-PZT composites. Their final equations read

$$\varepsilon = \varepsilon_p \left[1 + \frac{n\varphi_c(\varepsilon_c - \varepsilon_p)}{n\varepsilon_p + (\varepsilon_c - \varepsilon_p)(1-\varphi_c)} \right] \qquad (4)$$

$$d = \alpha_p \varphi_c G d_c \qquad (5)$$

$$E = E_p \left[1 + \frac{\varphi_c(E_c - E_p)}{E_p + n'(E_c - E_p)(1-\varphi_c)} \right] \quad \text{with} \quad n' = \frac{1+\nu_p}{3(1-\nu_p)} \qquad (6)$$

where $n = 4\pi/m$ is the parameter attributed to the shape of the ellipsoidal particles. Further, α is the poling ratio, $G = n\varepsilon/[n\varepsilon + (\varepsilon_c-\varepsilon)]$ is the local field coefficient and d_c is the piezoelectric constant of the piezoceramic while d is the piezoelectric constant of the composite. Finally the elastic modulus E contains, apart from the above mentioned quantities, a factor n' directly calculated from Poisson's ratio ν_p of the matrix. The condition that the particles are considered to be oriented ellipsoids might seem to be a significant restriction but it has been shown [26] that composites with an arbitrary distribution of ellipsoids with respect to the electric field direction can be transformed in to an equivalent composite with ellipsoids aligned along the electric field direction but with different aspect ratio's for the ellipsoids. This largely removes the restriction mentioned, although the interpretation in micro structural terms becomes more complex. Since their model also provides an expression for the elastic modulus, we have chosen this model mainly to analyze our experimental results.

Another model relatively simple model for the permittivity was provided by Jayasundere et al. [21]. The final expression reading

$$\varepsilon = \frac{\varepsilon_p\varphi_p + \varepsilon_c\varphi_c[3\varepsilon_p/(\varepsilon_c + 2\varepsilon_p)][1+3\varphi_c(\varepsilon_c - \varepsilon_p)/(\varepsilon_c + 2\varepsilon_p)]}{\varphi_p + 3\varphi_c\varepsilon_p/(\varepsilon_c + 2\varepsilon_p)[1+3\varphi_p(\varepsilon_c - \varepsilon_p)/(\varepsilon_c + 2\varepsilon_p)]} \qquad (7)$$

is a modification of the expression for a composite dielectric sphere by including interactions between neighboring spheres. The comparison with experimental data appeared to be excellent. Hence this model was applied as well.

Many other models resulting in analytical expressions have been proposed. We mention here only the models by Furukawa et al. [19], Bruggeman et al. [8], Maxwell-Wagner [22], Bhimasankaram et al. [20] and Wong et al. [27]. Most models deal only with part of the full piezoelectric problem and only partially combined solutions were given. E.g. based on the Bruggeman method [29, 30], taking permittivity and conductivity into account, or based on the Marutake method [31], taking

permittivity piezoelectric coefficients and elastic compliance into account. The latter already requires numerical solution. Recently complete numerical solutions to the fully coupled piezoelectric equations for ellipsoidal inclusions of the same orientation have been provided [28] predicting giant piezoelectric and dielectric enhancement. No experimental evidence for this effect was presented though while a significant conductivity is required rendering the options for practical applications probably less useful.

2. 4. Results and discussion

2.4.1. Optimization of PZT

X-ray diffraction

The XRD patterns of PZT5A4 powder before and after calcination at different temperatures (800 to 1300 °C) are shown in figure 2. The X-ray diffraction pattern of the PZT5A4 before calcination shows the coexistence of both rhombohedral (200)R and tetragonal phases [(002)T, (200)T] together with the presence of a pyrochlore phase. Calcination resulted in the disappearance of the rhombohedral perovskite structure and in the formation of peak splitting, indicating an increase of tetragonal distortion. The phenomenon of peak splitting and peaks shifting to higher angle with increasing calcination temperature was also reported in previous studies [13, 14].

As the calcination temperature increases, the intensity of the pyrochlore phase peaks decrease while the intensity of the tetragonal perovskite peaks increase. This indicates the transformation to almost single phase tetragonal PZT. The PZT calcined at 1100 °C shows a maximum intensity of the tetragonal perovskite peaks at (200)T and (211)T which indicates that at this temperature the material has become (XRD) single phase. From 1150 °C onwards, the peak height decreases as a result of lead loss and also the 2:1 ratio becomes more like 1:1. Zhang *et al.* reported that the shrinkage of the lattice is believed to result from loss of lead that creates some vacancies in the PZT lattice [14]. The optimal calcination temperature was found to be 1100 °C and PZT5A4 calcined at this temperature was used for composite fabrication.
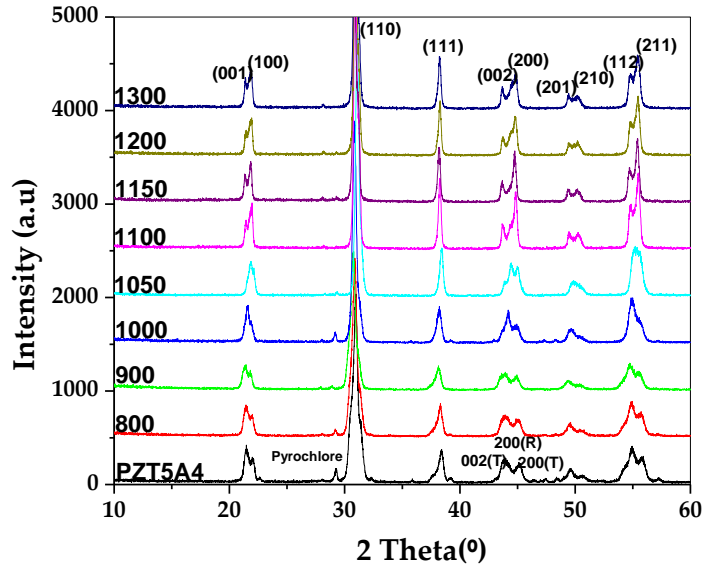
Figure 2. *XRD patterns of PZT5A4 at different calcination temperatures.*

Particle size analysis

The size of the particles was analyzed by both light scattering and by SEM. Table 1 illustrates the influence of different calcination temperatures on the particle size. The label d_{10}, d_{50} and d_{90} stands for the undersize percentage of the cumulative particle size distribution. The particles were also examined by SEM to get an average size of the individual particles. Comparing the particle size obtained from light scattering with SEM images indicates that the particles are agglomerates.

Table 1. *Particle sizes of calcined PZT5A4 as determined by light scattering.*

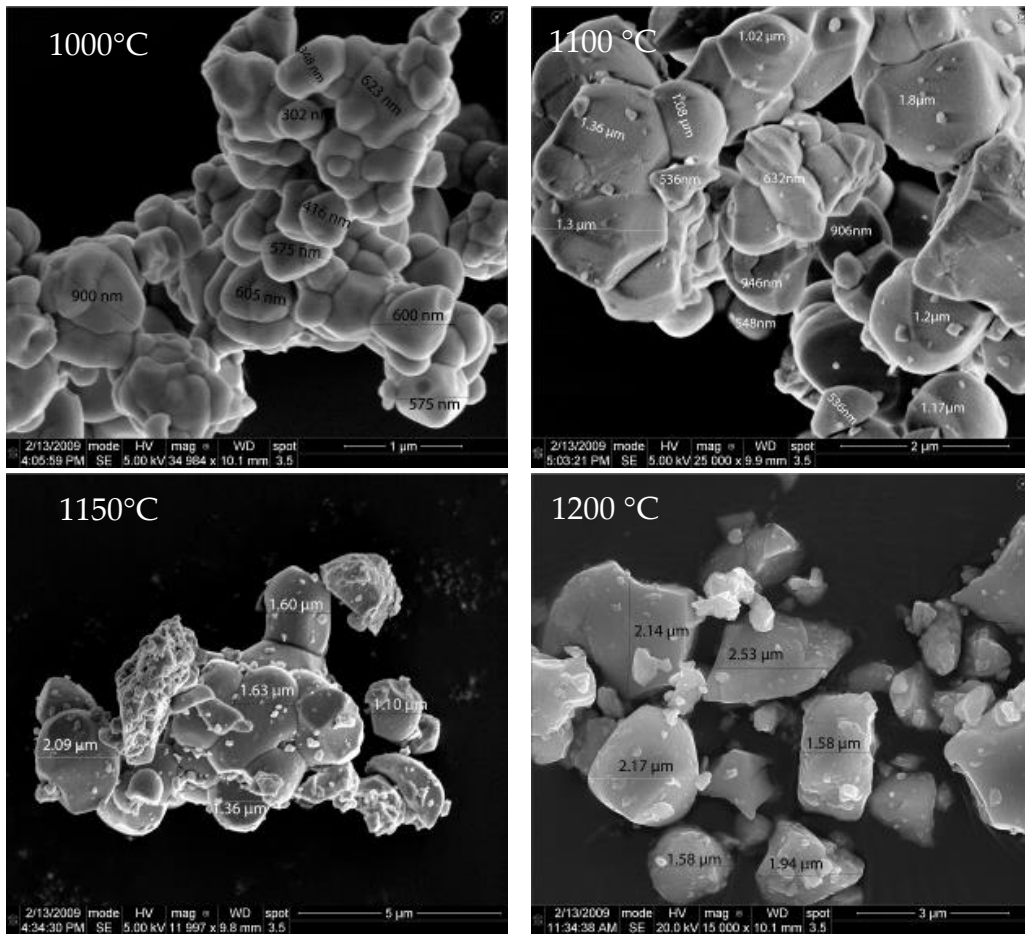| Calcination Temperature (°C)	d_{10} (μm)	d_{50} (μm)	d_{90} (μm)
PZT5A4 powder	0.23	1.47	3.4
800	0.88	1.78	3.74
900	1	1.94	3.98
1000	1.37	2.39	5.23
1050	1.25	2.16	4.17
1100	1.38	2.81	9.08
1150	1.51	3.56	11.07
1200	1.31	3.61	21.09
1300	0.71	3.61	17.39

Figure 3. *SEM micrographs of the PZT5A4 calcined at different temperatures.*

Figure 3 shows the SEM micrographs of the calcined PZT5A4 at different temperatures. From these micrographs it is observed that, as the calcination temperature increases, the grain size gradually increases, which implies that the particles sinter together during the calcination process. The approximate primary particle size in PZT5A4 calcined at 1000 °C is less than 600 nm, at 1100 °C the average size is about 1.0 μm and as the calcination temperature reaches to 1200 °C, the size of the primary particles becomes 2 to 2.5 μm. The aspect ratio of the particles was estimated by Image J software [15] on the SEM pictures of the calcined and milled powder. The number of particles per agglomerate can be estimated as about $(d_{50}/d_{SEM})^3$. For 1100 °C this yields $(2.8/1.0)^3 \cong 22$ primary particles which appears to be not an unreasonable number.

Impedance data

For the fabricated PZT/PA composites, the ac conductivity σ, relative permittivity ε_r, loss tangent $\tan\delta$, piezoelectric charge constant d_{33} and piezoelectric voltage constant g_{33} were determined. Figure 4 (a) and (b) show the dependence of σ, ε_r and $\tan\delta$ as a function of log frequency with increasing calcination temperature for the PZT/PA composites.
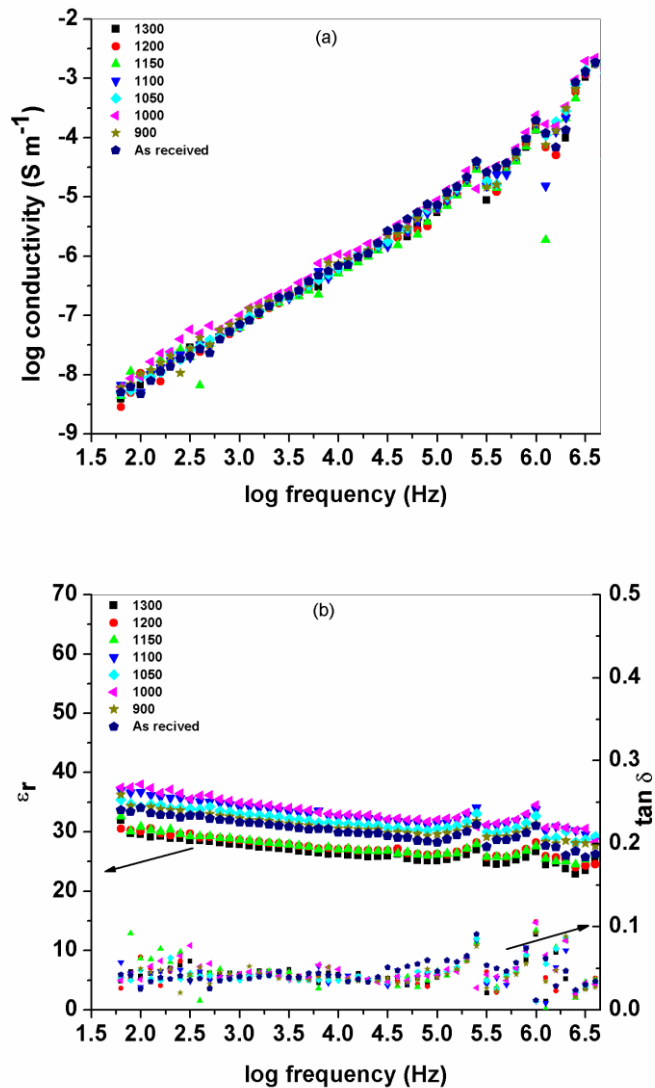
Figure 4 (a) and (b). *Dependence of σ, ε_r and $\tan\delta$ as a function of log frequency with increasing calcination temperature for the PZT/PA composites.*

From figure 4 (a) it is observed that the ac conductivity is the same for all calcination temperatures and equal to the value for the as-received PZT composite. From figure 4 (b) it is observed that the relative permittivity is in the range from 28 to 38 for the PZT calcined at different temperatures ranging from the as-received PZT

powder to the one calcined at 1300 °C. The maximum relative permittivity is observed at 1000 °C and 1100 °C. From 1200 °C, a small decrease in ε_r is observed which may be due to the loss of lead from PZT. The tan δ has a weak dependence on calcination temperature and is about 0.02 to 0.06 neglecting scattered points.

Piezoelectric charge and voltage constant

The dependence of d_{33} and g_{33} with increasing calcination temperature is shown in figure. 5. It is observed that the composite using PZT calcined at 1100 °C shows the maximum value of d_{33} and g_{33}. As the calcination temperature increases, a decrease in piezoelectric voltage coefficient is observed. Since ε_r is nearly constant up to 1150 °C and thereafter decreases but slightly, the g_{33} behavior mimics the d_{33} behavior closely. This may be due to the decrease in lead content, since the piezoelectric effect is highly dependent on the amount of lead in the PZT. From the above results it is clear that the best quality PZT powder is obtained with a calcination temperature of 1100 °C, consistent with the X-ray results on the PZT powder.

Figure 5. *The dependence of d_{33} and g_{33} of the PZT/PA composites on the PZT calcination temperature, measured at 110 Hz (lines drawn as guide to the eye).*

2.4.2 Fabrication of the PZT/LCT/PA composite with optimized PZT

Impedance data

Figure 6 (a) and (b) show the dependence of ac conductivity σ, permittivity ε_r and tan δ as a function of log frequency with increasing PZT volume fraction for the PZT/LCT/PA composites. From figure 6 (a) it is obser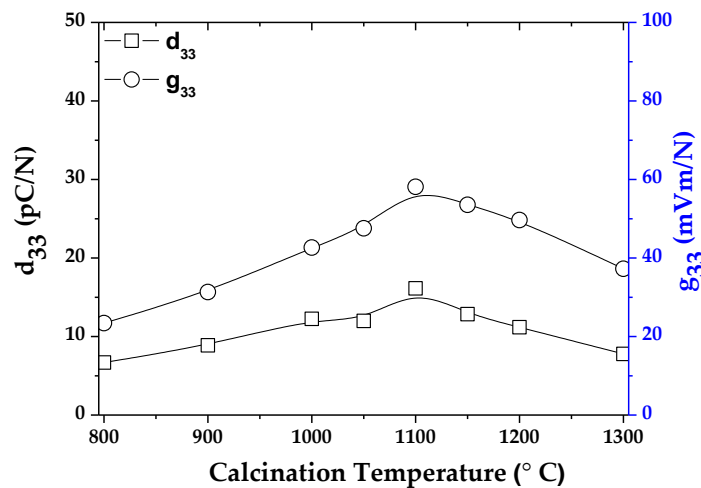ved that, as the volume percentage of PZT increases, the conductivity increases. Also an increase in ε_r is observed as the volume

percentage of PZT increases, due to the increasing contribution of the PZT. Because interface conductivity is usually higher then bulk conductivity, the increase in the conductivity with the increase in volume fraction of PZT is attributed to the increased contribution of interface conductivity, directly related to the increasing particle volume fraction.
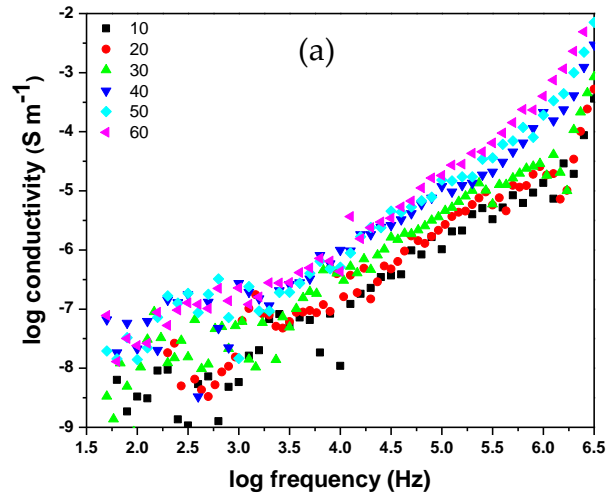

Figure 6 (a). *Dependence of σ as a function of log frequency with increasing PZT volume fraction for the PZT/LCT/PA composites.*

Since the particles in the composite are tightly packed with limited agglomeration and porosity, a homogeneous particle distribution results, even for a high volume percentage of PZT, as shown by the SEM images (Figure 11). This probably leads to the comparatively high ε_r values of the PZT/LCT/PA composite in comparison with those of other composites reported in literature (Table 3). The tan δ has a weak dependence on the volume fraction of PZT ranging from 0.01 to 0.06 if the scattered points are not considered.
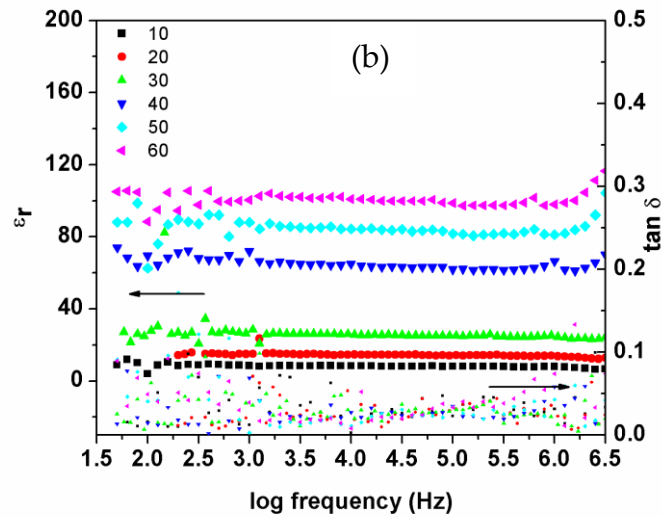
Figure 6 (b). *Dependence of ε_r and tan δ as a function of log frequency with increasing PZT volume fraction for the PZT/LCT/PA composites.*

Piezoelectric charge and voltage constant

The dependence of the d_{33} and g_{33} values of the PZT/LCT/PA composites with increasing volume fraction of PZT is shown in figure 7.

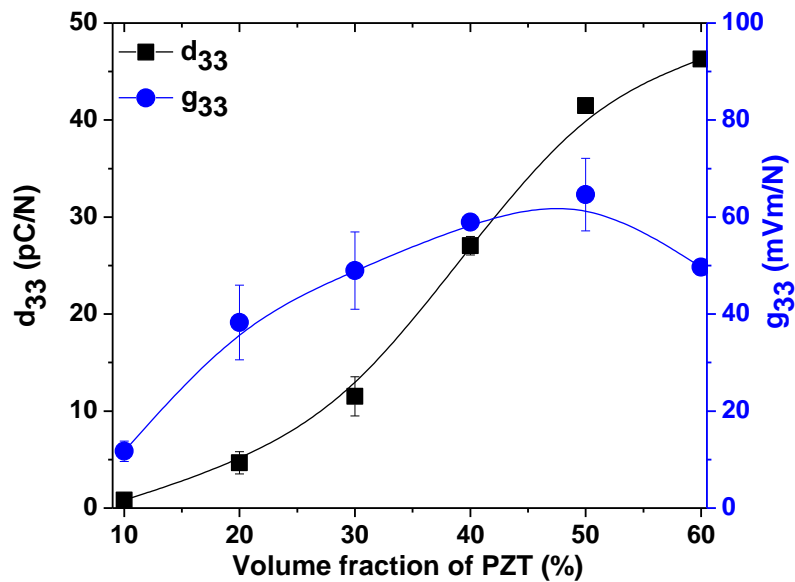**Figure 7.** *Dependence of the d_{33} and g_{33} of the PZT/LCT/PA composites with increasing volume fraction of PZT, measured at 110 Hz (lines drawn as a guide to the eye).*

The d_{33} value of the composite shows a continuous increase with increasing volume fraction of PZT, while the g_{33} value shows a maximum at 50 volume percent and then decreases when it reaches 60 volume percent. This decrease of g_{33} is due to the

behavior of d_{33} relative to ε_r. A maximum value for d_{33} of 46 pC/N is observed for the 60 volume percent PZT while for g_{33} a maximum value of 65 mVm/N is obtained, both for the 50 volume percent PZT composite.

Table 2: *Data of the various components used for the calculations for the composites.*

Type	ε_r	tan δ	d_{33} (pC/N)	E (GPa)	dc σ (S/m)
PZT	1820[a]	-	480	37[c]	-
LCT	3.6	0.0025[b]	0	1	1.22×10^{-11}
PA11	3.9	< 0.035[b]	< 0.5	0.83	3.82×10^{-11}

[a] Data from Morgan Electroceramics.

[b] Data measured at 110 Hz.

[c] Data from [32].

Table 3: *Data of ε_r, d_{33} and g_{33} obtained for the optimum PZT/LCT/PA and PZT/PA composites and comparison with literature data.*

Type	ε_r	d_{33} (pC/N)	g_{33} (mVm/N)
LCT/PA/0.5 PZT (present work)	73	42	65
PA/0.5 PZT (present work)	68	28	48
LCT/0.4 PZT [12]	30	13	48
PVDF/0.7 PZT [16]	100	26	30
Epoxy/0.685 PZT[a] [17]	120	50	47
PVDF/0.67 PZT [18]	152	48	36
PVDF/0.5 PZT (Hot-press) [9]	95	14	16
PVDF/0.5 PZT (Solution cast) [9]	30	9	36

[a] 1.5% carbon black added to the PZT-epoxy mixture.

The data used in the various calculations are given in Table 2. Table 3 provides the optimum data of ε_r, d_{33} and g_{33} obtained for the PZT/LCT/PA and PZT/PA composites and a comparison of different polymer/PZT composites as reported in the literature. The d_{33} and g_{33} values obtained in the present work follows the same trend as reported by Yamada et al. [18], Satish et al. [16] and Venkatragavaraj et al. [9]. Satish et al. reported that the hot-pressing is the most reliable method for the fabrication of 0-3 composites. Moreover hot-pressed composites are known to possess better piezoelectric properties than solution-cast composites [9].
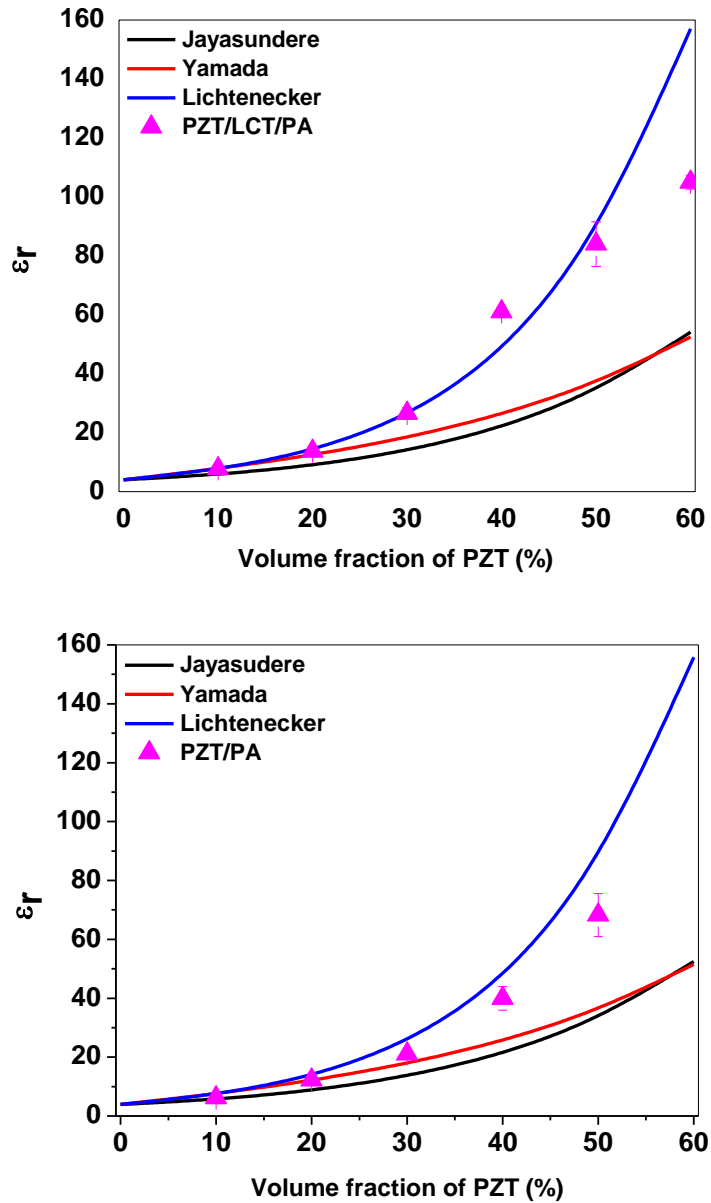
Comparison with theoretical models

Figure 8. *The relative permittivity values of the PZT/LCT/PA and PZT/PA composites as compared to 3 models for 0-3 composites.*

In figures 8-10 the experimental data of the PZT/LCT/PA and PZT/PA composites is compared to several models for 0-3 composites, both for dielectric and piezoelectric constants. It is observed that both the composites follow the same trend. In the PZT/LCT/PA, the relative permittivity of the matrix phase was taken to be the combined relative permittivity of the LCT and PA11 phases and was calculated by Lichtenecker's rule of mixtures [23] given by equation 3. The relative permittivity's of virgin LCT and PA11 materials were found to be 3.6 and 3.9, respectively, and the

relative permittivity of the ceramic phase was taken to ε_r = 1820 (data Morgan electroceramics, UK). The relative permittivity of the PZT/LCT/PA composite was calculated using Lichtenecker's formula and 2 models for high filler content 0-3 composites, namely Yamada's model [18] and Jayasundere's model [21].

The fit of the equation to the data points of the composites for both these models is plotted in figure 8. Both Yamada's and Jayasundere's model underestimate the permittivity of the composites, while Lichtenecker's mixing rule correlates well with the measured values up to 50 volume percent PZT for the PZT/LCT/PA composites. The dielectric behavior therefore, seems to satisfy the logarithmic mixing rule for the PZT/LCT/PA composites. The discrepancy at 60 volume percent is probably due to the fact that at this volume fraction processing becomes much more difficult.

The strong increase in relative permittivity with the increase in PZT volume fraction indicates good coupling of the PZT phase with the polymer phases up to high volume percentages. In both composites the discrepancy between the experimental data and theoretical models is higher at higher volume fraction. Two effects probably play a role here. According to theory the dielectric constant increases with increasing ellipticity of the particles [18, 24, 25]. Moreover, at higher volume fraction the composites, no more act as 0-3 but as 1-3 composites and this is another reason for the high relative permittivity.
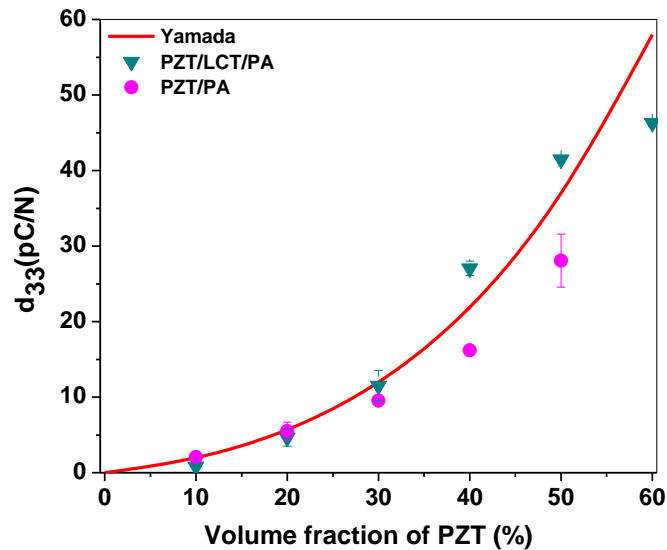

Figure 9. *The d_{33} values of PZT/LCT/PA and PZT/PA composites as compared to Yamada's model for piezoelectric composites.*

In figure 9 the d_{33} values are calculated using Yamada's model [18] for high PZT content composites with the d_{33} of the ceramic phase taken to be d_{33} = 480 pC/N (data Morgan electroceramics, UK). This model was originally developed for PZT/PVDF

composites and tested to a PZT content of 70 volume percent. Since the predicted values mainly depend on the permittivity of the composite and the volume fraction filler, both composites are represented by the same theoretical line. The model shows good correlation of measured d_{33} values up to 30 volume percent PZT for both composites, while at 40 and 50 volume percent some deviations occur. For 60 volume percent the estimated values are lower than expected, and as indicated, this may be due to the increased processing difficulties. It is observed that the presence of LCT results in an increase in ε_r and d_{33} values. This may be due to some preferred orientation of the LCT around the PZT particles, leading to increased polarisability.
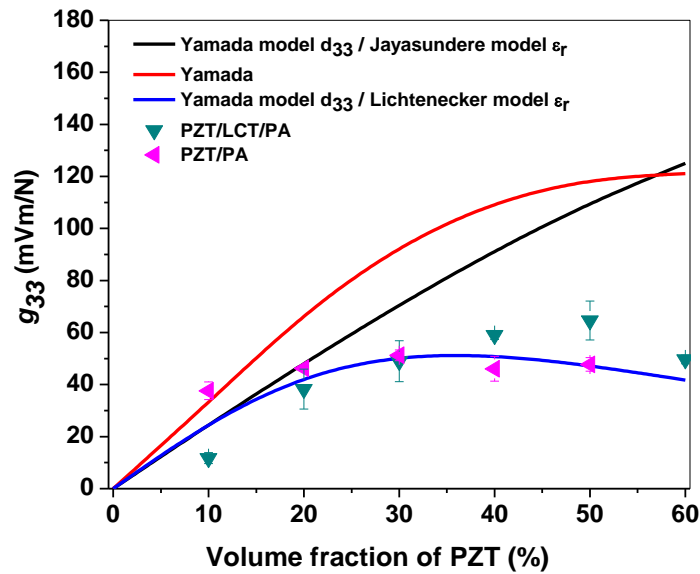

Figure 10. *The g_{33} values of the PZT/LCT/PA and PZT/PA composites as compared to 3 models.*

The Yamada model incorporates anisotropy effects of the particles by the parameter n. If $n = 3$, the particles are spherical while $n > 3$ reflects elongated particles. The best fit for d_{33} is obtained with a shape parameter of $n = 8.5$, which is similar to the value that Yamada et al. found for their composites. To corroborate this, the aspect ratio for 40 particles was estimated from SEM pictures resulting 1.6 ± 0.2, which corresponds to a value of $n = 4.6$. This factor is lower than the factor of $n = 8.5$ obtained from fitting the experimental d_{33} data to the model. This possibly can be explained by increasing particle-particle interactions at high filling fraction in the composites. When calculating piezoelectric constants using Yamada's model, this translates to a higher n value, which is explained by the model as a higher aspect ratio of the particles. In reality, simply more particles are directly connected which leads to a more direct electromechanical coupling between the particles themselves. Moreover,

Yamada's model assumes that all particles are oriented along the direction of the electric field. While this is obviously not true, it has been shown [16] that a random configuration of ellipsoids can be transformed to an equivalent, completely oriented configuration but with different (effective) aspect ratio's. Hence the aspect ratio as observed microscopically not necessarily agrees with the one determined by dielectric measurements.

The combination of LCT and PA11 increases the poling effectiveness, even at relatively low poling voltages. This is evident when comparing d_{33} results for the composite with a LCT/PA matrix (figure 7) to the composite with PA matrix only (figure 5). The 40% PZT composite with an LCT/PA matrix has a d_{33} value of 1.7 times the value for composite with a PA11 matrix only. The resulting g_{33} values are calculated using equation 1. It can be seen in figure 10 that the values calculated using the Lichtenecker model for the relative permittivity and Yamada's model for d_{33} correlate reasonably well with the g_{33} values of the PZT/LCT/PA composites, while values calculated with the relative permittivity predictions of both other models overestimate the g_{33} as a result of the underestimation in relative permittivity.

It is tempting to try to interpret the results also in terms of percolation theory, as has been done frequently for electrical conductivity. A number of aspects complicate the matter tremendously though. First, the configuration as encountered here is much more complex than for normal percolation. The ceramic component consists out of agglomerates with on average about 22 primary particles. These primary particles are sintered together to form these agglomerates during the calcination process. Therefore further percolation can only happen between agglomerates. However, the micrographs show a homogeneous distribution of ceramic particles for all volume fractions and we unable to distinguish between particles within an agglomerate and between agglomerates (see section 3.2.4). The fact that the experimental data are systematically above the prediction of mean field models like the Yamada model lead us to the idea that this effect is due to presence of agglomerates instead of single particles.

Secondly, this system is a dielectric system where both phases are non-conducting and so interfacial contact region between 2 particles will act as a system of parallel capacitors, instead of a system of parallel resistors as would be the case in a conducting filler in a non-conducting matrix. Obviously, the parallel resistor system is much more sensitive to point contacts between particles (which is always the case because of the calcined particle morphology) and a threshold can show up more easily.

Finally, the difference in permittivity between the two phases is about a factor of 450, much less then the factor between conductive and non-conductive phases which is usually 10^6 or 10^7 at least. This makes the transition much less clear. Also, note that experimentally there is no indication of a transition whatsoever, i.e. a clear threshold is

not observed, which makes it difficult to assess whether one is above or below the percolation threshold. A similar observation has been noticed before [33]. Estimating the critical exponents could help but the spacing of the experimental points renders such an analysis useless here.
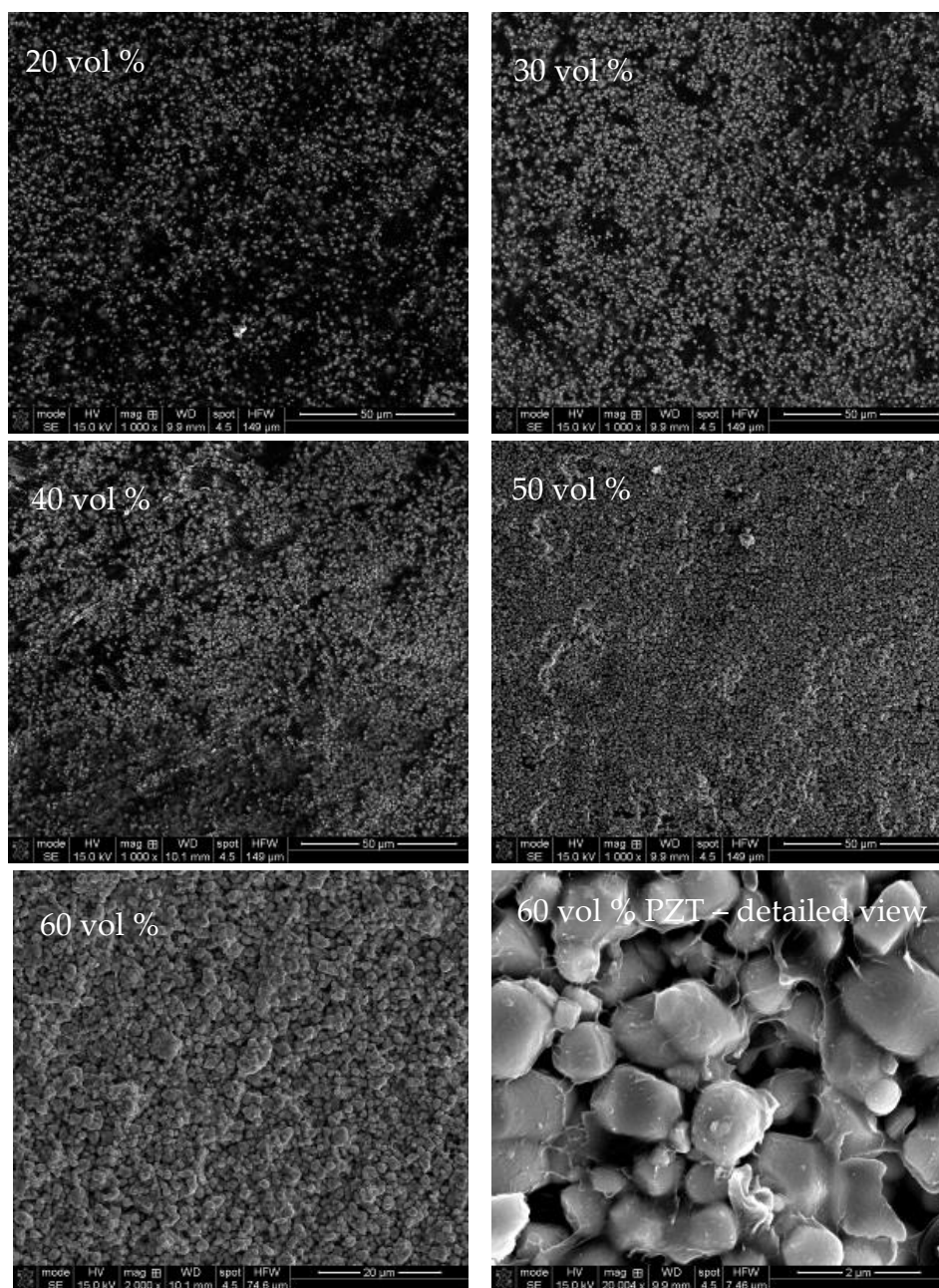
SEM Morphology

Figure 11. *SEM surface morphology of the PZT/LCT/PA composites with 20, 30, 40, 50 and 60 volume percent of PZT. The bright colour represents the PZT and the dark background the polymer.*

Therefore it seems unlikely that percolation plays a significant role but further analysis, e.g. along the line of [34] but now for agglomerates, is required to really elucidate whether this is the case or not.

Figure 11 shows the SEM surface morphology of PZT/LCT/PA composites with 20, 30, 40, 50 and 60 volume percent PZT. From these figures it is observed that all the composites have a relative density near to 100%. Moreover, on the scale of tens of micrometers the composites appear to be homogeneous and have a very similar microstructure. From the 60 volume percent PZT image it also becomes clear that the microstructure is also homogeneous at the micrometer scale. The detailed view of structure of the 60 volume percent PZT composite shows the good adhesion of polymer matrix with the ceramic particles. From these and similar pictures we conclude that the PZT particles are homogeneously dispersed in the polymer matrix and are well adhering to the polymer matrix.

Mechanical properties by DMA

Figure 12 shows the stress-strain curves of the PZT/LCT/PA and PZT/PA composites including the pure polymer and the ceramic volume fraction up to 40%. The measurements are done at a strain rate of 0.5% min^{-1} at room temperature. The three-point bending mode was utilized for these measurements with a preload force of 0.1 N. The upper limit of the static force of the machine is 18 N and the measurements stops when the force reaches this point. Young's modulus E is calculated from the slope near the origin.

From the graphs it can be observed that the resulting strain decreases strongly with increasing volume fraction of PZT leading to increasing Young's modulus. Young's modulus ranges from 1050 - 3000 MPa for the PZT/LCT/PA composites and from 850 to 4450 MPa for the PZT/PA composites. The modulus obtained for pure LCT (1.0 GPa) is lower than the value of 3.2 GPa as reported by Knijnenberg et al. [11]. However, since the strain rate in the static mode (as used by us) is about 4 orders of magnitude lower than the one for the dynamic mode (as used by [11]) and the former generally leads to lower Young's modulus values, this difference in measuring modes probably explains the difference in elastic values observed.

The elastic modulus of the composites was also calculated according to Yamada's model (Eq. 6) using E_c = 37 GPa and v_p = 0.35. While the agreement for the PZT/LCT/PA composites is fair, the agreement for the PZT/PA composites is less good (figure not shown) and we refrain from further discussion.
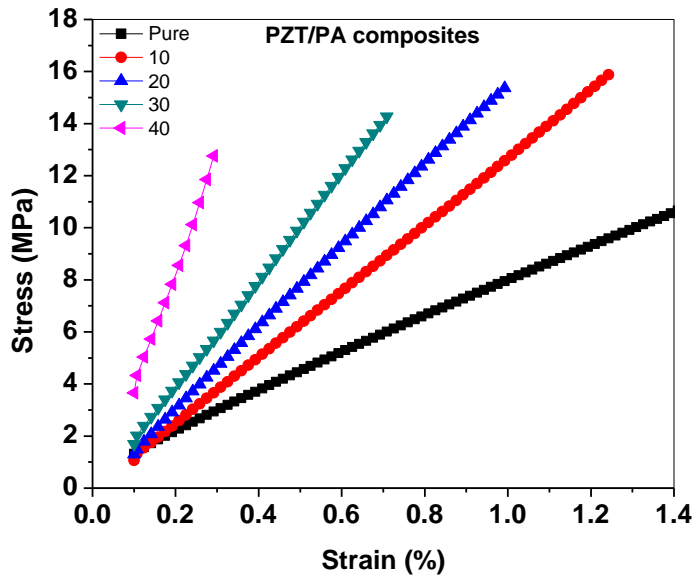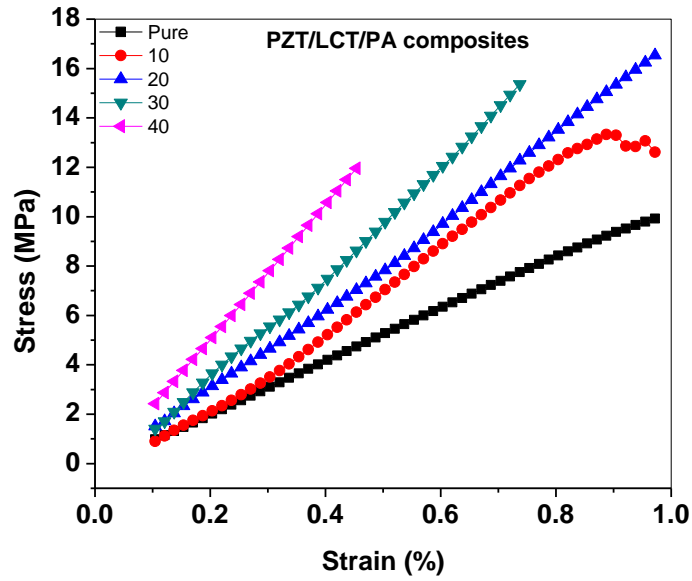
Figure 12. *Stress-strain curves of the PZT/LCT/PA and PZT/PA composites at room temperature as measured in three-point bending with DMA.*

2. 5. Conclusions

A series of new 0-3 PZT/LCT/20%PA composites was successfully fabricated and characterized. X-ray diffraction indicated that for the PZT powder used, calcination at 1100 °C shows the maximum intensity for the single phase tetragonal perovskite peaks. The obtained d_{33} and g_{33} values from PZT/PA composites are also the highest for the PZT calcined at 1100 °C, supporting the above conclusion. The experimental results from ε_r, d_{33} and g_{33} indicates that the new composites have high ε_r, and possess high d_{33} and g_{33}

values (50 volume percent PZT) of about 42 pC/N and 65 mVm/N. These results compare favourably and show the highest g_{33} value in comparison with other reported data in the literature. The experimental data for ε_r agree quite well with the Lichtenecker model for PZT volume fraction up to 50%, while the Yamada and Jayasundere model underestimate the experimental data. The experimental data for the piezoelectric constants agree well with the Yamada model, suggesting an elongated particle shape and confirmed by independent image analysis. Moreover, the addition of PA11 to PZT/LCT composites leads to a lower elastic modulus providing more flexibility to the materials. From the above observations we conclude that these composites are suitable candidate for both sensors and may even show possibilities for actuators.

References

[1]   T. Furukawa, K. Ishida and E.Fukada, *J. Appl. Phys.*, 1979, 50, p. 4904-4912.

[2]   D.K. Dasgupta and M.J. Abdullah, *J. Mat. Sci. Letters*, 1988, 7, p. 167-170.

[3]   H.L.W. Chan, Y. Chen and C.L. Choy, *Trans. Dielectrics and Electrical Insulation*, 1996, 3, p. 800-805.

[4]   E.K. Akdogan, M. Allahverdi and A. Safari, *Trans. Ultrasonics, Ferroelectrics and Frequency control*, 2005, 52, p. 746-775.

[5]   B. Jaffe, W.R. Cook and H. Jaffe, *Piezoelectric ceramics,* New York, 1971, p. 49-50.

[6]   R.E. Newnham, D.P. Skinner and L.E. Cross, *Mat. Res. Bull.*, 1978, 13, p. 525-536.

[7]   J. ChoiJ, B. Hahn, J. Ryu, W. Yoon, B. Lee and D. Park, *Sensors and Actuators A,* 2009, 153 p. 89-95 .

[8]   M. Wegener and K. Arlt, *J. Phys. D: Appl. Phys.,* 200, 41, p. 1-6.

[9]   E. Venkatragavaraj, B. Satish, P.R. Vinod and M.S. Vijaya, *J. Phys. D: Appl. Phys.,* 2001, 34, p. 487-492.

[10]   Y. Bai, Z. Y. Cheng, V. Bharti, H.S. Xu and Q. M. Zhang, *Applied Physics Letters,* 2000, 76 p. 3804-3806.

[11]   A. Knijnenberg, E.S. Weiser, T.L. StClair, E. Mendes and T.J. Dingemans, *Macromolecules*, 2006, 39, p. 6936-6943.

[12]   D.A. van den Ende, P de Almeida and S. van der Zwaag, *J. Mater. Sci.*, 2007, 42, p. 6417-6425.

[13]   A.M. Amer, S.A. Ibrahim, R.M. Ramadan and M.S. Ahmed, *J. Electroceramics, 2005,* 14 p. 273-281.

[14]   H. Zhang, A. Uusimaki, S. Leppavuori and P. Karjalainen, *J. Appl. Phys.*, 1994, 76, p. 4294-4300.

[15]   Image J: http://rsbweb.nih.gov/ij/ version 1.42 q release 08-06-09, accessed 20-01-10

[16]   B. Satish, K. Sridevi and M.S. Vijaya, *J. Phys. D: Appl. Phys., 2002,* 35, p. 2048–2050.

[17]   G. Sa-Gong, A. Safari, S.J. Jang and R.E. Newnham, *Ferroelectrics Lett.*, 1986, 5, p. 131-142.

[18]   T. Yamada, T. Udea and T. Kitayama, *J. Appl. Phys.*, 1982, 53, p. 4328-4332.

[19]   T. Furukawa, K. Ishida, E. Fukada, *J. Appl. Phys.*, 1979, 50, p. 4904-4912.

[20]   S. Firmino Mendes, C.M. Costa, V. Sencadas, J. Serrado Nunes, P. Costa, R. Gregorio jr., S. Lanceros-Méndez, *J. Appl. Phys. A*, 2009, 96, p. 899-908.

[21]   N. Jayasundere and B.V. Smith, *J. Appl. Phys.*, 1993, 5, p. 2462-2466.

[22]   D. Khastgir and K. Adachi, *J. Polymer Science*, 1999, 37, p. 3067-3070.

[23]   K. Lichtenecker, *Physikalische Zeitschrift*, 1926, 27, p. 115-158.

[24]   A. Sihvola, *Electromagnetic mixing formulas and applications*, 1999, London, p. 166-167.

[25]   R.W. Sillars, *J. Inst Electr*, 1937, 80, p. 378-394.

[26]   T. Zakri, J.P. Laurent and M.J. Vauclin, *j. Phys. D: Appl. Phys., 1998,* 31, p. 1589-1594.

[27]   C.K. Wong, Y. M. Poon, F.G. Shin, *J. Appl. Phys.*, 2001, 90, p. 4690-4700.

[28]   A.V. Turik, A.I. Chernobabov, G.S. Radchenko and S.A. Turik, *Physics of the Solid State*, 2004, 46, p. 2213-2216.

[29]   D.A.G. Bruggeman, *Ann. Physik*, 1935, 24, p. 636-664.

[30]   J.A. Reynolds and J.M. Hough, *Proc. Phys Soc.*, 1957, London, B70, p. 769-774.

[31]   M. Marutake, *J. Phys Soc. Japan*, 1956, 11, p. 807-814.

[32]   *Piezoelectric Materials Data Book*, 1996, Ferroperm, Kvistgård, Denmark.

[33]   C. Cui, R.H. Baughman, Z. Iqbal, T.R. Kazmar and D.K. Dahlstrom, *Synth. Metals*, 1997, 85, p. 1391-1392.

[34]   J.P. Calame, *J. Appl. Phys.*, 2006, 99, 084101-1 / 084101-11.

Chapter 3

Highly flexible piezoelectric 0-3 PZT/PDMS composites with high filler content*

Flexible piezoelectric composites offer alternative and/or additional solutions to sensor, actuator and transducer applications. Here high density, highly flexible piezoelectric composites with 0-3 connectivity using filler volume fractions up to 50 vol. % are realized by solution casting of dispersions of ferroelectric (Pb(Zr$_x$Ti$_{1-x}$)O$_3$ (PZT) in poly-dimethylsiloxane (PDMS). Excellent piezoelectric properties (permittivity ε_r up to ~ 40, piezoelectric charge constant d_{33} up to 25 pC/N, piezoelectric voltage coefficient g_{33} up to 75 mV.m/N), electrical properties (conductivity σ about $1 \cdot 10^{-6}$ S/m at 1000 Hz) and mechanical properties (storage modulus E' up to 10 MPa, loss modulus E'' less than 0.5 MPa, limited creep and stress relaxation) have been realized. The high flexibility combined with excellent properties of these composites opens new ways to 'soft touch' applications in a variety of transducer and sensor applications.

3.1. Introduction

Piezoelectric composites with 0-3 connectivity are of paramount importance for sensors, actuators and transducers in a variety of fields. In particular, flexible soft composite materials relate to transducer and sensor applications for the generation and detection of underwater acoustic signals (sonar), medical diagnostic systems (e.g. micropumps in micro- / nano-fluidic devices) and tactile sensors (energy scavenger for aerospace / automotive / domestic devices or touch-base switches for the consumer market). For each of the above mentioned applications, a different balance in properties is required. In many cases the most important requirements are that the composite films should be flexible and soft in the appropriate thickness range and still possess as good as possible piezoelectric properties [1-3].

Due to the increasing demands on structural performance for these electronic devices, there has been extensive research carried out in the design and fabrication of polymer-matrix composites (PMCs) in recent years [4-7]. Composite materials allow for optimization of electrical, magnetic and mechanical effects and this resulted in the emergence of many advanced functional materials. These PMCs offer several advantages over other types of materials: their ability to be tailored with properties by varying the volume fraction of the ceramic inclusions and their ease of production including the option to realize easily different sizes and shapes [8-10].

The most widely used ceramic for such composite materials is (ferroelectric) lead zirconate titanate ($Pb(Zr_xTi_{1-x})O_3$ or PZT) because of its excellent electromechanical properties [11, 12]. The properties of PMCs will depend not only on the nature of the phases but also the connectivity of the ceramic particles and the matrix. For the matrix of 0-3 composites various polymers are used.

In a previous study, we reported on the processing and characterization of 0-3 lead zirconate titanate / liquid crystalline thermotropic / polyamide (PZT/LCT/PA) composites [13]. Hot-pressing was utilized for the fabrication and the effect of the volume fraction of PZT on the piezoelectric and dielectric properties was studied. The experimental data of permittivity and piezoelectric constants were compared with several theoretical models (Jayasundere, Yamada and Lichtenecker) for these 0-3 composites. In order to assess the correlation of the experimental data with the theoretical models, the experimental data obtained from PZT/PA composites were also included. The matrix used leads to relatively stiff composite materials.

An interesting matrix material choice is poly-(dimethylsiloxane) (PDMS), a silicon-based elastomer with repeating unit of $SiO(CH_3)_2$. Due to its very low glass transition temperature T_g, PDMS exhibits rubbery behaviour at room temperature. Properties such as elastic behavior, resistance to high temperatures, resistance to

radiation and chemical attack make PDMS suitable for a wide range of applications in electrical and optical devices [14, 28].

In the present work, 0-3 PZT-PDMS composites were fabricated with volume fractions up to 50 vol. % PZT ceramic particles by solution casting. The electrical, dielectrical and mechanical properties were investigated as a function of ceramic volume fraction and frequency. These PZT-PDMS composites offer the advantage of high flexibility in comparison with other 0-3 composites, even with 50 vol. % PZT. These composites possess the ability to attain various sizes and shapes, each with high flexibility (Figure 1 a) due to the exceptional elastic behavior of PDMS, combined with good functional properties. Only a few papers report on flexible composites with relatively high ceramic volume fractions. Sakamoto et al. [15, 16] studied the electro-active properties of composites of PZT up to about 30 vol. % in a poly-urethane matrix. Ba-Sr-titanate-zirconate up to 40 vo% in an epoxy matrix was studied by Yang et al. [17] and these authors conclude that the Yamada model is inadequate because of the unknown shape factor. However, due to the nature of these matrices, the elastic moduli (not reported) is probably much higher than for PDMS composites.

Figure 1 (a). *Photograph showing the flexibility of a 40 vol. % PZT-PDMS composite film (thickness ~ 280 μm).*

Liou et al. [18] described the incorporation of Ba-Sr-titanate up to about 60 vol. % in PDMS rubber and studied in particular the dielectric tunability. However, their materials contained a bulk porosity of 4 to 7% and a surface porosity of 18 to 24%. These authors also observed a relatively high shape factor of 14.0 for the Yamada model and attributed that to clustering of the filler and the surface effect. No study was made of the flexibility. Sharma et al. [19] used PDMS composites with up to 32 vol. % PZT for active damping. No comparison of the experimental permittivity and elasticity results was made with theoretical expressions. Romasanta et al. [20] incorporated up to 8 vol. % Ca-Cu-titanate in PDMS and studied their electro-mechanical response. Also these authors observed a relatively high shape factor of 12.5 for the Yamada model,

stated that their results are in agreement with others and conclude that the Yamada model is applicable for these composites. As far as the authors are aware of, no other papers studied the mechanical properties of flexible 0-3 composites in some detail.

3. 2. Experimental

3.2.1. Materials

The PZT powder used in this research is a commercial half-product PZT5A4 (Morgan Electro Ceramics, Ruabon UK), a soft PZT with 1 mol% Nb added as dopant. Before use it was thermally treated, as reported in [13] where further details can be found. The average size of the filler is about 1.0 μm and the details of the filler size also can be found in [13]. The polymer used is linear vinyl-terminated poly (dimethylsiloxane) (PDMS17 with M_w = 17200 g/mol; ABCR GmbH & Co) cross-linked with the four-functional siloxane, tetrakis(dimethylsiloxane) (ABCR GmbH & Co). The hydrosilylation reactions were catalyzed by cisdichlorobis (diethylsulphide) platinum (II) catalyst (Strem Chemicals, Inc) previously dissolved in a toluene solution. Esteves et al. [14] reported on the details of the hydrosilylation addition reaction to obtain cross-linked (tri-dimensional network) PDMS composites by reacting functional end groups on the PDMS chains with a multifunctional cross-linker in the presence of a catalyst. We used the same hydrosilylation addition reaction to realize the PZT-PDMS composites.

3.2.2. Fabrication of composites

In brief, the materials PZT (10-50 vol. %) and PDMS (90-50 vol. %) were mixed in a speed mixer (DAC 150 FVZ) at 3000 rpm for 2 minutes and the appropriate amount of cross-linker is added and mixed again for 1 minute and finally the catalyst is added and mixed for 1 minute. This mixture is directly solution casted on a polycarbonate sheet and subsequently dried and cured under vacuum initially at 60 °C for 20 hours and at 110 °C for 5 hours. Attempts were made to realize composites with 60% PZT but the viscosity of the dispersion appeared too high to be able to cast the material properly. Composites with specific dimensions of 14 mm in diameter and 200-275 μm thickness were cut from the composite films. Circular gold electrodes with a thickness of 300 nm and an area of 7.85×10^{-5} m^2 were sputtered on both sides of the composites using an Edwards sputter coater (model S150B). The poling of the electroded sample is performed by applying an electric field of 12 kV/mm (Heinziger 10 kV power supply) at 120 °C for 30 minutes in a silicone oil bath to ensure uniform heating. The electric field was kept on during cooling to room temperature.

3.2.3. Measurements

The relative density of the composites were measured by the displacement of the solvent (2 wt % sodium dodecyl sulphate (Merck) in ultra-pure water) using dynamic contact angle measuring instrument and tensiometer (Dataphysics DCAT 21). Impedance data of the composites were collected by an impedance analyzer (EG&G Princeton Applied Research, Model 1025) coupled with a potentiostat (Potentiostat/Galvanostat, Model 283) at room temperature at a frequency range of 10 mHz - 5 MHz. The piezoelectric charge constant was measured with a d_{33} meter (Piezotest, PM300) at a fixed frequency of 110 Hz. The d_{33} and ε_r values obtained at 110 Hz were used to calculate the piezoelectric voltage coefficient g_{33} according to

$$g_{33} = d_{33} / \varepsilon_o \varepsilon_r \qquad (1)$$

where d_{33} is the piezoelectric charge constant in pC/N, ε_o is the permittivity of free space ($8.85.10^{-12}$ F/m) and ε_r is the relative permittivity of the composite. The microstructure of the composites was examined by SEM (FEI, Quanta 3D FEG). The mechanical properties of the composite films were tested in a tensile mode on DMA (TA Instruments Q800 series) at room temperature. The static elastic modulus E of the composites was measured by performing stress-strain tests with a strain rate of 0.5 % min^{-1}. Creep measurements were conducted at 0.1 MPa, a stress level within the linear viscoelastic region while stress relaxation measurements were conducted at a constant strain of 0.55%. Both were monitored for 140 min. The dynamic behavior of pure PDMS and 40 vol. % PZT-PDMS composites were studied using a temperature ramp and multi-frequency mode. The specimens are heated at a constant rate of 3 °C /min. While heating, the specimens are deformed at constant amplitude over a single frequency. The mechanical properties are also measured over a range of discrete frequencies. The frequencies 1, 5 and 10 Hz were used in this study. The dynamic tests were conducted at constant force amplitude of 5 μm with a preload force of 0.01 N. The temperature range used was from −120 °C to +120 °C at a frequency of 1 Hz.

3.3. Results and discussion

3.3.1. Density, morphology and electrical conductivity

The theoretical and experimental densities of the fabricated composites are shown in Figure 1 b.

The theoretical density values were calculated using the simple rule of mixtures,

$$\rho_c = \rho_P (1-\phi) + \rho_f \phi \tag{2}$$

where ρ_c, ρ_P and ρ_f are the densities of the composite, polymer and the ceramic filler and ϕ is the volume fraction of the ceramic filler. The values of ρ_P and ρ_f were taken to be 970 kg/m³ and 7950 kg/m³, respectively. The experimental density values are all approximately 90% of the theoretical prediction.
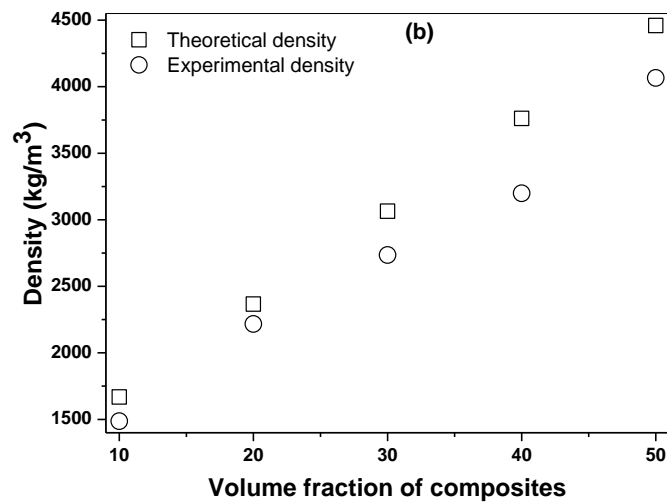

Figure 1 (b). *Comparison between the experimental and theoretical density values of the composites.*

The quality of many materials and in particular those of composites depends to a large extent on the homogeneity of the materials realized. Scanning electron microscopy (SEM) of cross-sections of the PZT-PDMS composite films was done to investigate the homogeneity of the dispersed particles (Figure 2 a and b). From these images it is observed that the PZT particles are homogeneously dispersed on the micrometer scale in the polymer matrix and are well adhering to the polymer matrix. Moreover the composites have hardly any residual porosity, rendering a positive influence on the structural integrity.

The dependence of ac conductivity σ of the PZT-PDMS composites as a function of frequency and volume fraction was determined (Figure 3 a and b). As the volume fraction of PZT increases, the conductivity increases about 1 decade from ~5x10⁻¹⁰ S/m (10 vol. %) to ~2x10⁻⁹ S/m (50 vol. %) at 1000 Hz. The latter is still a value corresponding to a highly insulating material, as required for sensor and transducer applications. Because interface conductivity is usually higher then bulk conductivity, the increase in the conductivity with the increase in volume fraction of PZT is attributed to the

increased contribution of interface conductivity between PZT and PDMS, directly related to the increasing particle volume fraction.

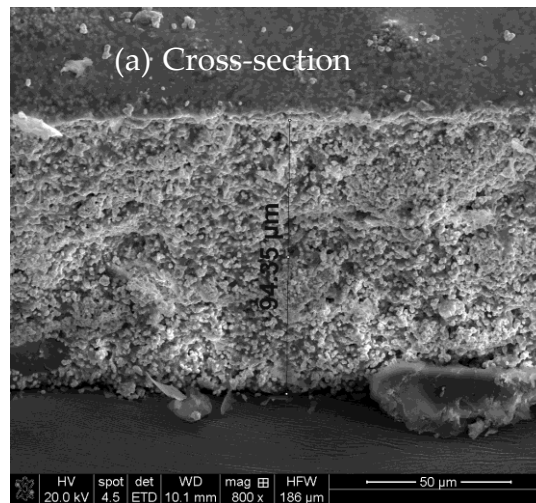**Figure 2 (a).** *SEM cross-section of the PZT-PDMS composite with 50 vol. % PZT having a thickness of ~100 μm.*
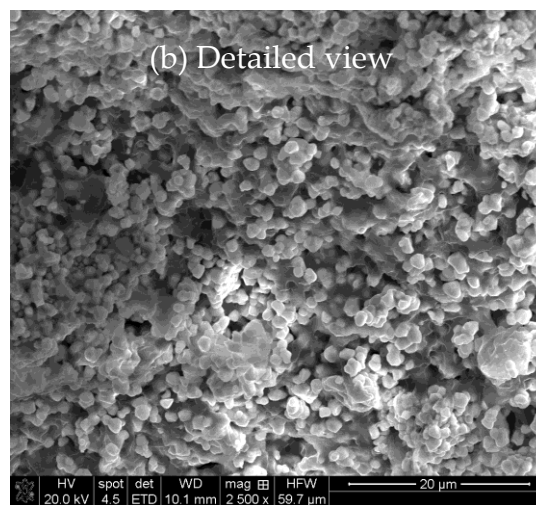

Figure 2 (b). *Detailed view of the cross-section of the PZT-PDMS composite with 50 vol. % PZT having a thickness of ~100 μm.*
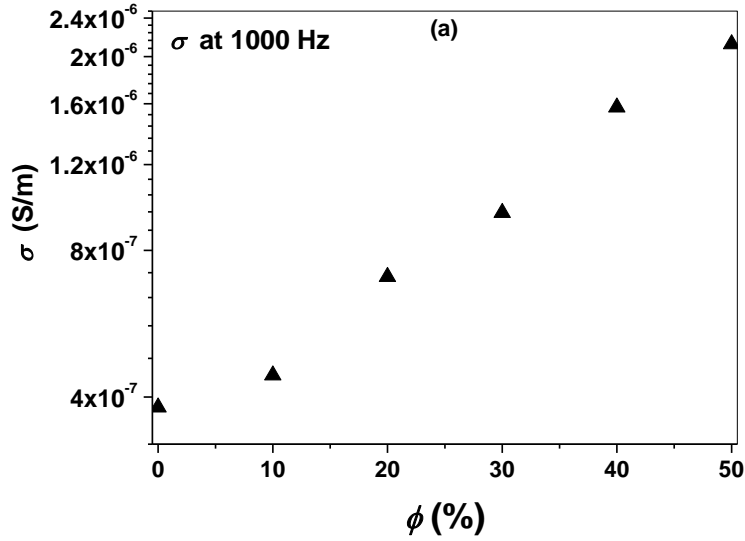
Figure 3 (a). *The ac conductivity σ of the PZT-PDMS composites at 1000 Hz as a function of volume fraction φ.*
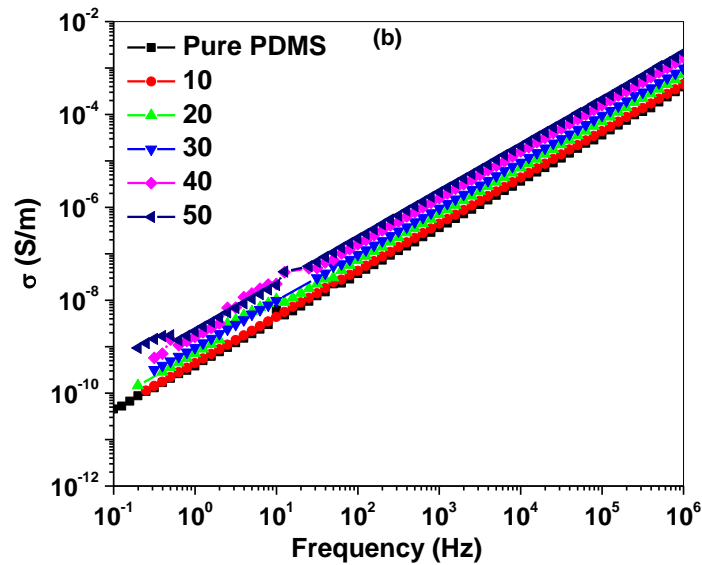
Figure 3 (b). *The dependence of σ of PZT-PDMS composites as a function of frequency.*

3.3.2. Piezoelectric properties

Generally models of piezo-and di-electric behavior employ descriptions based on spherical inclusions randomly distributed in the matrix. Only a few models result in the prediction for ε_r as well as d_{33} for 0-3 composites [21-23], the most well-known attempt

probably being the one by Yamada et al. [23]. The Yamada model incorporates anisotropy effects of the particles by the parameter n related to the shape of the particles but neglects particle-particle interactions. The expression for the permittivity ε of the composite reads

$$\varepsilon = \varepsilon_1 \left[1 + \frac{n\phi(\varepsilon_2 - \varepsilon_1)}{n\varepsilon_1 + (\varepsilon_2 - \varepsilon_1)(1 - \phi)} \right] \qquad (2)$$

where the ε_1 (ε_2) refers to the relative permittivity of the matrix (particles), ϕ to the volume fraction particles and n is a shape factor. The shape factor is $n = 3$ for spherical particles and has been used as a fitting parameter. A model that takes into account the polarization interaction of the inclusions induced by the applied electric field is the one by Jayasundere et al. [22] that describes ε_r based on spherical inclusions but pays no attention to d_{33}. Using the same notation their expression is

$$\varepsilon = \frac{\varepsilon_1(1 - \phi) + \varepsilon_2\phi[3\varepsilon_1/(\varepsilon_1 + 2\varepsilon_2)][1 + 3\phi(\varepsilon_2 - \varepsilon_1)/(\varepsilon_2 + 2\varepsilon_1)]}{(1 - \phi) + \phi(3\varepsilon_1)/(\varepsilon_1 + 2\varepsilon_2)[1 + 3\phi(\varepsilon_2 - \varepsilon_1)/(\varepsilon_2 + 2\varepsilon_1)]} \qquad (3)$$

The experimental ε_r values for the PZT-PDMS composites are compared with the theoretical predictions (Figure 4) given by Jayasundere and Yamada for 0-3 composites [22, 23], similarly as in [13]. The theoretical expressions were evaluated by substituting ε_r of virgin PDMS, measured to be 2.64 and ε_r of the ceramic phase, taken as 1820 (data Morgan Electroceramics, UK). For the Yamada model the optimum n-value is 14.2, leading to a shape anisometry ratio of $r = 4.2$, far above the independently determined value of $r = 1.4$ by microscopy [13]. The value $n = 14.2$ is therefore unrealistic. The line for $n = 8.2$ ($r = 2.6$) as determined by an optimum fit for d_{33} is also shown. Obviously in this case the Yamada model underestimates the experimental ε_r data. Apart from the properties of the matrix and particles, Jayasundere model contains no parameters. Obviously it underestimates the experimental ε_r data as well. The measured tan δ values of the PZT-PDMS composites are also shown in Figure 4. The tan δ value has a weak dependence on the volume fraction of PZT ranging from less than 0.0001 (detection limit of the equipment used) to ~ 0.018.
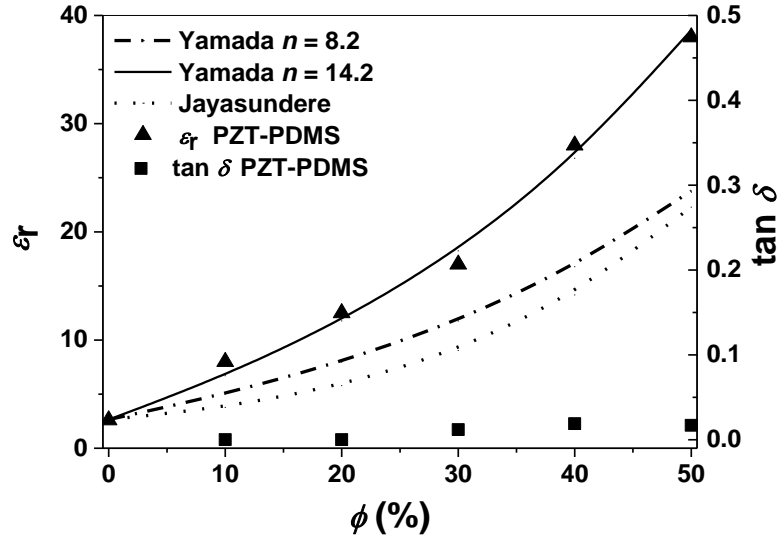
Figure 4. *The permittivity ε_r of the PZT-PDMS composites as compared with the Yamada and Jayasundere model (left) and the tan δ (right).*

Also the d_{33} and g_{33} values of the PZT-PDMS composites increase continuously with vol. % of PZT (Figure 5 a). Since PDMS exhibits rubbery behaviour at room temperature, the composites properties are appreciably affected by the stress-strain state. In order to be able to compare the data properly, all the d_{33} measurements were carried out at constant static force of 1 N. The maximum value for d_{33} and g_{33} are observed for the 50 vol. % composite, 25 pC/N and 75 mV·m/N, respectively. The obtained experimental d_{33} values are compared with the theoretical data as given by the Yamada model (Figure 5 b). The d_{33} values are calculated using Yamada's model for high PZT content composites with the d_{33} of the ceramic phase taken to be d_{33} = 480 pC/N (data Morgan Electroceramics, UK). For d_{33} the optimum n-value is 8.2, comparable to the value n = 8.5 obtained before for PZT/LCT/PA composites [13] as well as by Yamada [23]. The line for n = 14.2, being the optimum value for ε_r, is shown as well. Agreement is then absent. It thus appears impossible to describe both ε_r and d_{33} with the same n-value by the Yamada model, as was observed before [13]. The parameter g_{33}, often used as a figure-of-merit, has been reported to yield a value up to 60 mV·m/N for piezo-composites [13], typically containing 40 or 50% inorganic particles. The present value of 75 mV·m/N for the 40% composite thus compares favorably with the value for other materials.

Summarizing this part, it is observed that the experimental d_{33} values correlate well with the Yamada model using n = 8.2 (r = 2.6), contrary to the ε_r values for which the optimum value is n = 14.2 (r = 4.2). Two effects probably play a role here. According to theory the dielectric constant increases with increasing ellipticity of the particles [2,

23, 24]. This effect is estimated small in view of the independently determined experimental value $r = 1.4$. At higher volume fraction the composites no longer act as 0-3 but as 1-3 composites in which particle-particle interactions lead to enhanced permittivity, described by an artificially high n-value. Jayasundere model assumes spherical particles but since the r-value is only 1.4, the effect of ellipticity is considered small. The enhancement is incorporated in the Jayasundere model but obviously significantly underestimates the co-operative effect.
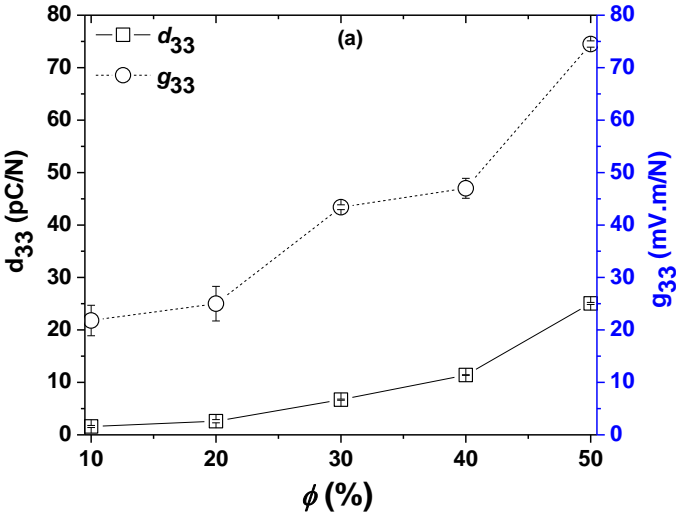

Figure 5 (a). *Dependence of d_{33} and g_{33} of the PZT-PDMS composites with increasing vol. % of PZT measured at constant static force of 1 N and at 110 Hz (lines drawn as a guide to the eye).*
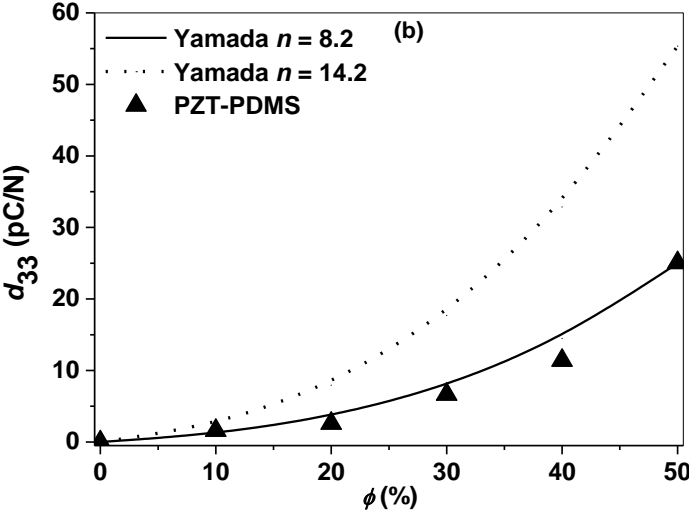

Figure 5 (b). *The piezoelectric charge constant d_{33} of the PZT-PDMS composites as compared with the Yamada model.*

60

3.3.3. Mechanical properties

Another important aspect of composites is their mechanical behavior. We studied the elastic modulus as well the creep and stress relaxation. The static elastic modulus E was measured between 2-10% strain and increases with increasing volume fraction of PZT (Figure 6 a). The experimentally obtained E moduli (Figure 6 b) are compared with the values obtained from the Yamada model. Input data are the measured E modulus for pure PDMS, $0.75 \cdot 10^6$ N/m^2 and that of PZT, $63 \cdot 10^9$ N/m^2 [25] while Poisson's ratio is estimated as $\sigma = 0.5$ (rubber value) [26]. The obtained results follow the same trend as those for ε_r, namely that the model underestimates the experimental values considerably. This conclusion is practically independent of the σ-value chosen. Contrary to this result, Yamada et al. [23] show good agreement with experiment for their PVDF/PZT composites[1], probably due to the much higher ratio of elastic moduli of the matrix and particles in their case. Apart from a low modulus, all composites show failure strains of more than 20%, while for the lower volume fraction composites the values are above 40 to 50%. In order to check the reproducibility of the stress-strain curve, three different samples for 30 vol. % PZT-PDMS composites were measured. The average modulus was 4.85 ± 0.22 MPa where $\pm$ indicates the sample standard deviation. We expect that the other composites have similar reproducibility.
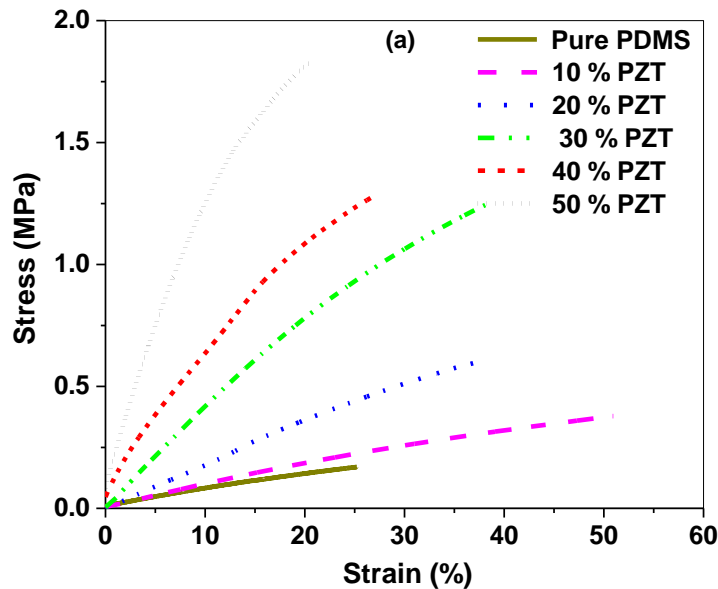

Figure 6 (a). *The stress-strain curves measured at a strain rate of 0.5% min^{-1}.*

To illustrate the temperature behavior, the storage and loss modulus of pure PDMS and the 40 vol. % PZT-PDMS composite were measured from −120 °C to +120 °C at a frequency of 1 Hz (Figure 7 a). At low temperature the storage modulus is high which is, as expected, due to the glassy state of the polymer. As the temperature rise and reaches room temperature, a drop by more than two orders of magnitude is observed due to the rubbery behavior. The glass transition temperature T_g measured for pure PDMS is −47 °C and we observed a small shift to −45 °C for the 40 vol. % PZT polymer composites. In addition, the loss modulus follows the same trend as the storage modulus and exhibits a plateau as the temperature rises. Mechanical properties of polymers and polymer composites are frequency dependent but the frequency range that can be addressed with DMTA is relatively limited. Hence we opted for using three frequencies and quasi-static measurements. The strain used for the DMTA measurements was ~ 5×10^{-4}, well within the linear regime as could be assessed from the quasi-static stress-strain curves.
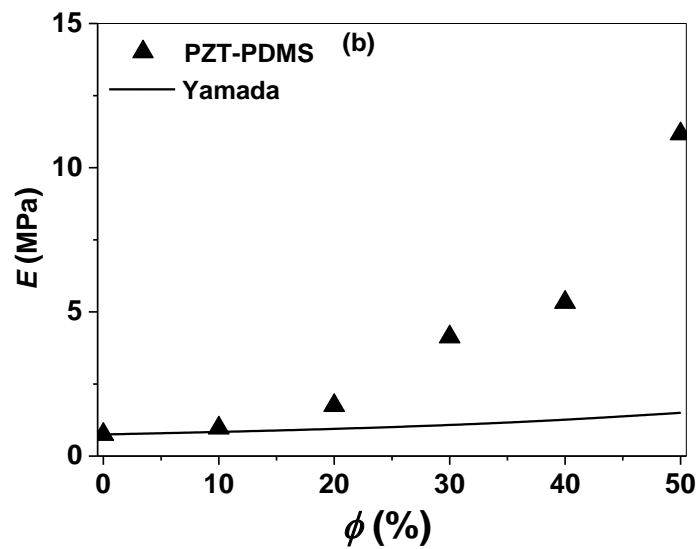
Figure 6 (b). *The elastic modulus E of the PZT-PDMS composites measured at a strain rate of 0.5 % min⁻¹ as compared with the Yamada model.*

The storage and loss modulus of 40 the vol. % PZT-PDMS composite, measured at 1, 5 and 10 Hz increase with increasing frequency, yielding a storage modulus of 7.5, 7.7 and 7.8 MPa at 1, 5 and 10 Hz, respectively while the loss modulus was 0.38, 0.43 and 0.46 MPa, respectively (Figure 7 b). The slight increase with frequency is typical for polymers (and their composites). Within the time interval used, the modulus is constant, consistent with the creep results (see below).
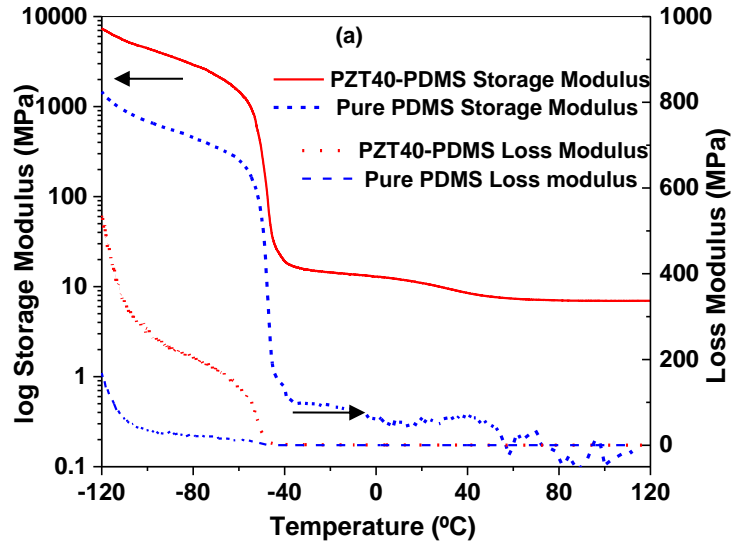
Figure 7 (a). *Dynamic behavior of pure PDMS and the 40 vol. % PZT-PDMS composite at 1 Hz using a heating rate of 3 °C/min.*
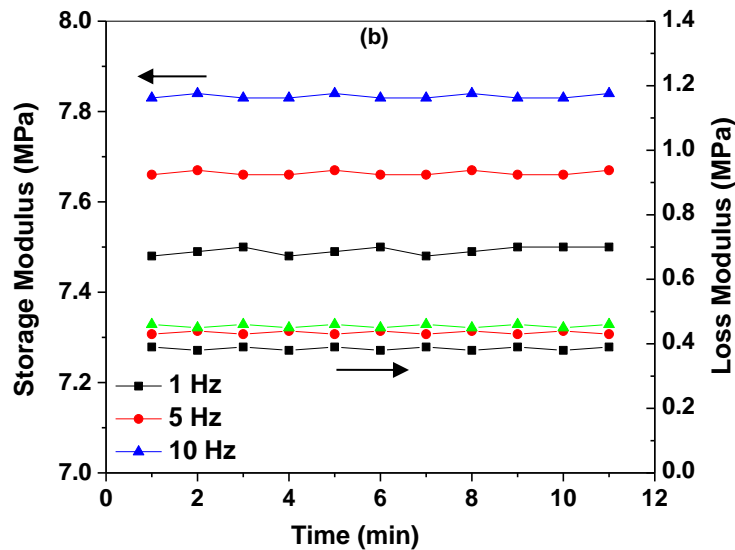
Figure 7 (b). *Dynamic behavior of 40 vol. % PZT-PDMS composites measured at 1, 5 and 10 Hz at room temperature.*

Creep measurements were conducted at a stress of 0.1 MPa in the linear viscoelastic region at room temperature for times up to 105 min (Figure 8 a). The specimens were allowed to recover for another 35 min after stress removal. The equilibrium elongation decreases strongly with increasing volume fraction of PZT. After stress removal, all the composites exhibit instantaneous recovery indicating that these composites are fully cross-linked and a three dimensional network is formed

encapsulating the ceramic particles. Stress relaxation measurements were conducted at a constant strain of 0.55% (value taken from creep measurements for the 50 vol. % composite) for 105 min and the strain recovery was followed for another 35 min (Figure 8 b). The obtained stress from the stress relaxation measurements for the 50 vol. % is equal to the applied stress in the creep measurements which indicates that the results obtained from these measurements are in excellent agreement.

Figure 8 (a). *Creep measurements at 0.1 MPa compared with the Burgers' four element model.*

Figure 8 (b). *Stress relaxation measurements at 0.55% compared with the Burgers' four element model.*
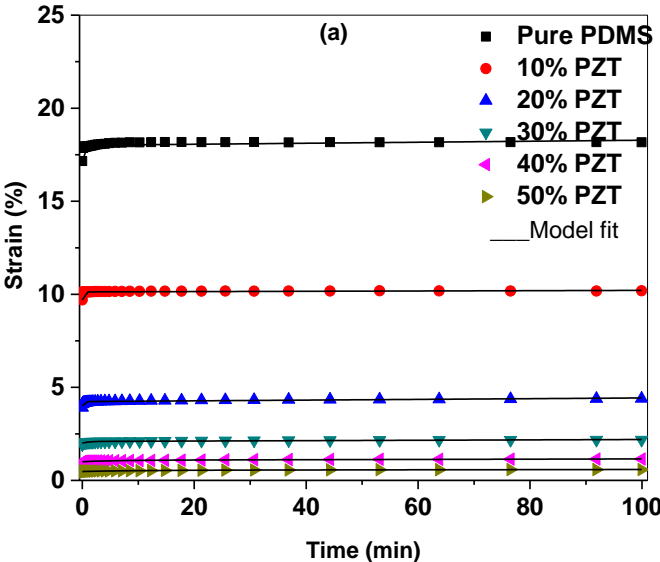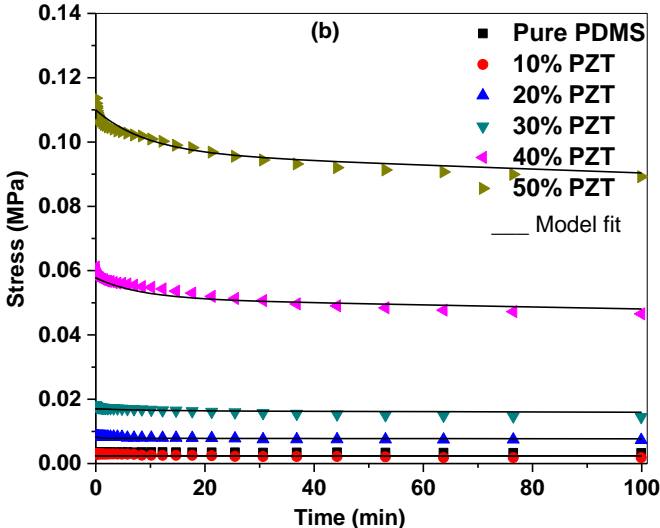
Table 1: Burgers' model parameters for creep at a stress of 0.1 MPa

Creep	E_M (MPa)	η_M (MPa.s)	E_K (MPa)	η_K (MPa.s)
Pure PDMS	0.00583	124	0.117	0.00168
10PZT-90PDMS	0.0103	124	0.234	0.00200
20PZT-80PDMS	0.0249	66.6	0.439	0.0885
30PZT-70PDMS	0.0492	102	0.821	7.68
40PZT-60PDMS	0.0993	142	1.28	7.95
50PZT-50PDMS	0.208	264	1.46	15.6

[a] The above shown parameters from the fitting of the Burgers' model to the creep data were used for the calculation of the stress relaxation curves.

Burgers' model, containing a Maxwell element (with elastic constant E_M and viscosity η_M) and a Kelvin element (with elastic constant E_K and viscosity η_K) in series, was used to analyze the creep data of the composites [27], resulting in a good fit for the higher vol. % composites and reasonable agreement for the lower vol. % composites (Figure 8 a). As expected, the elastic parameters E_M and E_K increase continuously with increasing vol. % of PZT (Table 1). Since both the Maxwell spring E_M and the Kelvin spring E_K increase with vol. % of PZT, both the instantaneous elastic deformation and anelastic relaxation decrease with increasing vol%. The viscous parameter η_M is approximately constant while the parameter η_K also increases continuously with increasing vol. % of PZT, rendering that creep of the composites decreased with respect to the pure PDMS, diminishing even further the already small effects present for pure PDMS. The parameters as obtained from the creep data were used to predict the stress relaxation data and the predicted curves show a good match with the experimental data, indicating the suitability of the model (Figure 8 b).

Finally we note that PDMS-based composites show excellent thermal stability. Thermal gravimetric analysis on similar composites have shown that these materials are thermally stable in nitrogen and air up to at least 300 °C [28]. In fact, the presence of the particles does seem to have a significant influence on the thermal stability. Since the Curie temperature of the PZT is about 360 °C [25], these composites can be used up to a temperature close to the Curie temperature.

Note: [1] Ref. [23] reports $n' = 0.67$ to fit the experimental data while we obtain $n' = 0.65$ using digitized data from fig. 6 in ref. [23], i.e. essentially agreement. Calculating Poisson's ratio σ from eq. 16 in ref. [23], $n' = (1+\sigma)/3(1-\sigma)$, results in $\sigma = 0.34$, a more reasonable value for a glassy polymer than $\sigma = 0.49$ as reported in ref. [23] . Moreover,

the value for the Young's modulus of the PZT is given as $E = 6.32.10^9$ N/m² which probably should read $E = 63.2.10^9$ N/m², an acceptable value for a PZT particle, and that value indeed yields $E \cong 3.1 \cdot 10^9$ N/m² as calculated from eq. 17 in ref. [23] for a volume fraction $\phi = 0.67$.

3.4. Conclusions

In conclusion, highly flexible piezoelectric PZT-PDMS composite films of 0-3 connectivity with filler volume fractions up to 50 vol. % could be successfully and easily fabricated by solution casting. SEM analysis of the composites shows a homogeneous distribution of PZT particles in the polymer matrix. The experimental relative density values proved to be about 90%. The relative permittivity and piezoelectric charge constant increase with the increasing contribution of PZT, maintaining a low ac conductivity. The experimental results were compared with theoretical models and we note that the Yamada model can either describe the piezoelectric charge constant d_{33} well meanwhile describing poorly the permittivity ε_r or vice versa, albeit in both cases with unrealistically high shape factors, but not both. Results obtained from static and dynamic mechanical analysis show that the present composites are highly compliant with a Young's modulus only a few times higher than for pure PDMS. The Yamada model underestimates the Young's moduli E significantly, though, as compared with the experimental data. A similar remark can be made for the permittivity with respect to the Jayasundere model. The good combination of the material properties, i.e. a decent value for permittivity, piezoelectric charge and voltage constant combined with low electrical conductivity, low elastic stiffness and very limited creep and stress relaxation, promotes the development of prototypes for transducer and sensors applications. Moreover, by varying the volume fraction a proper balance in dielectric and mechanical properties for various applications can be realized. It is highly likely that other piezoelectric oxide particles can be incorporated in PDMS without having any porosity in a similar easy way, thereby increasing the applicability range.

References

[1]   L. Dong , R. Li, C. Xiong, H. Quan., 2010, Polym Int.; 59(6):756- 758.

[2]   D. Khastgir, K. Adachi., Piezoelectric and dielectric properties of siloxane elastomers filled with bariumtitanate, 1999, J Polym Sci, Part B: Polym Phys., 37(21):3065-3070.

[3]   E. Venkatragavaraj, B. Satish, P.R. Vinod, M.S. Vijaya, 2001, J Phys D: Appl Phys., 34(4):487.

[4]   M. Akiyama, T. Kamohara, K. Kano, A. Teshigahara, Y. Takeuchi, N. Kawahara, 2009, Adv Mater., 21(5):593-596.

[5]   S.V. Glushanin, V.Y. Topolov, A.V. Krivoruchko, 2006, Mater Chem Phys., 97(2–3):357-364.

[6]   G. Rujijanagul, S. Jompruan, A. Chaipanich, 2008, Curr Appl Phys., 8(3–4):359-362.

[7]   J. Yao, C. Xiong, L. Dong, C. Chen, Y. Lei, L. Chen. et al, 2009, J Mater Chem., 19(18):2817-2821.

[8]   Y. Lin, H.A. Sodano., 2009, Adv Funct Mater., 19(4):592-598.

[9]   J.H. Park, T.Y. Kwon, D.S. Yoon, H. Kim, T.S. Kim., 2005, Adv Funct Mater., 15(12):2021-2028.

[10]   R.C. Twiney., Novel piezoelectric materials, 1992, Adv Mater., 4(12):819-822.

[11]   P. Moetakef, Z.A. Nemati., 2009, J Alloys Compd., 476(1–2):791-796.

[12]   C-B. Yoon, S-H. Lee, S-M. Lee, Y-H. Koh, H-E. Kim, K-W. Lee., 2006, J Am Ceram Soc. 89(8):2509-2513.

[13]   I. Babu, D. van den Ende, G. de With., 2010, J Phys D: Appl Phys., 43(42):425402.

[14]   A.C.C. Esteves, J. Brokken-Zijp, J. Laven, H.P. Huinink, N.J.W. Reuvers, M.P. Van et al., 2009, Polymer, 50(16):3955-3966.

[15]   W.K. Sakamoto, S. Shibatta-Katesawa, D.H.F. Kanda, S.H. Fernandes, E. Longo, G.O. Chierice., 1999, physica status solidi (a), 172(1):265-271.

[16]   W.K. Sakamoto, Ed. Souza, D.K. Das-Gupta., 2001, Materials Research, 4:201-204.

[17]   C-F. Yang, C-C. Wu, Y-C. Chen, C-C. Su., 2009, Appl Phys Lett., 94(5):052905-052905-052903.

[18]   J.W. Liou, B.S. Chiou., 1998, J Phys: Condens Matter., 10(12):2773.

[19]   S.K. Sharma, H. Gaur, M. Kulkarni, G. Patil, B. Bhattacharya, A. Sharma., 2013, Composites Science and Technology, 77(0):42-51.

[20]   L.J. Romasanta, P. Leret, L. Casaban, M. Hernandez, M.A. de la Rubia, J.F. Fernandez., et al, 2012, J Mater Chem., 22(47):24705-24712.

[21]   T. Bhimasankaram, S. Suryanarayana, G. Prasad., 1998, Current Science(India), 74(11):967-976.

[22]   N. Jayasundere, B.V. Smith., 1993, J Appl Phys, 73(5):2462-2466.

[23]   T. Yamada, T. Ueda, T. Kitayama., 1982, J Appl Phys, 53(6):4328-4332.

[24]   R.W. Sillars., 1937, Journal of the Institution, 80(484):378-394.

[25]   T.S. Low, W. Guo., 1995, J. MEMS, 4(4)230-237.

[26]   M.A. Jayaram., 2007, C. Prentice-Hall of India, p.19-20.

[27]   G. de With., 2008, Chapter 18, Structure, Deformation, and Integrity of Materials. Wiley-VCH Verlag GmbH, p. 569-591.

[28]   A.C.C. Esteves, J. Brokken-Zijp, J. Laven, G. de With., 2010, Progr Org Coat., 68: 12-18.

Chapter 4

Enhanced electromechanical properties of piezoelectric thin flexible films*

Highly flexible piezoelectric 0-3 PZT/PDMS (lead zirconate titanate - poly dimethyl siloxane) composites incorporated with carbon nanotubes (CNT) and carbon black (CB) were fabricated by solution casting technique using a constant PZT/PDMS ratio of 40/60 and conductive fillers ranging from 0 to 0.5 vol.%. Impedance measurements proved that a small addition of conductive fillers sufficiently enhanced the electrical conductivity to lead to improved poling efficiency. For too high volume fractions (and consequently too high conductivity), poling becomes impossible. For the optimum PZT/PDMS/0.125CNT a relative permittivity $\varepsilon_r \sim 50$ and conductivity $\sigma \sim 2.8 \times 10^{-6}$ S/m was obtained while for the optimum PZT/PDMS/0.125CB $\varepsilon_r \sim 35$ and $\sigma \sim 1.9 \times 10^{-6}$ S/m have been realized. The piezoelectric charge constant d_{33} of the PZT/PDMS/0.125CNT and PZT/PDMS/0.125CB composites were 25 and 18 pC/N, respectively. Dynamic mechanical analysis (DMA) shows better performance for PZT/PDMS/CB with lower volume fraction conductive fillers than for the PZT/PDMS/CNT composites. The excellent (di-)electrical properties and the relatively simple fabrication procedure of these composites make them promising candidates in piezoelectric sensors, actuators and high efficiency capacitors.

4.1. Introduction

Composites with piezoceramics and polymers have attracted much attention and have been the subject of many fundamental researches due to their technological potential. These composites, often named "smart materials", are optimized for special applications and can act as both sensors and actuators materials in many technical systems. The operation principle is the conversion of the mechanical energy into electrical energy [1-3]. Combining a piezoelectric ceramic and a polymer offers the advantage of flexibility and formability over ceramics with reduced sizes and lower operating voltages. The most widely used ceramic for such composite materials is lead zirconate titanate ($Pb(Zr_xTi_{1-x})O_3$ or PZT), with perovskite structure and a promising candidate material due to its excellent electromechanical properties [4-7]. Piezoelectricity produced by polar materials like PZT is applied over the whole range of piezoelectric devices that includes linear actuators, underwater acoustic signals, naval sonar devices, medical diagnostic systems and tactile sensors [8, 9].

The properties of these composites depend on the connectivity pattern of the ceramic and the polymer and the distribution and the size of the dispersed particles. The concept of connectivity was proposed by Newnham et al. to explain the piezoelectric behavior of the composites [10]. Many theoretical investigations have been carried out on such composites and the study done by Furukawa et al., Yamada et al. and Jayasundere et al. are considered to be the most extensive ones [11-13]. Out of these, composites with so-called 0-3 connectivity receive increasing attraction due to the ease of fabrication, high structural performance and the control of flexibility. The connectivity pattern 0-3 stands for the three dimensionally-connected polymer matrix filled with isolated ceramic particles.

Including nano-size conductive fillers like carbon nano tubes (CNT) and carbon black (CB) to 0-3 composites leads to a significant increase in the properties of the composites. Composites with conductive fillers have several advantages depending on the types used [14-19]. The use of CB as conductive filler is widely increasing because of its cost advantage and high surface area [20-22]. On the other hand, the addition of low concentration of CNT results in outstanding electrical and mechanical properties of the composites, but so far the use of CNT is limited due to their relatively high cost. As an advantage of the use of conductive fillers, previous research reported that their presence results in the formation of a continuous electric flux path between the ceramic grains and that poling can be carried out at low voltages and in shorter times [4, 23].

In a previous study, we reported on the processing and characterization of 0-3 PZT/LCT/PA composites [5]. Hot-pressing was utilized for the fabrication and the effect of the volume fraction of PZT on the piezoelectric and dielectric properties was studied.

71

In our recent work, the fabrication procedure and characterization of highly flexible 0-3 PZT/PDMS (lead zirconate titanate - poly dimethyl siloxane) composites is studied in detail [24]. The present work deals with the investigation of the enhancement of electromechanical properties of 0-3 PZT/PDMS composites incorporated with carbon nano tubes and carbon black.

4.2. Experimental

The ceramic powder used was a commercial PZT powder (PZT5A4) and the details of PZT powder used in this research are reported in [5]. The polymer used is linear vinyl-terminated poly (dimethylsiloxane) (PDMS17 with M_w = 17200 g/mol; ABCR GmbH & Co) cross-linked with the four-functional siloxane, tetrakis(dimethylsiloxane) (ABCR GmbH & Co). The same fabrication procedure [24] is followed with a constant PZT/PDMS ratio of 40/60 and conductive fillers ranging from 0 to 0.5 vol. % dispersed in low concentration, intended to result in isolated clusters. The incorporated carbon nano tubes (MWCNT-7000) from Nanocyl and carbon black CB Printex.

Impedance data of the composites were collected by an impedance analyzer (EG&G Princeton Applied Research, Model 1025) coupled with a potentiostat (Potentiostat/Galvanostat, Model 283) at room temperature at a frequency range of 10 mHz – 5 MHz. The piezoelectric charge constant was measured with a d_{33} meter (Piezotest, PM300) at a fixed frequency of 110 Hz. The microstructure of the composites was examined by SEM (FEI, Quanta 3D FEG). The mechanical properties of the composite films were tested in a tensile mode on DMA (TA Instruments Q800 series) at room temperature. The static elastic modulus of the composites was measured by performing stress-strain tests with a strain rate of 0.5% min^{-1}. The dynamic behavior of composites were studied using a temperature ramp. The specimens are heated at a constant rate of 3 °C/min. While heating, the specimens are deformed at constant amplitude over a single frequency.

4.3. Results and Discussion

4.3.1. Impedance Measurements

Figure 1 shows the dependence of the ac conductivity σ, the relative permittivity ε_r and the loss tangent tan δ of the PZT/PDMS/CNT composites, the 40PZT/PDMS composite and the pure PDMS as a function of log frequency and volume fraction filler. Figure 1 (a) presents the conductivity of the pure PDMS and 40PZT/PDMS composite compared with PZT/PDMS/CNT composites. The results showed that conductivity increases

significantly with increasing volume content of CNTs. It is observed that even with a 0.125 vol. % CNTs, the composites became electrically conductive to some extent and with higher volume fraction (0.25 and 0.5 vol.%) the composites show high electrical conductivity. Since an abrupt change in conductivity is observed between 0.125 and 0.25 vol. % , it is concluded that the percolation threshold is in the neighborhood of 0.125 vol. % CNTs. As the volume fraction of CNTs increases, they tend to link together to form conductive networks which leads to a significant increase in the electrical conductivity of the composite. The resulting high conductivity of these PZT/PDMS/CNT composites (0.25 and 0.5 vol. % of CNTs) prevents their poling.
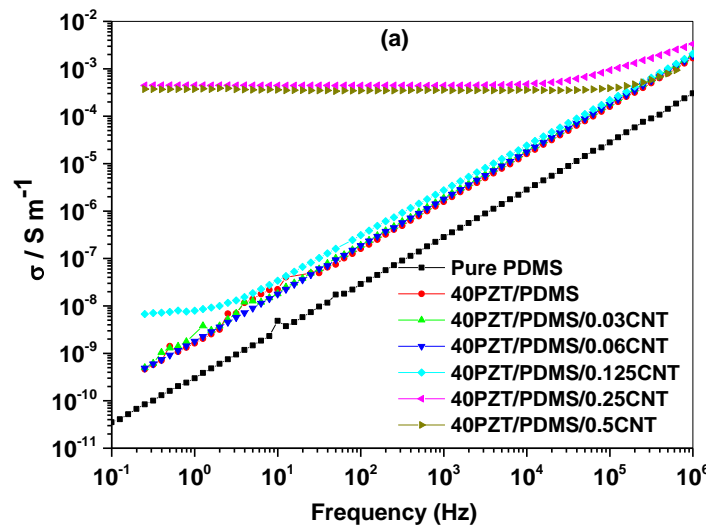

Figure 1(a). *The dependence of conductivity σ, of PZT/PDMS/CNT composites, 40PZT/PDMS composites and pure PDMS as a function of frequency.*

Figure 1 (b) presents the variation of the relative permittivity ε_r of the pure PDMS and 40PZT/PDMS composite compared with PZT/PDMS/CNT composites. It is observed that PZT/PDMS/CNT composites show significantly higher ε_r than the pure PDMS (ε_r = 2.64) and the 40PZT/PDMS composite. As the CNT concentration approaches to the percolation threshold, interfacial polarization (blockage of the charge carriers at internal interfaces) contributes to the steep increase in ε_r. Another reason for the abrupt enhancement in the ε_r is due to the formation of a micro-capacitor structure (isolated CNT clusters with the polymer matrix as a thin dielectric layer) originating from the interfaces of CNTs, PZT and the polymers, the so-called insulator-conductor interfaces. As the content of CNTs increases, the insulation layer between the CNT clusters decreases, the capacitance of the micro-capacitors increases and consequently the effective ε_r of the composite increases [25-27].

Figure 1 (c) shows the variation of tan δ and indicates that dielectric loss is less than 0.1 down to a frequency of 1000 Hz with composites containing 0.5 and 0.25 vol. %

CNTs but showing a strong increase with decreasing frequency. The increase in tan δ with the presence of a conductive phase is related to the increase of the electrical conductivity of the composite. Arbitrarily setting the maximum value for tan δ for a material to be applicable at 0.2, we note that for the composites containing 0.125 vol. % CNTs the tan δ = 0.09 in the low frequency region and showing a further decrease with increase in frequency.

Figure 1(b). *The dependence of permittivity ε_r of PZT/PDMS/CNT composites, 40PZT/PDMS composites and pure PDMS as a function of frequency. In the inset a magnified view of ε_r is shown.*

Figure 1(c). *The dependence of permittivity tan δ of PZT/PDMS/CNT composites, 40PZT/PDMS composites and pure PDMS as a function of frequency. In the inset a magnified view of tan δ is shown.*

Figure 2(a). *The dependence of the conductivity σ of PZT/PDMS/CB composites, 40PZT/PDMS composite and pure PDMS as a function of frequency.*

Figure 2(b). *The dependence of the permittivity ε_r of PZT/PDMS/CB composites, 40PZT/PDMS composite and pure PDMS as a function of frequency. In the inset for ε_r a magnified view is shown.*

Figure 2 shows the dependence of the conductivity σ, the relative permittivity ε_r and the loss tangent $\tan\delta$ of the PZT/PDMS/CB composites, the 40PZT/PDMS composite and pure PDMS as a function of log frequency and volume content. Figure 2 (a) shows that the PZT/PDMS/0.5CB composites become electrically conductive while the rest of the PZT/PDMS/CB composites have a conductivity only slightly higher than that of the 40PZT/PDMS composite. From Figure 2 (b) one observes that ε_r increases with increasing volume fraction of CB and that the PZT/PDMS/0.5CB composite shows a somewhat higher ε_r in the lower frequency region. The dielectric loss factor is

moderate in the low frequency region with composites containing a high volume fraction CB and for the rest of the composites the tan δ values are lower than 0.2.
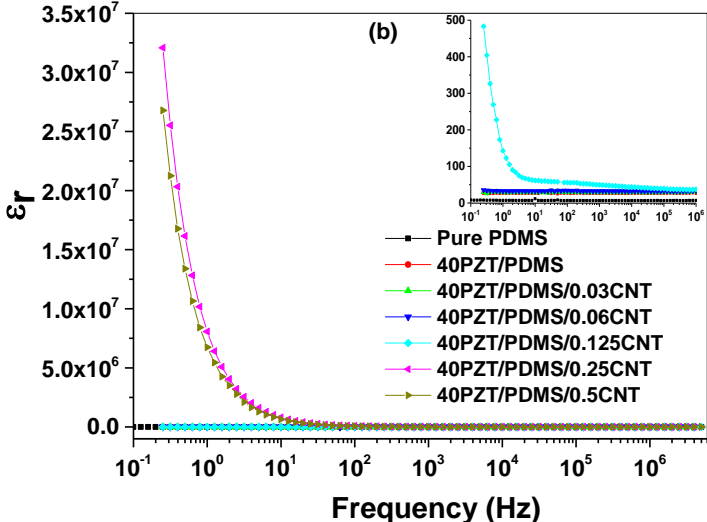

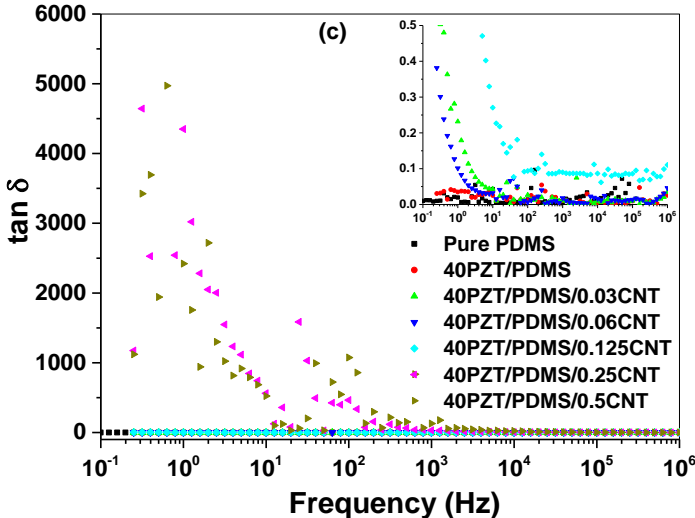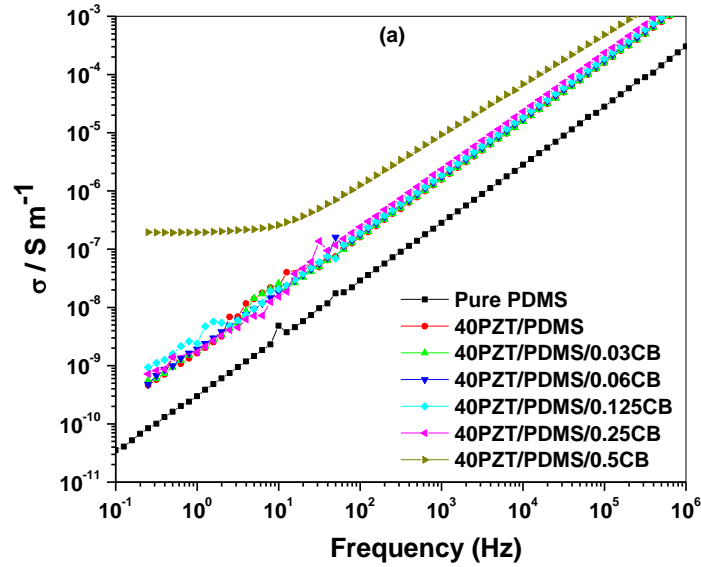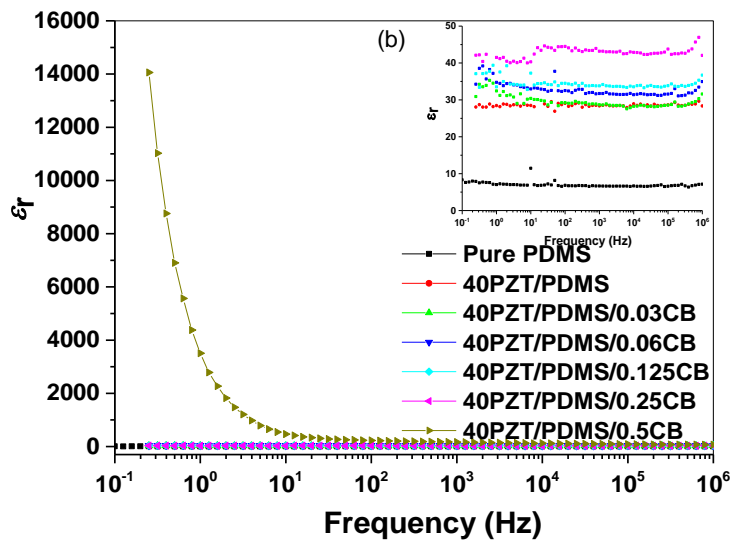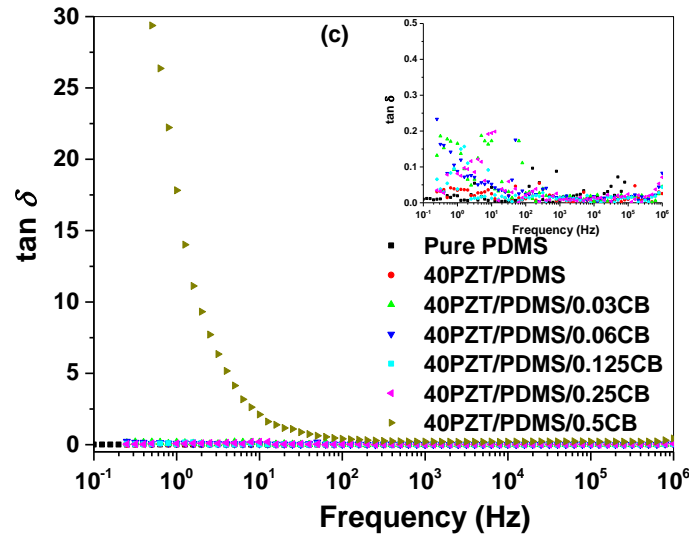**Figure 2 (c).** *The dependence of tan δ of PZT/PDMS/CB composites, 40PZT/PDMS composite and pure PDMS as a function of frequency. In the inset for tan δ a magnified view is shown.*

Table 1. *Comparison of measured values of σ, ε_r and tan δ at 1000 Hz. The piezoelectric charge constant d_{33} is also added for comparison.*

	σ (S/m)	ε_r	tan δ	d_{33} (pC/N)
Pure PDMS	2.83×10^{-7}	7	0.009	-
40PZT/PDMS	1.57×10^{-6}	28	0.01	11.4
40PZT/PDMS/0.03CNT	1.88×10^{-6}	29	0.011	12
40PZT/PDMS/0.06CNT	1.86×10^{-6}	32	0.014	16
40PZT/PDMS/0.125CNT	2.75×10^{-6}	50	0.083	24.6
40PZT/PDMS/0.25CNT	4.43×10^{-4}	7991	32	-
40PZT/PDMS/0.5CNT	3.58×10^{-4}	6500	123	-
40PZT/PDMS/0.03CB	1.59×10^{-6}	28	0.014	13
40PZT/PDMS/0.06CB	1.75×10^{-6}	31	0.014	14
40PZT/PDMS/0.125CB	1.87×10^{-6}	35	0.016	18
40PZT/PDMS/0.25CB	2.33×10^{-6}	43	0.021	-
40PZT/PDMS/0.5CB	9.38×10^{-4}	168	0.213	-

Table 1 summarizes the measured values of σ, ε_r and tan δ of pure PDMS, 40PZT/PDMS, PZT/PDMS/CNT and PZT/PDMS/CB composites at 1000 Hz. The observed higher electrical properties of PZT/PDMS/CNT and PZT/PDMS/CB composites is as expected and is due to the presence of conductive fillers that creates electric flux paths between the ceramic inclusions, which in turn increase the electric

field enabling improved poling efficiency. The PZT/PDMS/CNT composites exhibited an abrupt increase in electrical properties above 0.125 vol.% CNTs indicating that a percolation threshold is reached between 0.125 and 0.25 vol. % CNTs, while for the PZT/PDMS/CB composites the percolation threshold is reached in between 0.25 and 0.5 vol.% CB. The obtained percolation threshold is in accordance with the previous results [17, 19].

The frequency dependence of the permittivity ε_r of these composites shows a power law dependence, i.e. $\varepsilon_r \sim \omega^{u-1}$, where ω is the angular frequency and u an exponent with value between 0 and 1. A value of $u = 0.7$ is indicative for the presence of a percolating network [28-29]. We limited the fit range on the low side to 100 Hz since below that frequency a plateau is present, starting at ~ 50 Hz for the CNT composites and ~ 5 Hz for the CB composites. As shown in figure 3, for the optimum volume fractions the exponent $u = 0.95$ for the CNT composite and $u = 0.85$ for the CB composites. This indicates that the conductive fillers do not result in an ideal percolation network, as probably could have been expected. Nevertheless the homogeneity of the conductive network is sufficiently good that an improved poling can be realized.
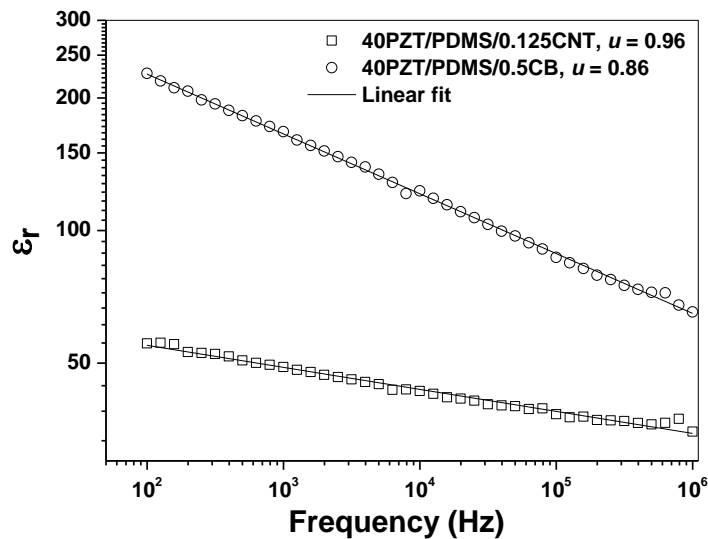
Figure 3. *Frequency dependence of the permittivity and line fit.*

Several investigators also reported similar results of obtaining a high ac conductivity σ and relative permittivity ε_r for slightly conductive composites. Rujijanagul et al. [16] and Liu et al. [4] reported that the presence of conductive phase creates a better conduction path between piezoelectric particles leading to better poling efficiency which enhances the dielectric properties. A similar result of obtaining a high conductivity with the presence of CNTs was reported by Lisunova et al. [30]. Using

CNTs, a percolation threshold can be achieved at a very low concentration, much lower than for CB. This sharp enhancement of conductivity with CNTs incorporated composites is due to the high aspect ratio and specific surface areas of the CNTs.

4.3.2. Piezoelectric properties

Figure 4 shows the dependence of the piezoelectric charge constant d_{33} of 40PZT/PDMS and PZT/PDMS composites containing CNTs and CB with a varying volume fraction of 0.03, 0.06 and 0.125. For the pure 40PZT/PDMS composite the obtained d_{33} is 11.4 pC/N. It is observed that the presence of conductive fillers enhances the piezoelectric charge constant, where the 40PZT/PDMS/CNT composites show a larger effect than 40PZT/PDMS/CB composites. The d_{33} of 40PZT/PDMS/CNT composites increases from 11.4 to 24.6 and from 11.4 to 18 for 40PZT/PDMS/CB composites. This increase in d_{33} is probably due to the presence of the conductive fillers that reduce the effective polymer resistivity thus leading to a more effective poling of the ceramic.
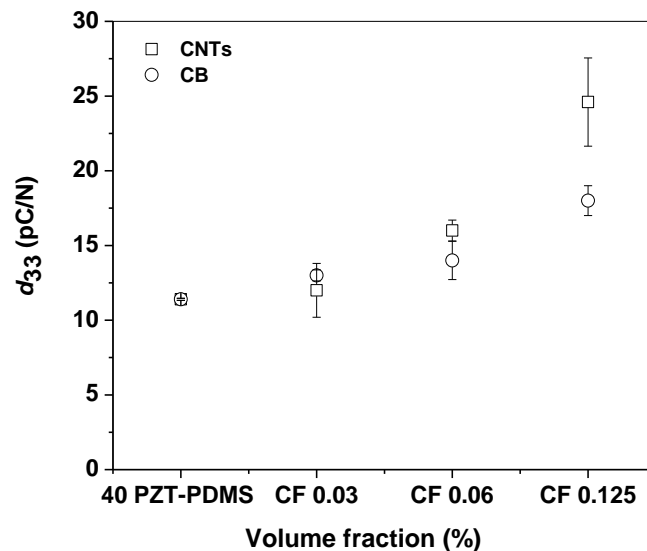
Figure 4. *Dependence of d_{33} of PZT/PDMS composites containing conductive fillers (CF).*

4.3.3. Morphology

Sakamoto et al. [23] reported similar results of enhancing the piezoelectric effect with the presence of conductive fillers by creating a continuous electric flux path between the PZT grains during poling. Twiney et al. [8] reported that the doping of polymer composites with conductive fillers reduces the effective polymer resistivity but that this also has the effect of increasing the material dielectric loss. Levi et al. [31] observed an enhancement in piezoelectric behavior with the CNTs inclusion in the PVDF/nanotube blends.

Scanning electron microscopy (SEM) analyzes were performed to investigate the homogeneity of the dispersed PZT, conductive fillers and the microstructure. Figure 5 (a) shows the SEM cross-section of the 40PZT/PDMS/0.5CNT composites. It is hard to see the dispersed conductive fillers due to the presence of PZT particles. Clearly the PZT particles are dispersed homogeneously in the PDMS matrix and are well adhering to the polymer matrix. Figure 5 (b) shows the photographs of 40PZT/PDMS and 40PZT/PDMS/0.5CNT composites demonstrating flexibility of the composites and their folding capacity.
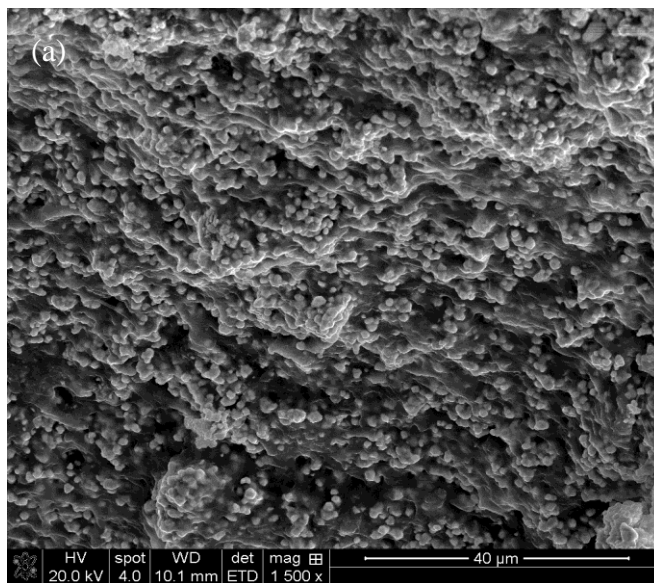

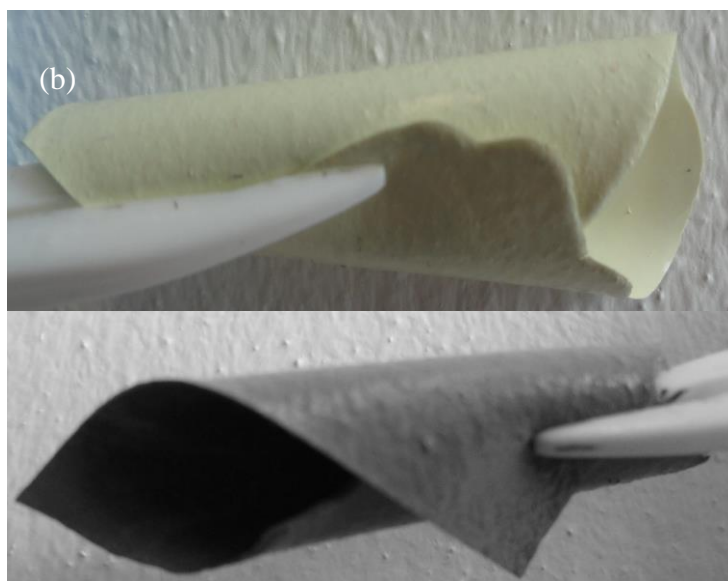**Figure 5 (a).** *SEM cross-section of the 40PZT/PDMS/0.5CNT composites.*

Figure 5 (b). *Photographs of 40PZT/PDMS (yellow) and 40PZT/PDMS/0.5CNT (black).*

4.3.4. Mechanical properties

Table 2 shows the static elastic modulus *E* obtained from the stress-strain curve of all the volume fractions of conductive fillers incorporated PZT/PDMS composites including the pure PDMS and 40PZT/PDMS. The static elastic modulus is measured using the 1-2 % strain range. It is observed that for the 40PZT/PDMS/CB (0.03 and 0.06 vol. %) composites, a slightly higher modulus is observed than for the 40PZT/PDMS composite. This is probably due to the good dispersion of CB at this volume fraction in the polymer matrix with reasonable adhesion to the matrix. But as the content of CB increases, the modulus decreases probably due to the formation of agglomerates, resulting in improper impregnation with less adhesion to the matrix, and effectively acting as voids.

Table 2. *Static elastic modulus of CNTs and CB incorporated PZT/PDMS composites.*

PZT/PDMS Composite	*E* (MPa)	CNTs (MPa)	CB (MPa)
Pure PDMS [a]	0.78 (–47 °C)	x	X
40PZT/PDMS [a]	7.32 (–45 °C)	x	X
0.03	x	7.42	7.59
0.06	x	2.51	7.9
0.125[a]	x	3.42 (–41°C)	5.05 (–41.5 °C)
0.25	x	2.51	3.03
0.5[a]	x	3.12 (–42 °C)	3.10 (–42 °C)

[a]T_gs are shown in brackets.

Similar behavior is observed for the 40PZT/PDMS/CNT composites, but the observed modulus is somewhat lower than for the 40PZT/PDMS/CB composites. This could be due to the strong attractive forces of CNTs leading even more easily to agglomeration. Gojny et al. [15] and So *et al*. [32] also reported similar results and indicated that the weak interfacial interaction between CNTs and the matrix could be one of the reasons for the reduction in the mechanical properties of the CNTs incorporated composites. Chen et al. [20] also reported similar results of deteriorating mechanical properties with increasing volume fraction of conductive fillers.
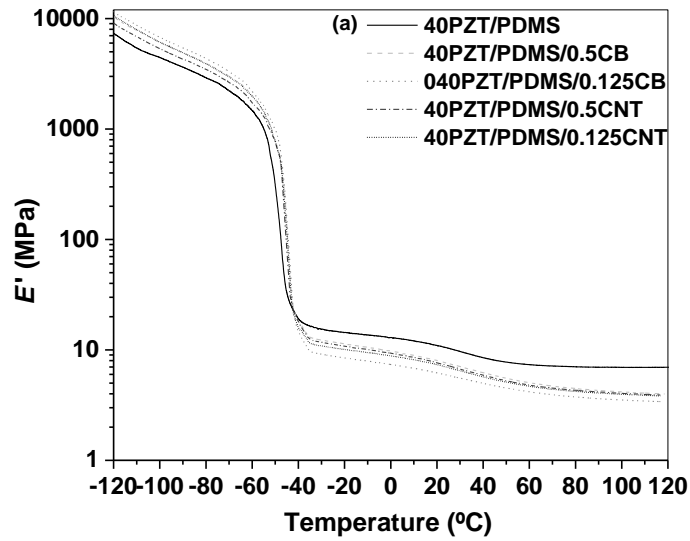
Figure 6 (a). *Dynamic behavior of composites incorporated with CNTs and CB (a) Storage modulus.*
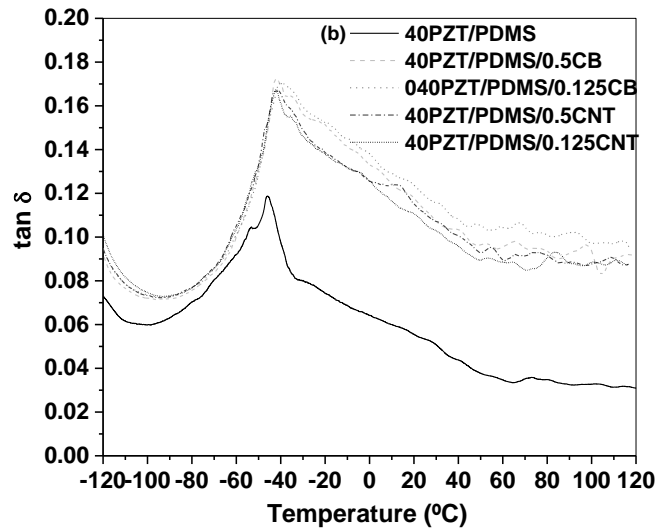
Figure 6 (b). *Dynamic behavior of composites incorporated with CNTs and CB (b) tan δ.*

Figure 6 shows the dynamic elastic behavior of 40PZT/PDMS, 40PZT/PDMS/CNT and 40PZT/PDMS/CB composites (0.125 and 0.5 vol. %) in tension as studied using a temperature ramp mode in the temperature range of –120 °C to +120 °C. The specimens are heated at a constant rate of 3 °C/min. While heating, the specimens are deformed at constant amplitude of 5 μm using a single frequency of 1 Hz.

Figure 6 (a) displays the variation of the storage modulus as a function of temperature. The variation of the profiles looks similar and the drop of storage

81

modulus by more than two orders of magnitude corresponds to the glass transition temperature. The T_g of the 40PZT/PDMS/CNT and 40PZT/PDMS/CB composites shifted to slightly higher temperature, which is attributed to the interaction between the matrix and the fillers. It is also evident from the modulus-temperature curves that the incorporation of conductive fillers leads to a decrease in storage modulus above T_g. This decrease in the storage modulus at room temperature is in agreement with the results obtained from the static measurements and probably due to the loss in structural rigidity of the composite because the conductive fillers are but weakly (or not at all) bonded to the matrix and consequently effectively act as voids. Below T_g the values of the conductive filler composites are above those of 40PZT/PDMS. The reason probably can be found in the large change of mechanical properties with temperature. Using a thermal expansion coefficient of 310 pp/K [33] and a T_g ~ −40 °C, the strain developed at −80 °C is about 0.012, far exceeding the external strain applied during the measurement. This implies that the contraction of the PDMS matrix provides a significant clamping of the conductive fillers, rendering them effectively to act as stiffeners.

Figure 6 (b) displays the (mechanical) tan δ curves exhibiting similar profiles. The peak in the loss curves corresponds to the T_g of the composites. The loss factor tan δ is an indication of the efficiency of the material to dissipate the mechanical energy, i.e. to damp vibrations. At room temperature tan δ = 0.05 for the 40PZT/PDMS composites, while for the 40PZT/PDMS/CNT and 40PZT/PDMS/CB composites tan δ ~ 0.12. In fact, tan δ is higher for the composites at all temperatures. Since the increase is similar for all composites, it is probably due to the further restraint by the fillers on the polymer network and not by any specific interaction.

4.4. Conclusions

Flexible 0-3 piezoelectric flexible PZT/PDMS/CNT and PZT/PDMS/CB composites were fabricated by solution casting. The electromechanical properties and the characterization of the composites were studied as a function of the volume fraction and frequency. The uniform distribution of the PZT and conductive fillers was realized by the step up increase in the conductivity and relative permittivity. Both set of composites show an optimum for which the enhanced electrical properties result in improved poling efficiency. The optimum compositions, limiting the (electrical) tan δ values to smaller then 0.2, are in the vicinity of percolation threshold and resulted in ε_r ~ 50, d_{33} ~ 25 pC/N and σ ~ 2.8×10^{-6} S/m for PZT/PDMS/0.125CNT and ε_r ~ 35, d_{33} ~ 18 pC/N and σ ~ 1.9×10^{-6} S/m for PZT/PDMS/0.125CB composites. In this study we realized a simple fabrication procedure for highly dense piezoelectric composites

containing CNTs and CB with a combination of high dielectric constant and low dielectric loss. The advancement in properties of this multifunctional composite material provides much benefit over other types of 0-3 piezoelectric composites in terms of relative permittivity and piezo-electric charge constant.

References

[1]   X. Chen, S. Xu, N. Yao and Y. Shi, *Nano Lett.,* 2010, *10* (6), p. 2133-2137.

[2]   Y. Lin and H.A. Sodano, *Adv. Funct. Mater.*, 2009, *19* (4), p. 592-598.

[3]   Y. Qi, N.T. Jafferis, K. Lyons, C.M. Lee and H.Ahmad, and M.C. McAlpine,*Nano Lett.* 2010, *10* (2), p. 524-528.

[4]   X.F. Liu, C.X. Xiong, H.J. Sun, L.J. Dong,R. Li, and Y. Liu, *Materials Science and Engineering: B* 2006, *127* (2-3), p. 261-266.

[5]   I. Babu, D. A. v. d. Ende and G. de. With, *J. Phys. D: Appl. Phys.* 2010, *43* (42), 425402.

[6]   G.L. Brennecka, C.M. Parish, B.A. Tuttle, L.N. Brewer, amd M.A. Rodriguez, *Adv. Mater.* 2008, *20* (8), p. 1407-1411.

[7]   P. Moetakef and Z.A. Nemati, *J. Alloys Compd.* 2009, *476* (1-2), p. 791-796.

[8]   R.C. Twiney, *Adv. Mater.* 1992, *4* (12), p. 819-822.

[9]   C.B. Yoon, S.H. Lee, S.M. Lee, Y.H. Koh, H.E. Kim, and K.W. Lee, *J. Am. Ceram. Soc.* 2006, *89* (8), p. 2509-2513.

[10]   R.E. Newnham, D.P. Skinner and L.E. Cross, *Mater. Res. Bull.* 1978, *13* (5), p. 525-536.

[11]   N. Jayasundere and B.V. Smith, *J. Appl. Phys.* 1993, *73* (5), p. 2462-2466.

[12]   T. Furukawa, K. Fujino, and E. Fukada, *Japanese Journal of Applied Physics* 1976, *15* (11), p. 2119-2129.

[13]   T. Yamada, T. Ueda and T. Kitayama, *J. Appl. Phys.* 1982, *53* (6), p. 4328-4332.

[14]   S. Tian and X. Wang, *Journal of Materials Science* 2008, *43* (14),p. 4979-4987.

[15]   F.H. Gojny, M.H.G. Wichmann, B. Fiedler and K. Schulte, *Composites Science and Technology* 2005, *65* (15-16), p. 2300-2313.

[16]   G. Rujijanagul, S. Jompruan and A. Chaipanich, *Curr. Appl. Phys.* 2008, *8* (3-4), p. 359-362

[17]   S. Banerjee and K.A. Cook-Chennault, *Composites Part A: Applied Science and Manufacturing* 2012, *43* (9), 1612-1619.

[18]   H. Gong, Y. Zhang, J. Quan and S. Che, *Curr. Appl. Phys.* 2011, *11* (3), p. 653-656.

[19]   M. Ma and X. Wang, *Mater. Chem. Phys.* 2009, *116* (1), p. 191-197.

[20]   G. Chen, B. Yang, S. Guo, *Journal of Applied Polymer Science* 2009, *114* (3), p. 1848-1855.

[21]   H. Gong, Z. Li, Y. Zhang and R. Fan, *J. Eur. Ceram. Soc.* 2009, *29*, p. 2013-2019.

[22]   M. Knite, V. Teteris, A. Kiploka and J. Kaupuzs, *Sensors and Actuators A: Physical* 2004, *110*, p. 142-149.

[23]   W.K. Sakamoto, E.d. Souza and D.K. Das-Gupta, *Materials Research* 2001, *4*, p. 201-204.

[24]   I. Babu and G. de. With, *Composites Science and Technology*. 2013; Submitted.

[25]   S.H. Yao, Z.M. Dang, M.J. Jiang and J. Bai, *Appl. Phys. Lett.* 2008, *93* (18).

[26]   J.K. Yuan, W.L. Li, S.H. Yao, Y.Q. Lin and A. Sylvestre, J. *Appl. Phys. Lett.* 2011, *98* (3).

[27]   Z.M. Dang, S.H. Yao, J.K. Yuan and J. Bai, *The Journal of Physical Chemistry C* 2010, *114* (31), p. 13204-13209.

[28]   L. Wang and Z.M. Dang, *Appl. Phys. Lett.* 2005, *87* (4), 042903.

[29]   Q. Chen, P. Du, L. Jin, W. Weng and G. Han, *Appl. Phys. Lett.* 2007, *91* (3), 022912.

[30]   M.O. Lisunova, Y. P. Mamunya, N.I. Lebovka and A.V. Melezhyk, *Eur. Polym. J.* 2007, *43* (3), p. 949-958.

[31]   N. Levi, R. Czerw, S. Xing, P. Iyer and D.L. Carroll, *Nano Lett.* 2004, *4* (7), p. 1267-1271

[32]   H.H. So, J.W. Cho and N.G. Sahoo, *Eur. Polym. J.* 2007, *43* (9), p. 3750-3756.

[33]   CTE data available at http://www.dowcorning.com.

Chapter 5

Design, fabrication and performance analysis of piezoelectric PZT composite bimorphs*

A disc type reinforced piezoelectric composite bimorphs with series connection was designed and the performance was investigated. The composite bimorphs (PZT/PA and PZT/PDMS (40/60 vol.%)) were successfully fabricated by compression molding and solution casting technique. The charge developed at an applied force of 150 N is 18150 pC (PZT/PA) and 2310 pC (PZT/PDMS), respectively. Electric force microscopy (EFM) is used to study the structural characterization and the piezoelectric properties of the materials realized. A clear inverse piezoelectric effect was observed when the bimorphs were subjected to an electric field stepped up through 2, 6 and 10 V, indicating the net polarization direction of the different ferroelectric domains. The as-developed bimorphs have the basic structure of a sensor and actuator and since they do not use any bonding agent for bonding, they can provide a valuable alternative to the present bimorphs where bonding processes required for their realization, can limit the application at high temperature.

5.1. Introduction

Knowledge on piezoelectricity enables the realization of new types of smart materials as sensors and actuators. This phenomenon is caused by the non-centrosymmetric crystal structure of certain materials, which has the ability to convert mechanical energy into electric energy and vice versa. Various structures (unimorphs, bimorphs, etc.) have been developed on the basis of such materials and the realization and characterization of such strained materials is important in developing devices for novel applications. In particular, flexible soft composite materials relate to transducer and sensor applications for the generation and detection of underwater acoustic signals (sonar), medical diagnostic systems (e.g. micropumps in micro- and nano-fluidic devices) and tactile sensors (energy scavenger for aerospace / automotive / domestic devices or touch-base switches for the consumer market). Piezoceramic materials are available in a large variety of shapes and forms. These materials are fabricated in many different ways: sputtering, metal organic chemical vapor deposition (MOCVD), chemical solution deposition (CSD), the sol gel method and pulsed laser deposition (PLD) which is a physical method by thermal evaporation. PLD technique is the most popular and powerful one in terms of stoichiometric transfer from the multi component oxide target to the growing film and its easy applications of PZT material. However, PLD has shortcomings too, in particular the oxygen content in the deposited layer may differ from that of the target and sometimes large entities are deposited, leading to a particulate nature of the films realized. The size of these particulates may be as large as few micrometers [1-3]. Several papers have been published on various designs using functionally graded layered piezoelectric materials, realized by different fabrication technique for a variety of applications [4-8].

A piezoelectric composite, incorporation of a piezoelectric-ceramic in a polymer, takes the advantage of the flexibility of a polymer and the piezoelectric effect of the piezoelectric-ceramics. The main advantage of these materials is the ease of formability into any shape and the flexibility of the resulting composite material. Moreover, this can also reduce the cost of the material. Conventionally, piezocomposites are fabricated by two ways; solid- and liquid-phase processes. Solid phase process usually involve mechanical approaches like direct compounding and melt compounding. Liquid-phase processes involve solvent assisted dispersion of the piezo-material in the polymer monomer followed by in-situ polymerization processes [9].

Conventional bimorphs have higher stroke value but develop lower force. The use of amplifiers in bimorphs can lead to large displacements. The magnitude of the generated voltage in the bimorphs is relative to the type of piezo active material, amount of deflection and the structure. Bimorphs are used as converters of electric

input to mechanical motion or vice versa, in applications such as actuators, sensors, loudspeakers, microphones, precise machining and phonographs [10-14]. Piezoelectric composite bimorphs are a good solution where more displacement is required and no high forces are needed. Piezoelectric composite bimorphs consists of two piezoelectric layers stacked on top of each other and can produce displacements in precise submicron increments. Typically two possible arrangements play the key role in making this structure smarter, series and parallel. For both series and parallel connections, outer surfaces are coated with electrodes. In some cases a third electrode is placed in between which act as an electrode and as reinforcement in bimorphs. In series connection, the two piezoelectric layers have opposite polarization, while in parallel bimorphs with same polarization direction [15-17]. Figure 1 shows the schematic representation of the type of bimorph used in this study.

In this work, we investigated the design and performance of two types of composite bimorphs with series connection. The design of bimorph is as follows: the bimorph consists of two circular piezoelectric disks, which are separated by a metal plate aluminium, which act as central electrode and also as reinforcement. The as fabricated bimorph operates in bending mode. An application of a bending moment will result in the signals from the two unimorphs, arising from the piezoelectric d_{31} coefficients, complimenting each other. During operation, the top half of the bimorph will be under compression while the bottom half in tension creating the signals with the same polarity (when the plates are of opposite polarity, the resulting electrical fields, and hence the voltages, have the same direction) because the applied stresses are of opposite signs.

We employed two types of composites, PZT/PA and PZT/PDMS, both using lead zirconate titanate (PZT) as piezoelectric filler. The matrix consisted of polyamide (PA) and poly dimethyl siloxane (PDMS). In the conventional fabrication process of bimorphs, the piezoelectric plates are bonded by bonding agents which limits there application at elevated temperatures due to the glass transition temperature of the bonding agents [18-22]. As a result the maximum application temperature at which piezo-bimorphs can be used is about 100 - 150 °C. The present fabricated piezo bimorphs (PZT-PDMS) have a good thermal stability up to 300 °C. Thermal gravimetric analysis on similar composites have shown that these materials are thermally stable in nitrogen and air up to at least 300 °C [23]. In fact, the presence of the particles does seem to have a significant influence on the thermal stability. Since the Curie temperature of the PZT is about 360 °C, these composites can be used up to a temperature close to the Curie temperature [24].

This new design using reinforced bimorphs overcome this limitation by fabricating the two piezoelectric plates together in a single operation via compression

molding (PZT/PA) and adhesion by solution casting (PZT/PDMS). These bimorphs have the basic structure of a sensor and/or actuator and have several advantages over other types of bimorphs that is the flexibility of obtaining different sizes and shapes due to easy processing and the possibility of tailoring the properties by varying the volume fraction of the ceramic inclusions and the low price.
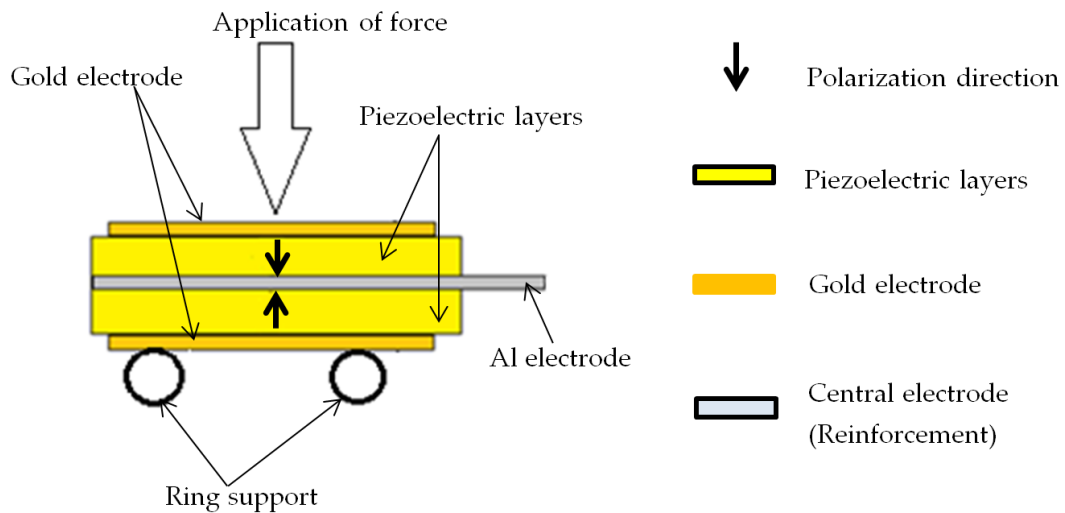
Figure 1. *Schematic side-view of the bimorphs realized in this study and the loading configuration using a ring support and central load for the charge measurement.*

5.2. Experimental

5.2.1. Materials

The PZT powder used in this research is a commercial half-product PZT5A4 (Morgan Electro Ceramics, Ruabon UK), a soft PZT with 1 mol% Nb added as dopant. Before use it was thermally treated, as reported in [25] where further details can be found. The average size of the filler is about 1.0 μm and the details of the filler size also can be found in [25]. The polymer used are polyamide PA 11 (Aldrich Chemical Company) and linear vinyl-terminated poly (dimethylsiloxane) (PDMS17 with M_w = 17200 g/mol; ABCR GmbH & Co) cross-linked with the four-functional siloxane, tetrakis(dimethylsiloxane) (ABCR GmbH & Co). The hydrosilylation reactions were catalyzed by cisdichlorobis (diethylsulphide) platinum (II) catalyst (Strem Chemicals, Inc) previously dissolved in a toluene solution. Esteves et al. [26] reported on the details of the hydrosilylation addition reaction to obtain cross-linked (tri-dimensional network) PDMS composites by reacting functional end groups on the PDMS chains with a multifunctional cross-linker in the presence of a

catalyst. We used the same hydrosilylation addition reaction to realize the PZT-PDMS composites [27].

5.2.2. Fabrication of composites

The disc type PZT/PA reinforced bimorphs with specific dimensions of 14 mm in diameter and ~350 μm thickness with an aluminum foil as central electrode (thickness 15 μm) were fabricated by hot-pressing with an applied force of 100 kN for 15 minutes. The disc type PZT/PDMS reinforced bimorphs with specific dimensions of 20 mm in diameter and ~250 μm thickness with an aluminum foil as central electrode (thickness 15 μm) were fabricated by solution casting.
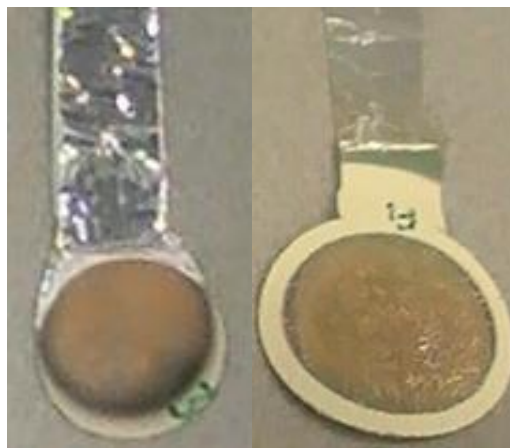
Figure 2. *Fabricated (a) PZT/PA and (b) PZT/PDMS bimorphs with aluminum foil as central electrode.*

In brief, the materials PZT (40 vol. %) and PDMS (60 vol. %) were mixed in a speed mixer (DAC 150 FVZ) at 3000 rpm for 2 minutes and the appropriate amount of cross-linker is added and mixed again for 1 minute and finally the catalyst is added and mixed for 1 minute. This mixture is directly solution casted on an aluminum foil and subsequently dried and cured under vacuum initially at 60 °C for 20 hours and at 110 °C for 5 hours. The other side of aluminum foil (dried and cured with adhering PZT/PDMS) is again solution casted with the same mixture as mentioned above and the process is repeated. This process resulted in a PZT/PDMS bimorph in which the central aluminium electrode is coated on both sides with the PZT/PDMS mixture. Using a cutter the required shape of the bimorphs is realized, while the outer electrodes are provided by sputter coating. Circular gold electrodes of thickness 30 nm and an area of 7.85×10^{-5} m^2 (PZT/PA) and 15.3×10^{-5} m^2 (PZT/PDMS) are sputtered on both sides of the composites using an Edwards sputter coater (model S150B). The poling of the

electroded sample is performed by applying an electric field of 60 kV/cm with a Heinziger 10 kV high voltage generator for 30 min at 60 °C in a silicone oil bath to ensure uniform heating. The two piezoelectric layers are poled in the opposites direction, by applying a positive DC bias to the middle electrode and the negative bias to the top electrode. The bottom electrode is grounded. The electric field was kept on during cooling to room temperature. Figure 2 shows the as fabricated PZT/PA and PZT/PDMS bimorphs.

5.2.3. Measurements

Electrical Measurements

The bimorphs were characterized with respect to their piezoelectric properties and electrical properties. The piezoelectric charge constant d_{31} was measured with a d_{33} meter (Piezotest, PM300) at a fixed frequency of 110 Hz. The capacitance and the loss tangent $\tan \delta$ of the composites were also measured with the d_{33} meter. The relative permittivity ε_r was calculated according to

$$\varepsilon_r = Ct / \varepsilon_0 A \qquad (1)$$

where C is capacitance, t is the thickness, ε_0 is the permittivity of free space (8.85×10^{-12} F/m) and A is the area of the deposited electrode on the bimorph.
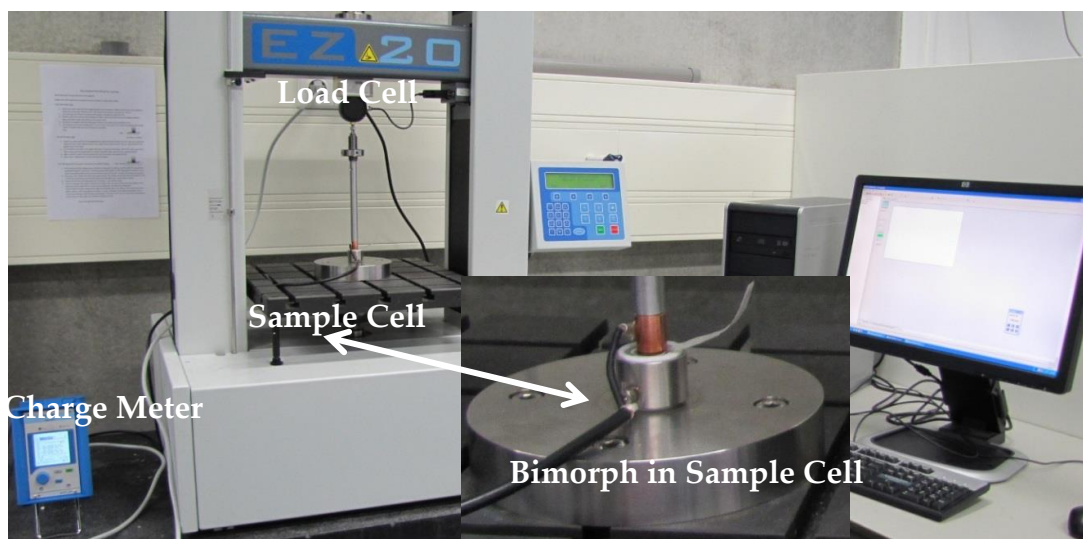
Charge Output Measurements

Figure 3. *Experimental setup for measuring the charge developed in the bimorphs.*

The charge developed in the bimorphs to a known applied static force was measured using a charge meter (Kistler, Type 5015A). The applied force is induced through a tensile machine (LLOYD Instruments). The setup consists of a computer operated tensile machine with a load cell of 500 N, charge meter, sample cell and the bimorph sample. The sample cell consists of two O-rings (insulating Teflon ring and conductive metal ring) with 20 and 10 mm in diameter, respectively. The insulating O-ring has a diameter similar to that of the sample, which rest on the metal O-ring having diameter lower than the sample. The sample rests on the metal ring (connected to the charge meter) and the outer edge of the sample is in connection with the insulating O-ring as insulation. Figure 3 shows the experimental setup for measuring the charge developed in the bimorphs when a known force is applied.

Structural characterization

Electrostatic force microscopy (EFM) is dynamic AFM where the electrostatic force is probed. Using a conductive tip, it is possible to electrically bias the oscillating tip with respect to the sample and to probe the long-range electrostatic interactions. Electric force microscopy (EFM) is a scanning probe technique to characterize the electrical properties of nanostructures, imaging the electric field and electric charge distributions on the sample surface [28, 29]. The measurements are performed with the NTEGRA-AURA (NT-MDT) using the procedure of the two-pass measurement. A two pass or lift up measurement scheme is a technique whereby each line of the scan is measured twice. In the first pass the surface topography of the scanning line is measured in the tapping mode, figure 4a, while in the second pass the tip is lifted above the surface at a height dz and a potential, the bias voltage *U*, is applied between the conductive tip and the sample, figure 4b. In this second pass the electrical properties or surface potential is detected.
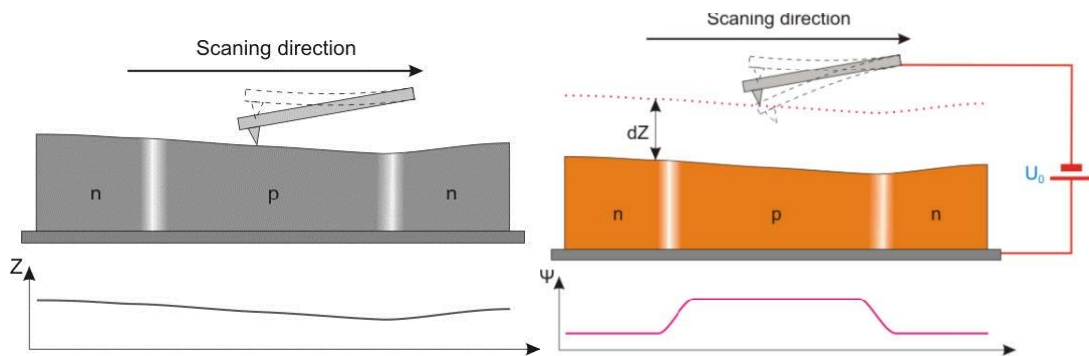

Figure 4. *a) First pass surface topography imaging. b) Second pass phase imaging.*

During the surface topography measurement the tip is close to the surface and the van der Waals forces are dominant. However, in the second pass the tip is moved from the surface whereby the electrical forces increases and become dominant. The tip is in the second pass lifted from the sample surface and retraces the measured surface profile achieved in the first pass moving at a constant predefined distance, dz, from the sample surface to eliminate the surface topography influence. In both passes the cantilever is oscillating with the resonance frequency resulting in a certain amplitude and phase. The attraction or repulsion of the tip depends of the force or electric field gradient. However, for the topography the amplitude signal is of importance while for the surface potential the change in the phase is used. The phase changes with the strength of the electrical field gradient which is used to construct the EFM image. This phase shift is proportional to the electrical field gradient. In this mode the tip together with the sample, separated at a distance dz, can be considered as a capacitor with capacitance C. The electrostatic force, F_{el}, is in this case approximately [30, 31]:

$$F_{el} = \frac{1}{2} U^2 \frac{dC}{dz} \tag{2}$$

where U is the applied bias voltage. This also reveals the importance of scanning with a constant height following the curvature of the sample topography. The electrostatic interaction depends on the distance. Figure 5 shows the schematic diagram of the EFM setup, using the NTegra. For the measurement a conductive gold coated tip NSG03/Au used. The sample is mounted on a conductive substrate and during the second pass the tip is kept 100 nm above the surface profile.
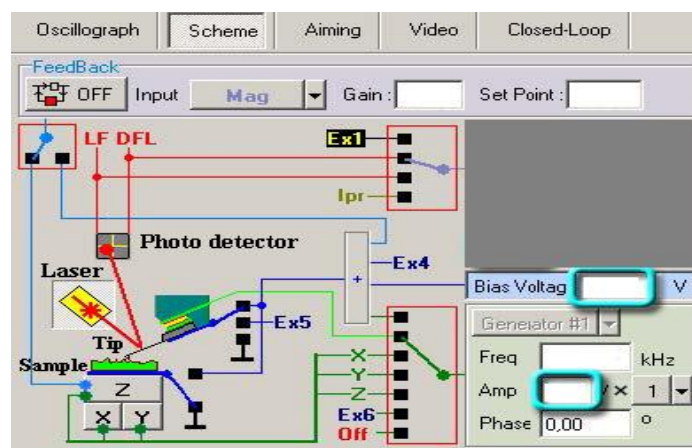

Figure 5. *Schematic diagram of the EFM setup. The feedback signal is not required because the tip is moved parallel to the topographic line maintaining a constant distance between tip and sample.*

5.3. Results and discussion

Electrical Measurements

Table 1 summarizes the measured values of piezoelectric charge constant d_{31}, relative permittivity ε_r and loss tangent $\tan \delta$ of PZT/PA and PZT/PDMS bimorphs. With the d_{33} meter, the d_{31} (induced polarization in direction 3 (parallel to direction in which ceramic element is polarized) per unit stress applied in direction 1 (perpendicular to direction in which ceramic element is polarized) measurement is possible only with the rigid samples (PZT/PA), while for the flexible (PZT/PDMS) samples, the measurement is impossible. Analysis of $\tan \delta$, which is the ratio of energy lost to energy stored, reveals a very low loss value indicating that only a small amount of the energy is dissipated as heat.

Table 1. *Comparison of measured values of d_{31}, ε_r and $\tan \delta$ of PZT/PA and PZT/PDMS bimorphs at a static force of 0.5 N.*

Bimorphs	d_{31} (pC/N)	ε_r	$\tan \delta$
PZT/PA	-7	4100	0.02
PZT/PDMS	-	3520	0

Charge Output Measurements

Piezoelectric materials produce an electric charge which varies in direct proportion to the load acting on the material. Figure 6 shows the charge output as a function of applied force on the PZT/PA and PZT/PDMS unimorphs. For both materials the output charge increases with increasing applied force. From the figure it is obvious that both composites behave linearly to the applied force and PZT/PA shows better piezoelectric properties than PZT/PDMS. Due to the rubbery behavior of PDMS at room temperature, the PZT/PDMS composites properties are appreciably affected by the stress-strain state. Figure 7 the charge output to the different force applied on PZT/PA and PZT/PDMS bimorphs. The maximum force that applied to the PZT/PA bimorph was 150 N (for preventing breakage) while to PZT/PDMS bimorph up to 400 N is applied. As expected, the PZT/PA bimorph exhibits better piezoelectric properties than the PZT/PDMS composites. From the figure it is also visible that at 150 N, PZT/PA bimorph acquired twice the charge compared to unimorph, while the charge of PZT/PDMS bimorph is lower than that of unimorph. The main reason could be the poor

adhesion of PDMS to the aluminum electrode resulting in poor electrical conductivity leading to lower poling efficiency.
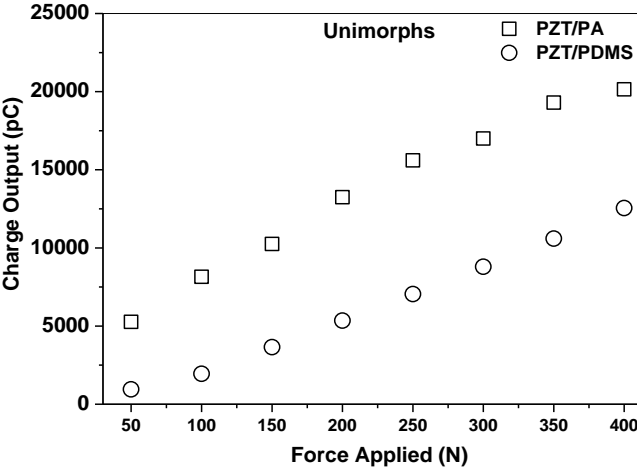
Figure 6. *The charge output to the different force applied on PZT/PA and PZT/PDMS unimorphs.*
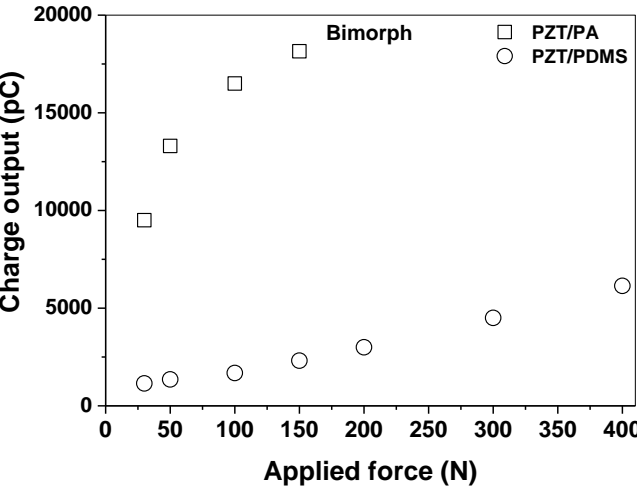
Figure 7. *The charge output to the different force applied on PZT/PA and PZT/PDMS bimorphs.*

Structural characterization

Figure 8 shows the topographic 3D images of PZT/PA bimorph. Due to the electrostriction or inversed piezoelectric effects the PZT/PA bimorph locally expand in accordance with the electric field. The domains experience a vertical expansion indicating the initial polarization of the electrical domain of the measured sample is

perpendicular to the sample surface and parallel to the applied electric field. The height image, figure 8a, resulted from the topography measurements in the first pass and the phase images with the applied bias voltages measured for the second pass, figure 8b till 8f. The phase change is proportional to this field. This indicates not only the position of the PZT material, which is easily polarized on or near the surface of the material, as shown by the mountains as shown in figure 8, but also the increase of the total polarization of the material. Of course, the PA polymer has a poor degree of polarization and it is unclear if the overall phase shift is caused by the surface effects or due to the bulk material. In the latter case the influence of the PZT plays a major role and is expected to be homogeneously distributed in the bulk.

Figure 8. *Topographic 3D images of PZT/PA (height and phase images).*

5.4. Conclusions

A new disc-type, reinforced piezoelectric composite bimorph has been designed and successfully fabricated by compression molding (PZT/PA-rigid) and solution casting (PZT/PDMS-flexible) technique. Th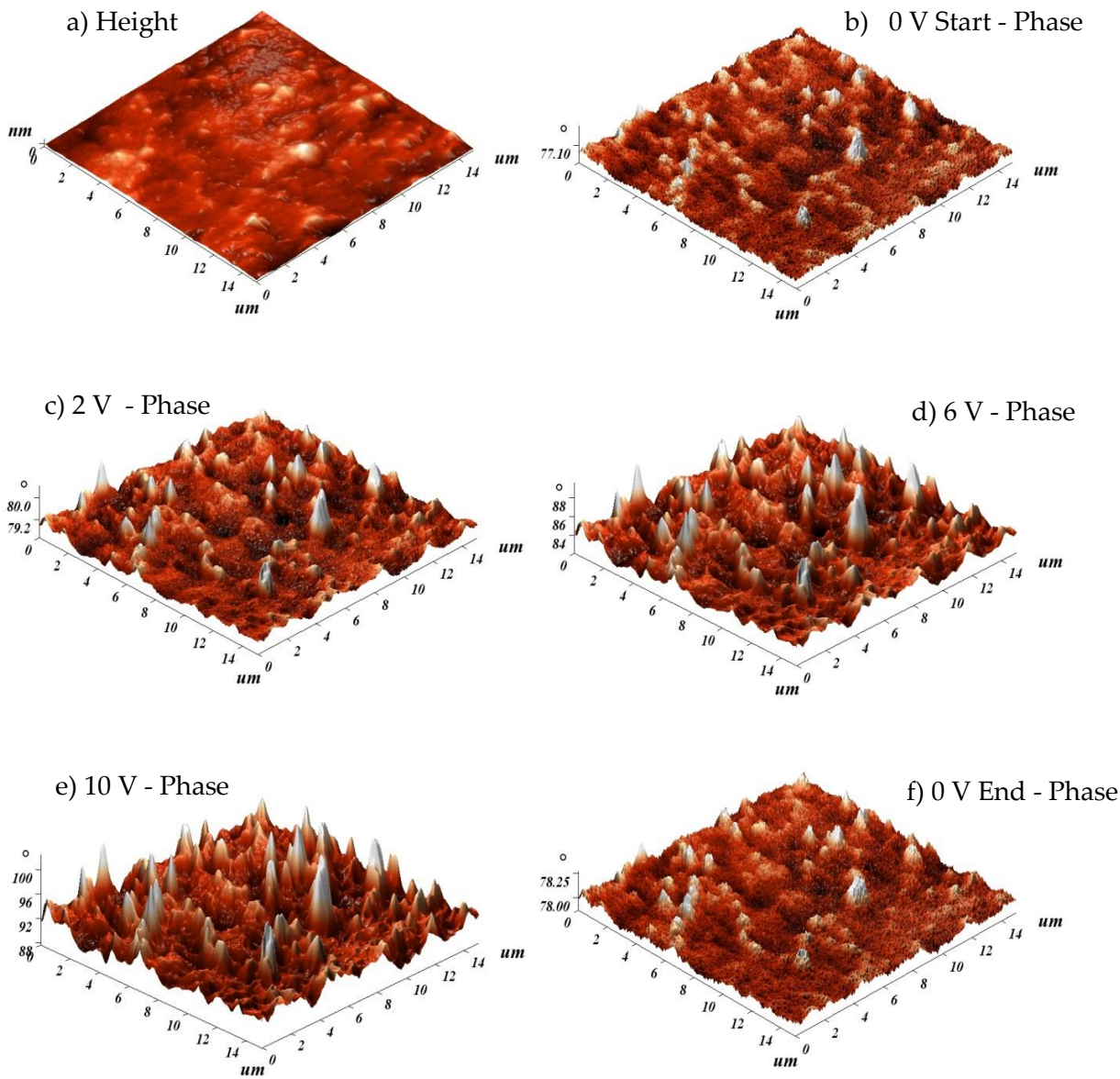e as-developed bimorphs have several advantages in terms of ease of fabrication, tailoring the properties and low price. Based on the charge output measurements, it is realized that PZT/PA bimorphs possesses excellent piezoelectric properties as compared to the PZT/PDMS bimorphs, but mechanically the latter can withstand much higher applied forces. The absence of any bonding agent in the fabrication process renders these bimorphs a useful alternative for high temperature applications.

References

[1]   S.B. Krupanidhi, N. Maffei, M. Sayer, K. El-Assal., 1983, J. Appl. Phys. 54, 6601-09.

[2]   T. Toyama, R. Kubo, E. Takata, K. Tanaka, K. Ohwada., 1994, Sensors and Actuators A: Physical 45 2 125–129.

[3]   M.D. Nguyen, H. Nazeer, K. Karakaya, S.V. Pham, R. Steenwelle, M. Dekkers, L. Abelmann, D.H.A. Blank, G. Rijnders., 2010, J. Micromech. Microeng. 20 085022.

[4]   V. Kugel, S. Chandran, L.E. Cross., 1996, Appl Phys Lett. 69 2021-2023.

[5]   R. Nath, S. Zhong, S.P. Alpay, B.D. Huey, M.W. Cole., 2008, Appl Phys Lett. 92 012916-012916-012913.

[6]   M.R. Steel, F. Harrison, P.G. Harper., 1978, J Phys D: Appl Phys. 11 979.

[7]   M. Taya, A.A. Almajid, M. Dunn, H. Takahashi., 2003, Sensors and Actuators A: Physical. 107 248-260.

[8]   M. Cleveland, H. Liang., 2012, Smart Mater.Struct. 21 047002.

[9]   Z.M. Dang, J.K. Yuan, J.W. Zha, T. Zhou, S.T. Li, G.H. Hu., 2012, Prog. Mat.Sci. 2012 57 660-723

[10]   A.B. Dobrucki, P. Pruchnicki., 1997, Sensors and Actuators A: Physical.58 203-212.

[11]   S. Dong, P. Bouchilloux, X-H. Du, K. Uchino., 2001, J. Intell. Mater. Syst. Struct. 12 613-616.

[12]   E.H. Hong, S. Trolier-McKinstry, R.L. Smith, S.V. Krishnaswamy, C.B. Freidhoff., 2006, J. Microelectromechanical Syst. 15 832-839.

[13]   I. Jung, Y. Roh., 1998, Sensors and Actuators A: Physical. 69 259-266.

[14]   C. Liu, S. Hu, S. Shen., 2012, Smart Mater.Struct. 21 115024.

[15]   C.W. Lim, L.H. He, A.K. Soh., 2001, Int. J. Solids. Struct. 38 2833-2849.

[16]   Q.M. Wang, Q. Zhang, B. Xu, R. Liu, L.E. Cross., 1999, J Appl Phys. 86 3352-3360.

[17]   B. Xu, Q.M. Zhang, V.D. Kugel, Q. Wang, L.E. Cross., 1996, Proc.Spie 271 217-220.

[18]   I. Chilibon, C. Dias, P. Inacio, J. Marat-mendes., 2007, J. Optoelectronics and advanced materials 9 6 1939-1943.

[19]   D. J. Cappelleri, M.I. Frecker, T.W. Simpson, A. Snyder., 2002, Transactions of the ASME 124 354-357.

[20]   Q. Wang, Q. Zhang, B. Xu, R. Liu, L.E. Cross., 1999, J.App Phy.86 3352- 3360.

[21]   J.G. Smits, S.I. Dalke, T.K. Cooney, 1991, Sensors and Actuators A: Physical. 28 41 01991.

[22]   J.G. Smits, W. Choi., 1991, IEEE Trans. Ultrason. Ferroelectr. Freq. Control 38 256.

[23]   A.C.C. Esteves, J. Brokken-Zijp, J. Laven, G. de With., 2010, Progr.Org.Coat. 68 12-18.

[24]   T.S. Low, W. Guo., 1995, J. MEMS 4(4)230-237.

[25]   I. Babu, D. van den Ende, G. de With., 2010, J Phys D: Appl Phys. 43 425402.

[26]   A.C.C. Esteves, J. Brokken-Zijp, J. Laven, H.P. Huinink, N.J.W. Reuvers, M.P. Van, et al., 2009, Polymer 50(16):3955-3966.

[27]   I. Babu, G. de With., 2013, Comp. Sci. Tech. Submitted.

[28]   T. Burnett, R. Yakimova, O. Kazakova., 2011, Nano Lett. 11 2324-2328.

[29]   E. Tevaarwerk, D.G. Keppel, P. Rugheimer, M.G. Lagally, M.A. Eriksson., 2005, Rev Sci Instrum. 76 053707-053707-053705.

[30]   P. Girard., 2001, Nanotechnology. 12 485-490.

[31]   Y. Minjun., 2006, Doctoral Thesis University of Notre Dame, Notre Dame, Indiana.

Chapter 6

Accurate measurements of the piezoelectric charge coefficient*

To realize proper measurements of the piezoelectric charge constant d_{33} of materials a certain mechanical load is required. This results in a contribution of the electric field dependence of the strain, i.e. dx/dE, to the experimentally determined d_{33}. While for stiff materials this contribution is negligible, it is shown that for compliant materials, such as composites using a low modulus matrix, a considerable contribution can arise and thus the experimental data should be corrected accordingly.

6.1. Introduction

The development of microelectromechanical systems (MEMS) pushed the physical limits of miniaturization of electronic devices creating a new frontier for research. These devices use the piezoelectric, electrostatic, thermal or electromagnetic properties of materials [1]. The piezoelectric effect provides the ability to use these "smart materials" as both sensor and actuator. The piezoelectric effect exists in several crystalline materials due to the polarity of the unit cells within the material. This polarity leads to the production of electric dipoles in the material which give rise to the piezoelectric properties. When these smart materials get strained an electric polarization is developed which is proportional to the magnitude and sign of the strain and refers to direct effect. Conversely, the indirect effect refers to the generation of a strain in a material due to the application of an electric field.

Both the direct and converse piezoelectric effects can be described mathematically through the piezoelectric constitutive equations. Accordingly the established linear constitutive equations in the reduced-matrix form [2] to describe the electromechanical interaction within a piezoelectric material are,

$$\{D\} = [\varepsilon^T]\{E\} + [d]\{T\} \qquad \text{Direct effect} \qquad (1)$$
$$\{S\} = [s^E]\{T\} + [d]\{E\} \qquad \text{Converse effect} \qquad (2)$$

The piezoelectric charge constant is defined by,

$$d_{33} = (\partial D_3/\partial T_3)_E + E(\partial \varepsilon^T/\partial T_3)_E = (\partial D_3/\partial T_3)_E + T(\partial s^E/\partial E)_T \qquad (3)$$

The constitutive equations are expressed in terms of the dielectric displacement D [C/m^2], mechanical stress and strain T [N/m^2] and S [-], applied electrical field E [V/m] through the dielectric permittivity ε [F/m], piezoelectric charge constant d [C/N] and the compliance s [m^2/N].

The piezoelectric activity of the material is defined by the piezoelectric charge coefficient d_{ij}, the subscript denotes the direction of the electric quantity (polarization or the electric field) and the mechanical quantity (stress or strain). The piezoelectric effect strongly depends on the polarization direction. In accordance with the IEEE standard on piezoelectricity [3], the three-dimensional behavior of the piezoelectric material (electric, elastic and piezoelectric) are based on an orthogonal coordinate system.

Conventionally there are various techniques to measure the piezoelectric effect. Accurate knowledge of the piezoelectric charge coefficient d_{ij} is essential to understand

the behavior of the piezo-material. Since equipment to measure the d_{33} is conventionally used for stiff, ceramic-like materials and the expected load dependence for polymer matrix piezo-composites is expected to be larger than for ceramics, a study on the load dependence of d_{33} for polymer matrix composites was done. To that purpose we used the composites as described below and compared measurements of d as a function of load for these materials as well as for ceramic reference samples.

6.2. Experimental

6.2.1. Materials

Cylindrical samples of bulk ceramics and 0-3 composites were used in this study. The ceramic used in this study was PZT disks (PC4 and PC5) marked as reference A and B with a reported d_{33} value of 336 and 370 pC/N, respectively. The three types of fabricated thin 0-3 composites used were PZT/LCR/PA, PZT/PA and PZT/PDMS for which the details of the fabrication procedure are reported in [4, 5]. The PZT used for the fabrication of 0-3 composites thin films is a soft PZT with 1 mol% Nb added as dopant.

6.2.2. Measurements

The samples were characterized with respect to their piezoelectric properties in terms of a static preload, imposing a varying load and constant frequency of 110 Hz using a d_{33} meter (Piezotest, PM300, UK). Conventionally d_{33} is defined as charge per unit force, both in the direction of polarization of the piezoelectric material. Figure 1 shows the picture of d_{33} meter used in this study. The piezoelectric sample is clamped within the jaws of the force head and is subjected to an oscillating force applied by means of an electromagnetic transducer. This force is preset to 0.25N rms, and is regulated by means of a current controlled amplifier. The oscillator may be set to any frequency in the range from 30 Hz to 300 Hz.

Figure 1. *Picture of d_{33} meter used in this study.*

6.3. Results and Discussion

Figure 2a and 2b shows the effect of static preload on the d_{33} value of bulk ceramics and 0-3 composites thin films. Two different trends are observed in the figures indicating the nature of PZT material used. The bulk ceramics shows an increasing trend with load, as reported for hard PZT [6]. The thin films (PZT/PA and PZT/LCR/PA) show a decreasing trend with load since we used a soft PZT material as piezo-filler and for soft PZT d_{33} decreases with load [7].

From figure 1a, showing the d-dependence on applied force F for the ceramic reference samples, a rather linear increase with load can be observed. Nevertheless, a second order polynomial was fitted but the R-test [8] showed that this fit is not significantly better at the 5% significance level. Hence the parameters a and b for a linear fit $d = a + bF$ are given in table 1. The recommended value to measure d is given as 10 N and the calibration values are given in table 1 as well [9]. Also indicated are the values of d at $F = 10$ [N]. From table 1 it is clear that the differences are small, about 1.5%; nevertheless for an accurate determination of d the load dependence should be taken in to account. Actually figure 1a shows a small change in slope at about 5 N for both reference samples. However, fitting only the range from 5 to 20 N does not change the value for a significantly. This change is probably due to a somewhat less good contact between the measuring force head and the (rather stiff) ceramic reference sample at a load less than 5 N.

From figure 1b, showing the d-dependence on applied force F for the composite samples, also a rather linear increase with load can be observed. Similarly as for the

reference samples, here also a second order polynomial was fitted to the data with the same result: this fit is not significantly better than a linear fit using the *R*-test at the 5% significance level. The resulting *a* and *b* values for the linear fit of the composite materials are also given in table 1. The advised value for the load is independent of the type of material. However, from the data in table 1 it is clear that for the various composites a significant discrepancy between *d* at 10 N and *d* at 0 N exist. While for the PA composites the difference is about 14%, the difference for the PA/LCR composites is about 16%. The value of these differences is significant so that a load-dependent measurement is required to get really reliable *d*-values. The data for the PDMS composites do deviate substantially from that of the other composites. First, the *d*-values increase with load and, second, they show a somewhat erratic behavior. The reason for this is unclear. Probably it is due to the rather large difference in stiffness between the PZT piezo-filler ($E \sim 63$ GPa [5]) and the PDMS matrix in the rubbery state ($E \sim 0.00075$ GPa) while for the other matrices the modulus is higher (PA ~ 0.15 GPa and PA/LCR ~ 1 GPa [5]).

Table 1. *Comparison of d values.*

Samples	d_{33} (pC/N)[*]	a (pC/N)[#]	b (pC/N²)[#]
Reference A	334 (336)	329.6 (0.2)	0.43 (0.02)
Reference B	370 (370)	365 .0 (0.3)	0.54 (0.02)
PZT/PA 1	13.4	14.59 (0.05)	−0.107 (0.004)
PZT/PA 2	11.3	12.18 (0.04)	−0.079 (0.003)
PZT/PDMS 1	18.5	13.5 (0.3)[$]	0.45 (0.02) [$]
PZT/PDMS 2	28.2	21.6 (1.3) [$]	0.38 (0.10) [$]
PZT/LCR/PA 1	28	31.06 (0.08)	−0.294 (0.007)
PZT/LCR/PA 2	22.2	23.57 (0.09)	−0.127 (0.008)

[*] Value as determined at $F = 10$ N. For the reference samples calibration values are given in parentheses.

[#] Standard error values are given in parentheses for fit using the data range 5-20 N.

[$] The large errors for the PDMS composites reflect the erratic behavior as shown in figure 1b.
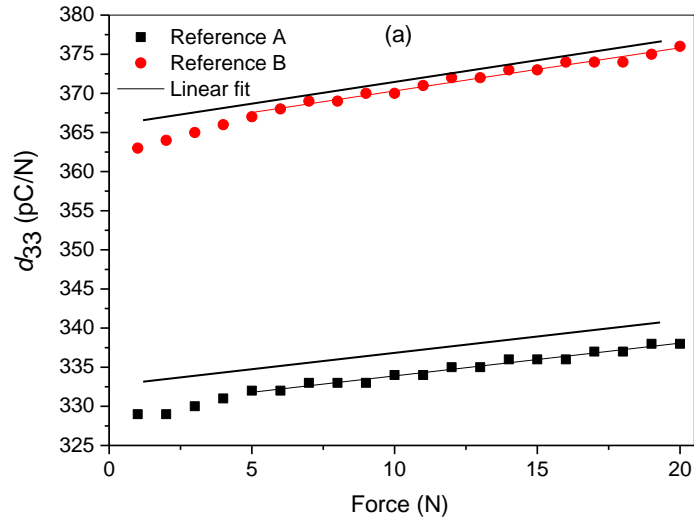
Figure 2 (a). *The d-dependence on applied force F for the ceramic reference samples. The linear fit line uses the data range 5-20 N.*

Figure 3a and 3b show the time dependence of the piezoelectric charge constant d measured at a constant static preload of 10 N. From figure 2a it can be seen that d-value for the ceramic reference samples does not change with time for the interval used. However, figure 2b shows the d-values for the PA/LCR composites decrease by about 2% while those for the PA composites decrease by about 5%. This limited change with time in d-values renders these composites suitable for various sensor and actuator applications. The time dependence of PDMS composites also differs from that of the other composites. Figure 2b indicates that the values increase by about 15%. Although the precise reason is unclear, this is probably related to the mechanical relaxation of the rubbery matrix under the load applied.
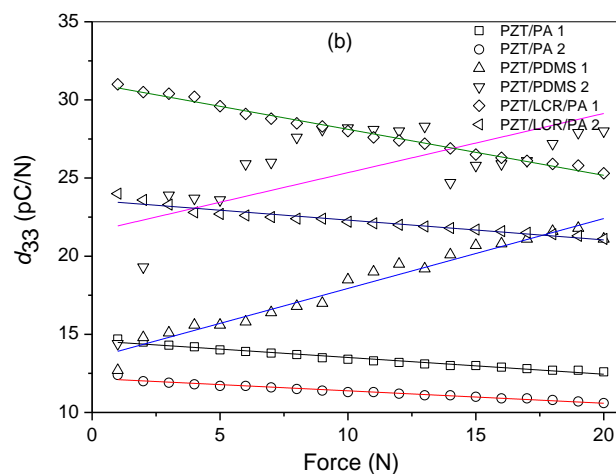
Figure 2 (b). *The d-dependence on applied force F for the composite samples.*
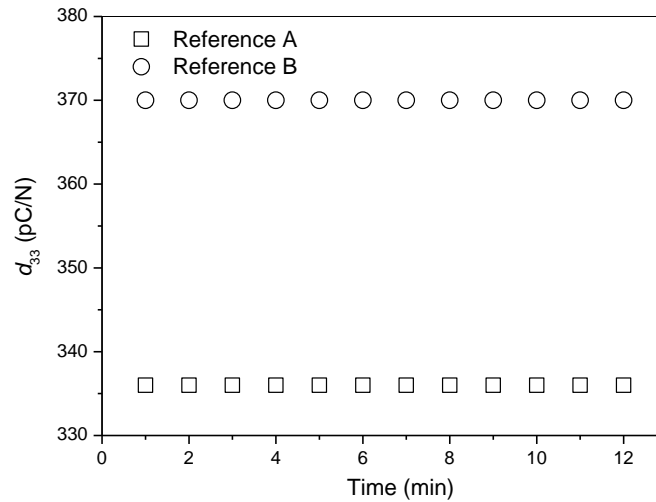
Figure 3 (a). *The time dependence of the piezoelectric charge constant d measured at a constant static preload of 10 N.*
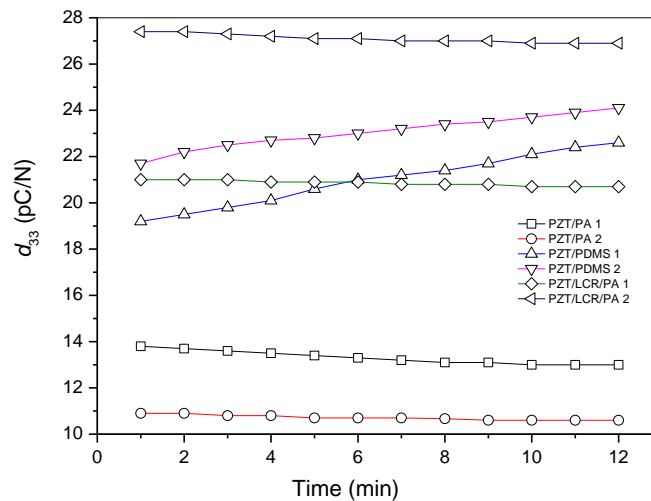
Figure 3 (b). *The time dependence of the piezoelectric charge constant d measured at a constant static preload of 10 N.*

6.4. Conclusions

The mechanical load applied to realize proper measurements of the piezoelectric charge constant d_{33} leads to electric field dependence of the strain, i.e. dx/dE, to the experimentally determined piezoelectric charge constant d_{33} of materials. In this manuscript, we investigate this effect using cylindrical samples of bulk ceramics (PZT disks) and 0-3 composites (PZT/LCT/PA, PZT/PA and PZT/PDMS). The samples were

characterized with respect to their piezoelectric properties in terms of a static preload, imposing a varying load and constant frequency of 110 Hz using a d_{33} meter. The discrepancy in the value of d measured at 0 N and 10 N is about 14% and 16%, respectively, for PA and PA/LCT composites. In the case of PDMS composites, the d-value first increases with load and at higher load shows a somewhat erratic behavior, probably due to the rather large difference in stiffness between the PZT piezo-filler and the matrix. Ceramic reference samples do not show any time dependence of d-values whereas the d-values for the PA/LCT and PA composites decrease by about 2% and 5%, respectively. The time dependence of PDMS composites indicates that the values increase by about 15%, probably related to the mechanical relaxation of the rubbery matrix under the load applied. The limited change of d-value observed for PA/LCT and PA composites with time renders these composites suitable for various sensor and actuator applications.

Acknowledgements

References

[1]   M. S. Vijaya, *Piezoelectric materials and devices*, New York, 2013, p. 39-40.

[2]   M E Lines and A M Glass *Principles and Applications of Ferroelectrics and Related Materials*, Oxford University Press, Great Britain 1977 128-131.

[3]   IEEE standard on piezoelectricity *IEEE Ultrasonics, Ferroelectrics, and Frequency Control Society* USA 1987 21-22.

[4]   I. Babu, D.A. van den Ende and G. de With. *J. Phys. D: Appl. Phys.* 2010, *43* (42), 425402.

[5]   I. Babu and G. de With, *Composites Science and Technology*, 2013, Submitted.

[6]   G. Yang, S F Liu , W Ren and B K Mukherjee *Ferroelectrics* 262:1 2001 207-212.

[7]   Q. M. Zhang and J Zhao, *IEEE Ultrasonics, Ferroelectrics, and Frequency Control Society*, 1999, 46.

[8]   W.C. Hamilton, *Statistics in physical science*, Ronald Press, New York, 1964, 157.

[9]   Piezometer system PM300 technical specifications.

Chapter 7

Summary and Outlook*

In this chapter a summary of the results and conclusions are given. An outlook to future developments is presented, which offer transducer characteristics with possibilities for new markets in the form of novel materials and processing techniques, related to existing polymer based composite processing techniques.

7.1 Summary

The design and fabrication of 0-3 piezoelectric composites (three types of unimorphs and two type of bimorphs) developed with improve material properties and to obtain integrated structures such as self-standing films are described. The development of soft flexible elastomeric piezocomposites like PZT/PDMS composite, proved to be the newest candidate novel materials which will offering oppourtunities for sensor and actuator applications in all fields. The above mentioned piezocomposites can break up the limitation for the application at high temperature, by avoiding bonding agents to be used in application.

In **chapter 2** we report on the processing and characterization of new series of fairly flexible 0-3 PZT/LCT/PA (Lead Zirconate Titanate $Pb(Zr_{1-x}Ti_x)O_3$/Liquid crystalline thermosets/Polyamide) piezoelectric composites with high permittivity and piezoelectric charge constant by incorporating PZT5A4 into a matrix of LCT and polyamide (PA11). Commercially available PZT powder was calcined at different temperatures for the optimization of the composite properties. The phase formation during calcination of the powder was studied by X-ray diffraction and the particle size by light scattering and scanning electron microscopy. X-ray diffraction indicated that for the PZT powder used, calcination at 1100 °C shows the maximum intensity for the single phase tetragonal perovskite peaks. The obtained d_{33} and g_{33} values from PZT/PA composites are also the highest for the PZT calcined at 1100 °C, supporting the above conclusion. The relative permittivity ε_r, piezoelectric charge constant d_{33}, electrical conductivity σ and elastic modulus E of the composites were found to increase with increasing ceramic volume fraction ϕ. Good agreement was found between the experimental data of relative permittivity and piezoelectric constants with several theoretical models (Jayasundere, Yamada and Lichtenecker) of 0-3 composites. The experimental data for ε_r agree quite well with the Lichtenecker model for PZT volume fraction up to 50%, while the Yamada and Jayasundere model underestimate the experimental data. The experimental data for the piezoelectric constants agree well with the Yamada model, suggesting an elongated particle shape and confirmed by independent image analysis. Moreover, the addition of PA11 to PZT/LCT composites leads to a lower elastic modulus providing more flexibility to the materials.

In c**hapter 3** we report on the realization of highly flexible piezoelectric composites with excellent functional properties which opens new ways to 'soft touch' applications in a variety of transducer and sensor applications. Highly flexible piezoelectric composites with 0-3 connectivity, filler volume fractions up to 50 vol. % and having hardly any pores are realized by solution casting of dispersions of $(Pb(Zr_xTi_{1-x})O_3$ (PZT) in poly-(dimethylsiloxane) (PDMS). SEM analysis of the

composites shows a homogeneous distribution of PZT particles in the polymer matrix without any porosity. The relative permittivity and piezoelectric charge constant increase with the increasing contribution of PZT, meanwhile maintaining a low ac conductivity. The experimental results were compared with theoretical models and we note that the Yamada model can either describe the piezoelectric charge constant d_{33} well meanwhile describing poorly the permittivity ε_r or vice versa, albeit in both cases with unrealistically high shape factors, but not both. Results obtained from static and dynamic mechanical analysis show that the present composites are highly compliant with a Young's modulus only a few times higher than for pure PDMS. The Yamada model underestimates the Young's moduli E significantly, though, as compared with the experimental data. Excellent piezoelectric properties (permittivity ε_r up to ~ 40, piezoelectric charge constant d_{33} up to 25 pC/N, piezoelectric voltage coefficient g_{33} up to 75 mV.m/N), electrical properties (conductivity σ about $1 \cdot 10^{-6}$ S/m at 1000 Hz) and mechanical properties (storage modulus E' up to 10 MPa, loss modulus E'' less than 0.5 MPa, limited creep and stress relaxation) have been realized. The good combination of the material properties, i.e. a decent value for permittivity, piezoelectric charge and voltage constant combined with low electrical conductivity, low elastic stiffness and very limited creep and stress relaxation, promotes the development of prototypes for transducer and sensors applications.

In **chapter 4** we present a simple fabrication procedure for highly dense piezoelectric composites with a combination of high dielectric constant and low dielectric loss and demonstrate the enhancement of electromechanical properties by incorporating carbon nanotubes (CNT) and carbon black (CB) into 0-3 PZT/PDMS (lead zirconate titanate - poly dimethyl siloxane) composites. Composites were fabricated by solution casting technique using a constant PZT/PDMS ratio of 40/60 and conductive fillers ranging from 0 to 0.5 vol.%. Impedance measurements proved that a small addition of conductive fillers sufficiently enhanced the electrical conductivity to lead to improved poling efficiency. For too high volume fractions (and consequently too high conductivity), poling becomes impossible. For the optimum PZT/PDMS/0.125CNT a relative permittivity ε_r ~ 50 and conductivity σ ~ 2.8×10^{-6} S/m was obtained while for the optimum PZT/PDMS/0.125CB ε_r ~ 35 and σ ~ 1.9×10^{-6} S/m have been realized. The piezoelectric charge constant d_{33} of the PZT/PDMS/0.125CNT and PZT/PDMS/0.125CB composites were 25 and 18 pC/N, respectively. Dynamic mechanical analysis (DMA) showed better performance for PZT/PDMS/CB with lower volume fraction conductive fillers than for the PZT/PDMS/CNT composites. The excellent (di-)electrical properties and the relatively simple fabrication procedure of these composites make them promising candidates in piezoelectric sensors, actuators and high efficiency capacitors.

In **chapter 5** we investigated the design, fabrication and performance analysis of two new disc-type types of composite bimorphs with series connection by compression molding (PZT/PA-rigid) and solution casting (PZT/PDMS-flexible) technique. The charge developed at an applied force of 150 N is 18150 pC (PZT/PA) and 2310 pC (PZT/PDMS), respectively. Charge output measurement demonstrates that PZT/PA bimorphs possesses excellent piezoelectric properties as compared to the PZT/PDMS bimorphs, but mechanically the latter can withstand much higher applied forces. A clear inverse piezoelectric effect was observed when the bimorphs were subjected to an electric field stepped up through 2, 6 and 10 V, indicating the net polarization direction of the different ferroelectric domains. The as-developed bimorphs have the basic structure of a sensor and actuator and since they do not use any bonding agent for bonding, they can provide a valuable alternative to the present bimorphs where bonding processes required for their realization, can limit the application at high temperature. Furthermore, these new bimorphs offer several advantages in terms of ease of fabrication, tailoring the properties and low price.

In **chapter 6** we describe contribution of the electric field dependence of the strain, i.e. *dx/dE*, to the experimentally determined d_{33}. This issue is arising because certain mechanical load is required to realize proper measurements of the piezoelectric charge constant d_{33} of materials. While for stiff reference materials this contribution is small, ~ 1.5%, for the compliant composite materials it is about 15%. Hence for an accurate determination of the *d*-value the experimental data extrapolated to load zero. Since equipment to measure the d_{33} is conventionally used for stiff, ceramic-like materials and the expected load dependence for polymer matrix piezo-composites is expected to be larger than for ceramics, a study on the load dependence of d_{33} for polymer matrix composites was done. We used the composites as described and compared measurements as a function of load for these materials as well as for ceramic reference samples.

7.2 Outlook

In the last few decades piezomaterials gained much importance due to their high potential as "smart materials". The emergence of new processing technologies continue to enlarge the performance of piezo composites and the results of this research suggest several promising directions for future investigations. The development of novel piezoelectric materials and processing technologies has great potential for further developments and creates a fertile ground for fundamental research. However, further developments and fundamental research are required in translating it into for sensing

applications with higher reliability. The integration of composite into a sensing device and its performance analysis in relation to demonstrator applications under its normal operating conditions will translate the outcome of this research into the next phase of development. The good combination of the material properties, i.e. a decent value for permittivity, piezoelectric charge and voltage constant combined with low electrical conductivity, low elastic stiffness and very limited creep and stress relaxation, promotes the development of prototypes for transducer and sensors applications. It is highly likely that other piezoelectric oxide particles can be incorporated into PDMS matrix without having any porosity in a similar easy way, thereby increasing the applicability range.

Samenvatting

Het ontwerp en de fabricage van 0-3 piëzo-elektrische polymeer composieten (drie soorten unimorphs en twee soorten bimorphs), ontwikkeld om materiaaleigenschappen te verbeteren en om geïntegreerde structuren zoals op zichzelf staande films te verkrijgen, zijn beschreven. De ontwikkeling van zachte flexibele elastomeer piezocomposieten, zoals PZT / PDMS, zijn de nieuwste kandidaten van onbekende materialen die mogelijkheden bieden voor sensor- en actuator -toepassingen op allerlei gebieden. De bovengenoemde piezocomposieten kunnen de beperking voor de toepassing bij hoge temperatuur doorbreken omdat lijmen vermeden wordt.

In **hoofdstuk 2** rapporteren we over de verwerking en karakterisering van nieuwe, redelijk flexibele 0-3 PZT / LCT / PA (Loodzirkoontitanaat $Pb(Zr_{1-x}Ti_x)O_3$ / vloeibare kristallijne thermoharders / Polyamide) piëzo-elektrische composieten met een hoge diëlektrische constante en piëzo-elektrische ladingsconstante door het opnemen van PZT5A4 in een matrix van LCT en polyamide (PA11). Commercieel verkrijgbaar PZT poeder werd gecalcineerd bij verschillende temperaturen voor het optimaliseren van de composieteigenschappen. De fasevorming tijdens het calcineren van het poeder werd bestudeerd met behulp van Röntgendiffractie en de deeltjesgrootte door middel van lichtverstrooiing en scanning elektronenmicroscopie. Röntgendiffractie laat zien dat het gebruikte PZT poeder, gecalcineerd bij 1100 °C, de maximale intensiteit van de pieken voor éénfase tetragonaal perovskiet geeft. De verkregen d_{33} en g_{33} waarden voor de PZT / PA composieten zijn ook het hoogst voor PZT gecalcineerd bij 1100 ° C, hetgeen de bovenstaande conclusie ondersteunt. De relatieve diëlektrische constante ε_r, de piëzo-elektrische ladingsconstante d_{33}, de geleidbaarheid σ en de elasticiteitsmodulus E van de composieten bleken toe te nemen met toenemende keramische volumefractie ϕ. Goede overeenkomst werd gevonden tussen de experimentele data voor de relatieve diëlektrische constante en piëzo-elektrische constanten met diverse theoretische modellen (Jayasundere, Yamada en Lichtenecker) voor 0-3 composieten. De experimentele gegevens voor ε_r komen goed overeen met het Lichtenecker model voor PZT met een volume fractie tot 50%, terwijl het Yamada en Jayasundere model de experimentele waarden onderschatten. De experimentele gegevens voor de piëzo-elektrische constanten komen overeen met het Yamada model en suggereren een langgerekte deeltjesvorm, zoals bevestigd door de resultaten van onafhankelijke beeldanalyse. Bovendien leidt de toevoeging van PA11

aan PZT / LCT composieten tot een lagere elasticiteitsmodulus die meer flexibiliteit geeft aan de materialen.

In **hoofdstuk 3** beschrijven we de realisatie van flexibele piëzo-elektrische composieten met uitstekende functionele eigenschappen hetgeen nieuwe wegen opent naar 'soft touch' toepassingen voor een verscheidenheid van transducer en sensor toepassingen. Zeer flexibele piëzo-elektrische composieten met 0-3 connectiviteit, met vulmiddel volume fracties tot 50% en vrijwel zonder poriën werden gerealiseerd door gieten van dispersies (met wat extra oplosmiddel) van $(Pb(Zr_xTi_{1-x})O_3$ (PZT) in poly-(dimethylsiloxaan) (PDMS). SEM analyse van de composieten laat een homogene verdeling van de PZT deeltjes in de polymeermatrix zien, wederom vrijwel zonder enige porositeit. De toename van de relatieve diëlektrische constante en piëzo-elektrische ladingsconstante met toenemende PZT fractie leidt niet tot een hogere AC elektrische geleidbaarheid. De experimentele resultaten werden vergeleken met theoretische modellen. Opgemerkt wordt dat het Yamada model ofwel de piëzo-elektrische ladingsconstante d_{33} goed beschrijft en de diëlektrische constante ε_r slecht, of vice versa, hoewel in beide gevallen met onrealistisch hoge vormfactoren, maar niet beide grootheden tegelijkertijd. Resultaten verkregen uit statische en dynamische mechanische analyse tonen aan dat de composieten zeer een zeer lage stijfheid bezitten met een Young's modulus maar enkele malen hoger dan voor puur PDMS. Het Yamada model onderschat de Young's modulus E aanzienlijk vergeleken met de experimentele data. Uitstekende piëzo-elektrische eigenschappen (diëlektrische ε_r tot ~ 40, piëzo-elektrische ladingsconstante d_{33} tot 25 pC/N, piëzo-elektrische spanning coëfficiënt g_{33} tot 75 mV·m/N), elektrische eigenschappen (geleidbaarheid σ ongeveer $1·10^{-6}$ S/m bij 1000 Hz en mechanische eigenschappen (opslagmodulus E' tot 10 MPa, verliesmodulus E'' minder dan 0,5 MPa, beperkte kruip en spanningsrelaxatie) zijn gerealiseerd. De goede combinatie van de eigenschappen van het materiaal, dat wil zeggen een goede waarde voor de diëlektrische constante, piëzo-elektrische lading en spanning constante in combinatie met een lage elektrische geleidbaarheid, lage elastische stijfheid en zeer beperkte kruip en spanningsrelaxatie, maken een verdere ontwikkeling van prototypen voor transducer en sensoren toepassingen mogelijk.

In **hoofdstuk 4** presenteren we een eenvoudige fabricage procedure voor zeer dichte piëzoelektrische composieten met een combinatie van hoge diëlektrische constante en lage diëlektrische verliezen. Tevens tonen we de verbetering van de elektromechanische eigenschappen door het opnemen van koolstof nanotubes (CNT) en koolzwart (CB) in 0-3 PZT / PDMS (loodzirkonaat titanate - poly dimethylsiloxaan) composieten. De composieten werden gefabriceerd door eerder genoemde giettechniek met een constante PZT / PDMS -verhouding van 40 / 60 en de geleidende vulstoffen van 0 tot 0,5 vol%. Impedantiemetingen geven aan dat een kleine toevoeging van

geleidende vulstoffen de elektrische geleidbaarheid voldoende verhoogt om een verbeterde efficiency voor polen te realiseren. Voor te hoge volume fracties (en dus te hoge geleidbaarheid) wordt polen onmogelijk. Voor de optimale samenstelling PZT/PDMS/0.125CNT werd een relatieve diëlektrische constante ε_r ~ 50 en geleidbaarheid σ ~ 2,8 × 10^{-6} S/m verkregen, terwijl voor de optimale samenstelling PZT/PDMS/0.125CB ε_r ~ 35 en σ ~ 1,9 × 10^{-6} S/m werd gerealiseerd. De piëzo-elektrische ladingsconstante d_{33} van de PZT/PDMS/0.125CNT en PZT/PDMS/0.125CB composieten zijn, respectievelijk, 25 en 18 pC/N. Dynamische mechanische analyse (DMA) toonde betere prestaties voor PZT / PDMS / CB met een lagere volume fractie geleidende vulstoffen dan voor de PZT / PDMS / CNT composieten. De voortreffelijke (di-) elektrische eigenschappen en de relatief eenvoudige fabricage werkwijze van deze composieten maken dat ze veelbelovende kandidaten voor piëzoelektrische sensoren, actuatoren en hoge efficiency condensatoren zijn.

In **hoofdstuk 5** wordt het ontwerp, de fabricage en de prestatie van twee nieuwe disc-types van composiet bimorphs met serieschakeling verkregen door persen (PZT / PA - rigide) en gieten (PZT / PDMS - flexibel) techniek onderzocht. De ontwikkelde lading bij een aangebrachte kracht van 150 N is, respectievelijk, 18150 pC (PZT / PA) en 2310 pC (PZT / PDMS). De gegenereerde lading toont aan dat PZT / PA bimorphs betere piëzoelektrische eigenschappen bezitten dan de PZT / PDMS bimorphs, maar dat de laatste veel hogere mechanisch krachten kan weerstaan. Een duidelijk invers piëzo-elektrisch effect werd waargenomen wanneer de bimorphs werden onderworpen aan een elektrisch veld door middel van het aanbrengen van 2, 6 en 10 V bij EFM metingen, waarbij de netto polarisatierichting van de ferroelektrische domeinen zichtbaar wordt. De ontwikkelde bimorphs hebben de basisstructuur van een sensor en actuator en omdat zij geen lijm gebruiken kunnen zij een waardevol alternatief zijn voor de bimorphs waar lijmprocessen nodig zijn voor de realisatie, hetgeen de toepassing bij hoge temperaturen kan beperken. Bovendien bieden deze nieuwe bimorphs verdere voordelen in termen van gemak van de fabricage, het afstemmen van de eigenschappen en de lage prijs .

In **hoofdstuk 6** beschrijven we de bijdrage van het elektrische veld afhankelijk van de rek x, namelijk dx/dE, aan de experimenteel bepaalde waarde van d_{33}. Deze bijdrage ontstaat omdat een bepaalde mechanische belasting nodig is om een correcte meting van de piëzo-elektrische ladingsconstante d_{33} van de materialen te kunnen doen. Voor een nauwkeurige bepaling van de d-waarde werden de experimentele gegevens geëxtrapoleerd naar een mechanische belasting van 0 N. Aangezien apparatuur voor de bepaling van d_{33} gewoonlijk gebruikt wordt voor stijve, keramische materialen en het verwachte effect voor polymeermatrix piëzo-composieten hoger is dan voor keramiek, werd een studie van de afhankelijkheid van de mechanische belasting voor d_{33} van

polymeermatrix composieten uitgevoerd. We gebruikten de samenstellingen zoals beschreven en vergeleken metingen als functie van de belasting voor deze materialen en voor keramische referentiemonsters. Terwijl voor stijve referentiematerialen de bijdrage van dx/dE klein is, ~ 1,5%, is deze voor de composietmaterialen ongeveer 15%.

Publications

Publications related to the work presented in this thesis

1. I. Babu, D.A. van den Ende and G. de With, "Processing and characterization of piezoelectric 0-3 PZT/LCT/PA composites," Journal of Physics D: Applied Physics, 43, 425402 (2010).
2. I. Babu and G. de With, "Highly flexible piezoelectric 0-3 PZT-PDMS composites with high filler content," Composites Science and Technology (In review)
3. I. Babu and G. de With, "Enhanced electromechanical properties of piezoelectric thin flexible films," Composites Science and Technology (In review)
4. I. Babu, M M R M. Hendrix and G. de With, "Piezoelectric composite bimorphs: Design, fabrication and performance analysis," Smart materials and structures (In review)
5. I. Babu and G. de With, "Accurate measurements of the piezoelectric charge coefficient," Applied Physics Letters (In review)
6. I. Babu, N. Meis and G. de With, "Review of piezoelectric composites," Journal of Materials Chemistry (In review)
7. I. Babu and G. de With, "Highly flexible 0-3 PZT/PDMS composite films," 6th Coatings Science International, Noordwijk, The Netherlands (2010).
8. I. Babu and G. de With, "Processing and characterization of new 0-3 PZT/LCR/PA composites," Proceedings of European congress and exhibition on advanced materials and process, Euromat 2009, UK (2009).
9. I. Babu and G. de With, "Processing and characterization of 0-3 PZT/LCR/PA composites," 5th Coatings Science International, Noordwijk, The Netherlands (2009).
10. D.A. van den Ende, I. Babu, Y. Jia, W.A. Groen, G. de With and S. van der Zwaag, "PZT-polymer composites: Material combinations and design routes for optimal device performance," Proceedings of European congress and exhibition on advanced materials and process, Euromat 2009, UK (2009).

Other publications

11. K. A. J. Dijkhuis, I. Babu, J. S. Lopulissa, J.W.M. Noordermeer and W. K. Dierkes, "A mechanistic approach to EPDM devulcanization," Rubber Chemistry and Technology, 81 (2), 190-208 (2008).

12. K.A.J. Dijkhuis, I. Babu, J.S. Lopulissa, J.W.M. Noordermeer and W.K. Dierkes, "A Mechanistic Approach to EPDM Devulcanization," Kautschuk Gummi Kunststoffe (2007).

13. K.A.J. Dijkhuis, I. Babu, J.S. Lopulissa, J.W.M. Noordermeer and W.K. Dierkes, "A Mechanistic Approach to EPDM Devulcanization," The fall 172nd Technical Meeting of the American Chemical Society Rubber Division, Cleveland, USA (2007).

14. W. K. Dierkes, K.A.J. Dijkhuis, I. Babu and J.W.M. Noordermeer, "Study on the reversibility of EPDM Vulcanization," Salvador, Brazil (2007).

Acknowledgements

The research presented in this thesis is the result of my work conducted at the Materials and Interface Chemistry group of Technical University of Eindhoven. During this period, I have been fortunate to be accompanied, supported and inspired by several people professionally as well as personally, to whom I would like to express my sincere acknowledgements here.

First of all, I would like to express my profound respect and gratitude to my promotor Bert de With. It's my great pleasure and privilege to have you as my daily supervisor. You were always there with a smiling face for discussion. Dear Bert, thank you very much for your invaluable suggestions, affectionate advices and for all the support throughout the years, which helped me in completing this thesis. Hartelijk bedankt Bert!

I would like to thank my co-promoter Rolf van Benthem for his support. I really appreciate your open minded constructive remarks and suggestions about my thesis. Thank you for being a friendly professor.

The contribution of the promotion committee constituted probably the most feedback from the outside. I acknowledge Prof. J.C. Schouten, Prof. J.Th.M. de Hosson, Prof. S.J. Picken and Prof. C.W.M. Bastiaansen for their valuable comments and for being the committee members of my defense.

This work was financially supported by the Smartmix funding program (grant SMVA06071), as part of the program "Smart systems based on integrated Piezo (SmartPIE)". I wish to express my sincere gratitude to Jan Peters (Chairman of the Applied Piezo foundation), Prof. Sybrand van der Zwaag (Delft University), Dr. Pim Groen (TNO, Eindhoven), Dr. Daan van den Ende (TNO, Eindhoven), Dr .Yan Min Jia (Delft University) and Benjamin for their interest and for the fruitful discussions.

Special thanks to Jos Laven and Catarina for being significant sources of support individually and also in the technical progress of this project. You were always willing to help me in all possible ways and with a smiling face.

I wish to acknowledge Huub van der Palen (always ready to help me) and Marco Hendrix (bedankt voor de samenvatting) for their technical assistance and for their interest in this project. Thank you very much for being so helpful !

I had a great time during this period at my research group. My room mates Camille (thanks for being my paranimfen and a nice friend), Marcos and Yvvone are acknowledged for creating a very friendly working atmosphere. I am indebted to all the

past and present members of the SMG group: Leendert, Nico, Heiner, Frank Peters, Gunter, Sasha, Niek, Paul, Mark, Beulah (thanks for being my paranimfen), Kangboo, Baris, Dina, Katya, Yogesh, Vladimir, Isabelle, Maarten, Qingling, Beryl, Marcel, Koen, Cem, Jos, Karthik, Niels, Delei, Gokhan, Hesam, Maurizio and all the new members for their creative ideas and support. Special thanks to Imanda for her support and for making all the administrative work very smooth.

I extend my heartfelt gratitude to all my Indian friends for making my life in Netherlands so memorable. Thanks to Ajin, Abraham-Denny, Arbind-Selina, Biju-Reshmi, Berni-Kamalamma, Chetan-Poornima, Hrudya, Jincy, Kiran-Kavitha, Musthafa-Shahina, Rajesh-Sheba, Sandeep-Jalaja, Seshan-Jayanthi, Shaji-Mercy, Shaneesh-Rashija, Tony-Sheril, Vinay-Uma, Vipin-Tintu for making me feel at home.

Thanks to Alberto-Ilaria, Ben-Lidi, Elena and Natallia for the nice evening gatherings.

I express my hearty thanks to my loving parents-in-law for their affection, constant support and prayers extended to me. Thank you so much for always being very supportive and helpful. Many thanks to my brother-in-law's and sister-in-law's: Jose-Sheeba, Poly-Treesa, Francis-Lissy, Babu-Annie and Sabu for all their support and wishes.

I express my hearty thanks to my sister Bindu and brother-in-law Joshy for their love, continuous support and prayers.

My loving parents always gave great care and priority for me and for my studies. It is with your sacrifices, support and prayers that I reached up to here. Without your unconditional love and blessings, I would not have come so far and this thesis would not have materialised. Thank you so much for always being with me.

Dear Iva (*Ponnu*), you are the most wonderful blessing in my life. Nothing is comparable to the happiness of being your mother. You cherishes each and every moment of my life. You don't know how much I love you and how much I missed you when I was busy with this thesis. Finally, I would like to thank the person without whom this day would never have come ! Dear Babu, I am very fortunate to have you as my partner. You have always provided steadfast support throughout the years. During the most difficult times, you were always there to keep me happy and smiling with your true affection and dedication that you always had towards me. Dear Babu, I owe this thesis to you.

Above all, I thank God for the uncountable blessings showered upon me and I lift my exuberant heart with utmost gratitude and honor.

Thank you all,

Indu Babu

Curriculum Vitae

Indu Babu was born in Trichur, Kerala, India. She obtained Bachelor of Science (B.Sc.) degree in Chemistry from University of Calicut in 1998 and Master of Science (M.Sc.) degree in Analytical Chemistry from Mahatma Gandhi University in 2001. As a part of the M. Sc course she carried out a research project on the permeation of organic vapors through Nylon/NBR polymer blends at School of Chemical Sciences, Mahatma Gandhi University, India. Later, she worked as Research Assistant at Central Instruments Laboratory, India during the period 2001-2004.

In 2004 she came to Netherlands for pursuing post-graduation in Material Science and Technology and she received Masters in Chemical Engineering from University of Twente in 2006. She carried out Masters research project on the devulcanization of EPDM-Rubber vulcanizates at the Department of Elastomer Technology and Engineering, University of Twente, The Netherlands and internship project on the surface modification of X-Flow PES/PVP hollow fiber membranes to control fouling at X-Flow, Norit, Enschede, The Netherlands. Later she worked (2007-2008) as a Junior Researcher on magnetostrictive sensing materials at MESA+ Institute of Nanotechnology, University of Twente, The Netherlands. In 2008 she started her PhD research at Laboratory of Materials and Interface Chemistry, Department of Chemical Engineering and Chemistry, Eindhoven University of Technology, The Netherlands under the supervision of Prof. Dr. Gijsbertus de With. The topic of research was "Processing and properties of piezoelectric polymer-ceramic composites for sensor applications". The results of this research project are presented in this thesis.